UNIVERSITY OF PAVIA

“Department of Brain and Behavioral Sciences”

IRCCS Mondino Foundation

PhD Thesis in Biomedical Sciences

Development of innovative three dimensional cell culture for modelling neurodegenerative diseases

Tutor:
Prof. Mauro Ceroni

Supervisor:
Dr. Cristina Cereda

Experimental thesis by
Matteo Bordoni

Academic Year 2017/2018

Summary

1. INTRODUCTION 4

1.1. Neurodegenerative diseases 5

1.1.1. Alzheimer's disease 6

1.1.2. Parkinson's disease 10

1.1.3. Amytrophic Lateral Sclerosis 13

1.1.4. Huntington disease 16

1.1.5. Neurodegenerative diseases' modelling 20

1.2. Induced Pluripotent Stem Cells in NDDs' study 23

1.2.1. iPSCs 24

1.2.2. iPSCs in Disease Modelling 26

1.2.3. iPSC-based drug discovery 29

1.2.4. IPSCs in Alzheimer's disease 32

1.2.5. IPSCs in Parkinson's disease 34

1.2.6. IPSCs in amyotrophic lateral sclerosis 36

1.2.7. IPSCs in Huntington's disease 38

1.3. 3D Bioprinting 39

1.3.1. Bioprinting techniques 41

1.3.2. Bioplotters 45

1.3.3. Bioinks 46

1.3.4. Bioprinting and neurodegeneration 50

2. AIM 52

3. MATERIALS AND METHODS 55

3.1. Gelatin-based hydrogel 56

3.2. Conductive hydrogel 59

3.3. Induced Pluripotent Stem Cells 62

4. RESULTS 66

4.1. Gelatin-Based Hydrogel 67

4.1.1. Pasteurization is the best sterilization method available 67

4.1.2. Gelatin seems to improve cells viability 68

4.1.3. Viability tests in SH-SY5Y cell line 69

4.1.4. The 4% SA / 4% GEL hydrogel maintains the 3D structure 70

4.1.5. Cells organize themselves into 3D clumps 71

4.1.6. Analysis of repeatability 72

4.1.7. 3D bioprinting of SH-SY5Y cell line 74

4.2. Conductive hydrogel 76

4.2.1. Finding the best drying method for scaffolds 77

4.2.2. The attachment of SH-SY5Y cells is charge-dependent 78

4.2.3. Functionalization with CNTs allows conductivity improvement of NFC 79

4.2.4. The conductive ink improves differentiation of SH-SY5Y cells 80

4.3. iPSCs 83

4.3.1. Fibroblasts and PBMCs reprogramming 83

4.3.2. iPSCs bioprinting 86

5. DISCUSSION AND CONCLUSION 87

6. REFERENCES 91

1. INTRODUCTION

1.1. Neurodegenerative diseases

Neurodegenerative diseases (NDDs), such as Alzheimer's disease (AD), Parkinson's disease (PD), amyotrophic lateral sclerosis (ALS), and Huntington's disease (HD), are a broad class of several pathologies that lead to the degeneration of a disorder-specific group of neural cells and affect millions of people across the world. Since NDDs occur easily in elder people, they are increasing in prevalence in the last decades because of the increasing average age of the population (Peden and Ironside, 2012). NDDs cause a wide range of symptoms such as memory impairment, cognitive disabilities and motor problems. There are many differences not only between diverse diseases, but also between patients with the same pathology. Moreover, overlaps between the different disorders complicate the diagnosis. In fact, the clinical diagnosis of NDs such as PD is often inaccurate and a definitive diagnosis can only be made with a neuropathological examination of the brain during autopsy (1). Another common issue shared by NDDs is the presence of two main forms of the disease, i.e. a sporadic form and a familial one, based on the existence of a familial history of the pathology. Usually, NDDs appear in the sporadic form, while the familial form represents only rare cases. Both the types of disorders can have a well-defined and known genetic mutation, but probably there are many susceptibility genes that have to be discovered. Finally, in other cases the pathogenesis is not caused by a genetic mutation but by other molecular pathways (2).

Despite they are very common diseases and many research studies tried to unravel the pathogenesis of them, the exact cause of these chronic disorders is not fully understood. Actually, current treatments only try to slow down the progression or to ameliorate the symptoms of these pathological conditions (3). The main limit for the study of NDDs is the lack of a realistic model of the neural tissue, because of the hardness to obtain it from human beings. Moreover, after NDDs cause the death and the degeneration of the neural tissue and cells. Thus, it is necessary to develop a model system that can recapitulate the pathogenesis

and the hallmarks of these disorders, in order to know more about NDDs. Therefore, different *in vivo*, *ex vivo*, and *in vitro* models have been generated. Mouse, fruit fly, nematode worm, and yeast have been used as important experimental model for many years, providing key insights into disease mechanisms (4-7). But *in vitro* models present several advantages over *in vivo* models in many aspects. For example, the role of a particular type of cells can be studied, investigating also the environment that surrounds cells, simulating the disease. With *in vitro* models, it is possible to investigate molecular pathways of specific molecules and other compounds, e.g. oligonucleotide, that can have possible deleterious or protective role (3).

Many models have been developed to better understand the molecular pathways that underlie the degeneration of the neural tissue, causing the establishment of a NDD.

1.1.1. Alzheimer's disease

AD is the most common cause of dementia in the whole world and it is characterized by progressive memory loss, deficits in cognitive abilities and behaviour impairments (8). AD was firstly described in 1907 by Alois Alzheimer, who noticed an atrophic brain of one of his patients during the autopsy (9). AD is a severe neurodegenerative disorder that affects several areas of both the cerebral cortex and the brain's memory area, the hippocampus. The frontal and the temporal lobes are the first areas involved by the disease, but then the degeneration and abnormalities slowly progress at rates very different between patients, involving other areas of the neocortex (10).

Recently acquired data suggest that about 25 million of people have AD, and every year about 5 million new cases arise (11). The prevalence of AD in Western Europe and North America is about 6% of the population at age 60, representing the highest prevalence of the disease respect other countries. Intriguingly, the prevalence rate for AD increases exponentially with age. For example between the ages of 60 and 85 years dementia

(predominately AD) increases of 15 times (12, 13). This data suggest that age is probably the most important risk factor for the development of the disease. Moreover, AD is usually classified by the age of the manifestation of symptoms: when they start to manifest before age 65 patients are classified as patients with early-onset AD, while patients with the late-onset form of AD manifest symptoms after the age of 65. As expected, the most common form of AD is the late one, with only 10% of cases being diagnosed before the age of 65, usually between 45 and 60 years (14). Only 1–5% of AD cases have a genetic cause and almost all of these involve early-onset disease, while in the other cases the real pathogenesis is still unknown (14, 15). Other factors have been associated with increased risk of AD, such as diabetes, smoking, obesity, and dyslipidaemia (Table I). Among these, cerebrovascular diseases are the most consistently reported to be associated with AD (12). As protective factors, we can find education, leisure activities, Mediterranean diet and physical activity (Table I). All of those are involved in pathways that lead to the activation of brain plasticity, the improvement of lipids metabolism and an anti-inflammatory response (12).

Antecedent	Direction	Possible mechanisms
Cardiovascular disease	Increased	Parenchymal destruction and ↑ Aβ
Smoking	Increased	Vascular effects and oxidative stress
Type II diabetes	Increased	Insulin and Aβ compete for clearance
Obesity	Increased	Increased risk of type II diabetes
Traumatic head injury	Increased	↑Aβ
Education	Decreased	Provides cognitive reserve
Leisure activity	Decreased	Improves lipid metabolism
Mediterranean diet	Decreased	Anti-inflammatory
Physical activity	Decreased	Activates brain plasticity

TABLE I. FACTORS THAT CAN INCREASE OR DECREASE THE RISK OF PROVOKE AD (12)

On average, the duration of the disease is about 8–10 years, but a preclinical and prodromal stage, which can extend over 2 decades, precedes the symptomatic clinical stages.

AD has two main hallmarks (Fig. 1):

- the accumulation of insoluble amyloid-β (Aβ42) in extracellular and blood vessels plaques in extracellular spaces;
- the formation of neurofibrillary tangles in neurons due to the aggregation of the microtubule protein tau.

Until now, the progression of the disease has been studied using post-mortem reconstructions, but the development of new molecular imaging techniques has allowed a better tracking of accumulation and aggregation of both Aβ and tau, helping to study longitudinal dispersal of pathological changes with a real-time *in vivo* approach (10). Aβ42 deposition usually precedes neurofibrillary changes, involving specific regions of the brain, in particular the frontal and temporal lobes, hippocampus and limbic system. Sometimes, AD starts from other areas, such as parietal and occipital lobes, with the accumulation of the neurofibrillary tangles in the medial temporal lobes and hippocampus, and progressively spread to other areas of the neocortex (10).

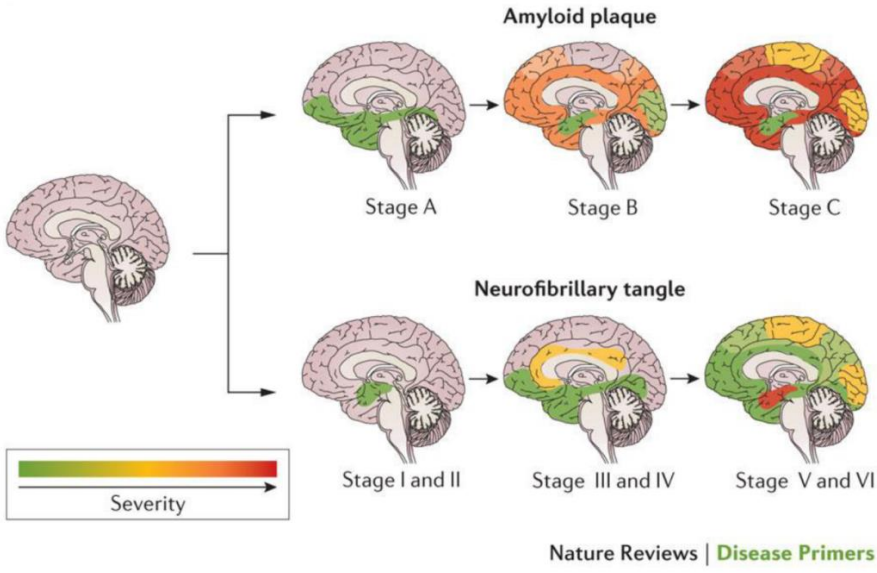

FIGURE 1. PATHOLOGICAL PROGRESSION OF AMYLOID PLAQUES AND NEUROFIBRILLARY TANGLES (ADAPTED FROM MASTERS ET AL., 2015)

Rare mutations in three genes involved in the aggregation of Aβ42 have been implicated in familial disease: *APP*, *PSEN1*, and *PSEN2* (16-18). The penetrance of these mutations is extremely high, and they have mostly an autosomal dominant inheritance. All of the mutations lead to an increase of relative levels of Aβ42 peptide and to its aggregation. Usually, these mutations cause the beginning of the disease in the fourth or fifth decade of life (19). Missense mutations of *APP* influence APP processing and/or aggregation, since they are located in or close to the Aβ-coding exons (16 and 17) of *APP*. In some case also microduplication at the *APP* locus on chromosome 21 have been found. Single-nucleotide substitutions represent the most common mutations of *PSEN* genes, but small deletions and insertions have also been described. The proteolytic cleavage of APP by γ-secretase is altered by *PSEN* mutations, leading to an increased $A\beta42/A\beta_{40}$. Probably *PSEN* mutations cause a partial loss-of-function rather than a gain-of-function in *PSEN* (20). *Al*though these mutations represent rare causes of AD, their discovery greatly highlighted the main role of Aβ in the pathogenesis of AD.

Finally, genetic analysis identified *APOE4* as one of the main risk factors for late-onset AD (21), while *APOE2* as protective against the disease (22). By now, it is known that one allele of *APOE4* shifts of 5 years earlier the risk curve for AD, two copies of *APOE4* 10 years earlier, and one copy of the *APOE2* allele of 5 years later (23). Very intriguingly to understand the role of *APOE* allele's role in disease pathogenesis is the finding that all of the loci identified map to pathways involved in immunity, inflammation, cholesterol metabolism, or endosomal vesicle recycling (24). However, genome-wide association study (GWAS) and whole-exome/genome sequencing allowed to identify many other loci, but they have much smaller effect sizes than that of *APOE*, that has an odd ratio of about 4, while other loci is usually between 1.1. and 1.3 (25). Finally, many other genes were found to increase or decrease the risk of AD (26).

1.1.2. Parkinson's disease

Parkinson's disease (PD) is the second common adult-onset neurodegenerative disorder and it is characterized by the progressive loss of a neuronal subtype, notably dopaminergic neurons in *substantia nigra pars compacta* (27). PD is usually characterized by three main symptoms that occur in motor function, i.e., bradykinesia, rigidity, postural instability, and rest tremor. Moreover, many other nonmotor manifestations are recognized in the last years (28). Like other adult-onset neurodegenerative disorders, PD is primarily sporadic, in the absence of any obvious genetic linkage. However, in rare cases, PD is inherited and the phenotype is transmitted either as a recessive or dominant trait (27).

The prevalence of PD is about 0.3% in the general population, with a prevalence of 1.0% in people older than 60 years, and 3.0% in those aged 80 years and older, with incidence rates of PD of about 13 per 100,000 person-years (29, 30). The mean duration of the disease from the first diagnosis to death is usually 15 years, with 60 years as median age of onset (31, 32). Moreover, as the older age, male sex is considered a risk factor to develop PD. In fact, both incidence and prevalence of PD are about 2.0 times higher in men than in women (33, 34). Studies conducted on animals suggest that a neuroprotective role to striatal dopaminergic neurons may is played by estrogen (35).

The discovery of monogenic forms of Parkinson's disease highlighted the contribution of genetics in PD (36). One of the most important genes involved in PD is *SNCA*, which encodes the protein α-synuclein, and it was the first gene to be associated with inherited form of PD (37). The most common mutations dominant and recessive forms of PD are respectively mutations in *LRRK2* and *Parkin* (38). In the last year it was found that the greatest genetic risk factor for developing PD is mutations in the *GBA* gene, which encodes for the β-glucocerebrosidase protein, which is the lysosomal enzyme deficient in Gaucher disease (39). An odds ratio greater than 5 for any GBA mutation in PD patients resulted from

a large multicentre study (40). Advances in genomics and bioinformatics have discovered throughout the human genome up to 500,000 variants and polymorphisms associated to PD (Table II) (41).

Gene	Protein	Inheritance
SNCA	α-synuclein	AD
LRRK2	Leucine-rich repeat kinase 2	AD
VPS35	Vacuolar protein sorting 35	AD
EIF4G1	Eukaryotic translation initiation factor 4-γ 1	AD
DNAJC13	Receptor-mediated endocytosis 8 (REM-8)	AD
CHCHD2	Coiled-coil-helix-coiled-coil-helix domain containing 2	AD
Parkin	Parkin	AR
PINK1	PTEN-induced putative kinase 1	AR
DJ-1	DJ-1	AR

TABLE II. GENES INVOLVED IN PD. AD: AUTOSOMAL DOMINANT, AR: AUTOSOMAL RECESSIVE (41)

Epidemiological findings, pathological observations, and genetic discoveries helped to understand the pathogenesis of PD. For example, important molecular pathways of both familial and sporadic forms have been identified by fitting genes that are associated with the disease (41). In PD pathogenesis seem to be implied cellular pathways involved in the protein homeostatsis, called also proteostasis, such as abnormal protein aggregation, intracellular protein and membrane trafficking, impairments of the ubiquitin-proteasome and lysosome-autophagy systems (Fig. 2). Moreover, in PD patients seems to be altered synaptic structures and also mitochondrial dysfunction has been found. For example, the impairment of mitochondria has been used to develop a toxic model of the disease, e.g., 6-hydroxy-dopamine (6-OHDA) and 1-methyl-4-phenyl-1,2,3,6-tetrahydropyridine (MPTP) (42) (Fig.2).

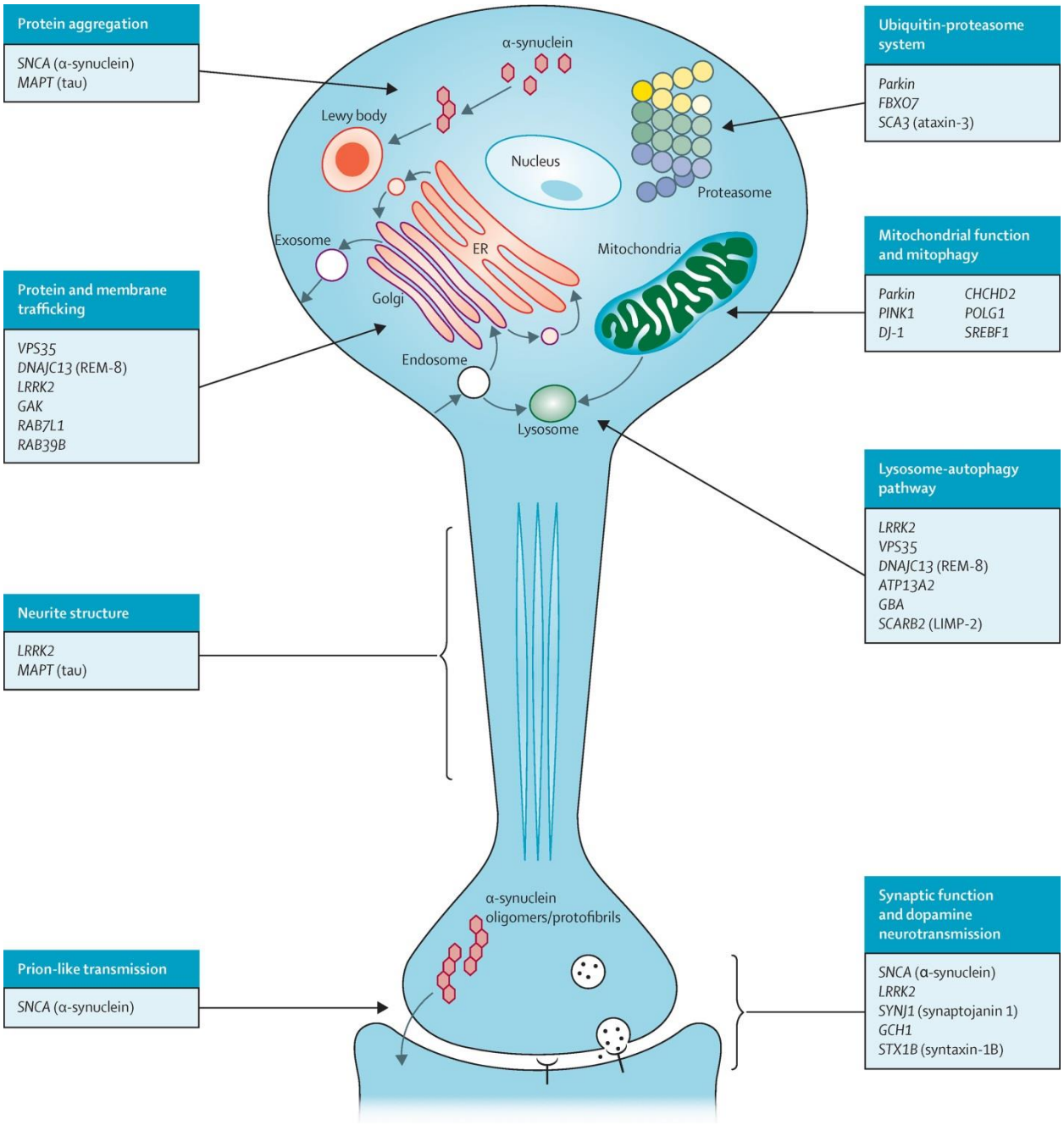

FIGURE 2. IMPAIRMENT OF SEVERAL CELLULAR PATHWAYS INVOLVED IN THE PATHOGENESIS OF PD (41)

The Braak's hypothesis on PD suggests that pathological process spreads in a pattern from one susceptible brain region to the next. He hypothesised that the process begins peripherally, e.g., nasal or gastric route, and spreads between neurons trans-synaptically (43, 44). For example, PD patients who received transplant of embryonic neurons showed

inclusions in the grafted cells, suggesting a prion-like transmission of α-synuclein between neurons (45). Neuroinflammation is a feature of many neurodegenerative diseases, but it still unknown if it promotes or protects from neurodegeneration. GWAS data identified a polymorphism within the human leucocyte antigen region that improves the risk of developing PD, suggesting the immune-related susceptibility (46). Moreover, an epidemiological study showed reduced risk of developing the disease using anti-inflammatory drugs, specifically non-steroidal anti-inflammatory drugs, indicating that inflammation might promotes the pathogenesis (36). Finally, evidences, provided by the use of calcium channel blockers and elevated concentration of serum urate, suggested the role of oxidative stress in the pathogenesis of PD, although the mechanistic details have yet to be elucidated (36, 41).

1.1.3. Amytrophic Lateral Sclerosis

ALS is the most common neurodegenerative disease that leads to the degeneration of motor neurons, specifically the loss of both of upper and lower motor neurons in the cortex, brainstem and spinal cord. The main symptoms of ALS are weakness of limb, bulbar, and respiratory muscles. Usually, patients die within 3-5 years from the diagnosis, mainly for respiratory failure (47).

The disease was described fby Jean-Martin Charcot as "sclérose latérale amyotrophique" in 1869 (48), since glial cells replace degenerated motor neurons, causing the hardening of the lateral cortico-spinal tract (sclérose latérale), while “amyotrophique” refers to the progressive degeneration of muscles (49).

As AD and PD, also ALS can occur in both sporadic (90-95%) and familial (5-10%) forms. Clinically there are no differences between the two forms.

The incidence of ALS is about 2 per 100,000 person-years in Europe. Peak age at onset is 58-63 years for sALS and 47-52 years for fALS (50). In some case (5%) ALS appears

as juvenile onset disease, when it is diagnosed before the age of 30 years (51). There is a slight excess of males affected by sporadic forms more than females, with a M:F ratio about 1.5:1 (52).

When family pedigrees have at least two ALS cases, the disease is considered as familial form. *SOD1* was the first causative gene linked to ALS in 1993 and it codes for a Cu/Zn enzyme that catalyses the reaction that changes toxic O_2^- into O_2 and H_2O_2, (53). More than 150 mutations have been described over the last two decades and in almost all cases the inheritance is autosomal dominant (54). Actually, *SOD1* mutations explain about for 12% of fALS cases and around 1% of sALS (55). Mutation in *TARDBP* was found for the first time in 2006 thanks to presence of cytoplasmic ubiquitin-positive inclusions of TDP-43, encoded by the gene, seen in ALS (56). Usually mutations are found in exon 6 within the glycine-rich C-terminal region involved in protein–protein interactions. *TARDBP* mutations account for 4% of fALS and <1% of SALS worldwide and, as *SOD1*, no phenotypic correlations can be drawn for TARDBP (57). Shortly after identification of the *TARDBP* gene, also *FUS/TLS* gene was linked to ALS and the protein coded is involved in DNA/RNA machinery, as *TARDBP* (58). Mutations in this gene explain about 4% of fALS but are extremely rare in sALS cases and usually are located in exon 13 of the gene and in the C-terminal of the protein, leading to aberrant cytoplasmic distribution of the protein (59-61). Finally, mutations on *VCP* were found in 1-2% of fALS cases and rarely in sALS. Then gene encodes for a protein that seems to play an important role in the maturation of ubiquitin-containing autophagosomes (62). However, the most common gene found mutated in ALS is *C9ORF72*, notably the expansion of the GGGGCC hexanucleotide. The pathophysiology in C9orf72-linked patients is still unknown but probably it is due to the of aggregation of RNA-binding proteins in G4C2 transcripts enconded by the expansion (63). Finally, other genes seem to be linked to ALS, such as VAPB, ANG, and FIG4 (Table III) (57).

Gene	Protein	Inheritance
SOD1	Superoxide dismutase 1	AD, AR
TARDBP	TAR DNA-binding protein 43	AD
FUS/TLS	Fusion malignant liposarcoma	AD, AR
C9ORF72	Chromosome 9 open reading frame 72	AD
VAPB	Vesicle-associated membrane protein B	AD
ANG	Angiogenin	AD
FIG4	FIG4 phosphoinositide 5-phosphatase	AD
OPTN	Optineurin	AD, AR
ATXN2	Ataxin-2	AD
VCP	Valosin-containing protein	AD
UBQLN2	Ubiquilin 2	X-linked

TABLE III. GENES INVOLVED IN ALS (57)

As suggested by genetic evidences and many pathological hallmarks, there are several pathogenic cellular mechanisms that might cause ALS, but the exact pathway is still uncertain (64). In degenerating motor neurons of ALS patients there is the swelling of not only the perikarya but also of proximal axons (65). Also Bunina bodies, that are eosinophilic intracytoplasmic inclusions, spheroids (Lewy-body like) and strands (skein-like) of ubiquitinated materials were found in motor neurons of ALS patients (66, 67). The presence of reactive gliosis usually indicates that neuroinflammation and also that non-neuronal cells concurs in the pathogenesis of the disease. Moreover, excitotoxicity (cause by glutamate), oxidative stress, mitochondrial dysfunction, impaired axonal transport, neurofilament aggregation, protein aggregation and deficits in neurotrophic factors as well as dysfunction of signalling pathways are the principal mechanisms that cause ALS. In Fig. 3 is clear that every pathological mechanism can play a major or a minor role in the degeneration of ALS patients and many pathways may concur in the pathogenesis of the disease (68).

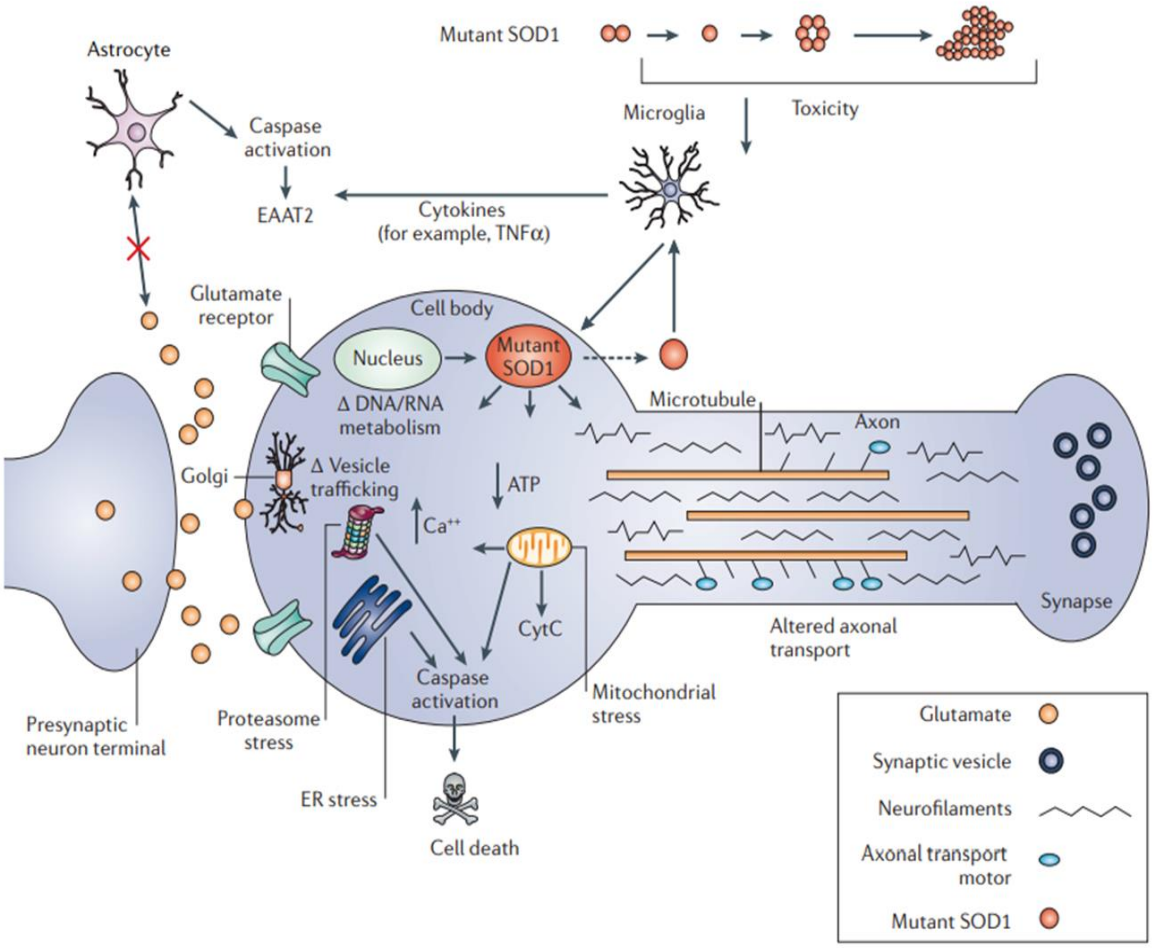

FIGURE 3. FIGURE 2: CELLULAR MECHANISMS IN THE PATHOGENESIS OF ALS (68)

1.1.4. Huntington disease

HD is a degenerative disorder that affects mainly the central nervous system, notably the striatum, but also the cerebral cortex and other subcortical structures. The disease is recognized by several symptoms, such as progressive dementia with chorea, that means brief and irregular movements, athetosis, impaired coordination, abnormal speech, swallowing difficulties and other neuropsychiatric symptoms, such as depression (69). One of the most influential descriptions of HD was made by George Huntington in 1872, and the disease has since borne his name. He examined the medical histories of several generations of a particular family that exhibits similar symptoms, recognizing that their diseases were linked (70).

The average prevalence rate among Caucasian populations is about 10 per 100,000 people (71). Some evidences suggested that probably different haplotypes between East Asians and Europeans may be associated with differing prevalence of the disease (72).

HD is a single-gene disorder with autosomal dominant transmission, meaning that the presence of the mutation in one allele leads to the disease. The mutation is an expansion of the CAG triplet on the exon 1 of the Huntingtin gene (*HTT*). During translation, the expansion leads to the presence of a polyglutamine (polyQ) stretch at the N-terminus of Huntingtin protein (73).

In healthy people the wild-type gene carries from 10 to 35 repeats, with a mean value of 18 CAG repeats among the population (74). The mutation is considered fully penetrant when the gene has 40 or more repeats, while between 36 and 39 repeats the penetrance is reduced, that means that carriers may develop or not HD symptoms. Finally, *HTT* gene with 27–35 CAG repeats is usually classified as an "intermediate allele" (75).

CAG repeat is intrinsically instable during meiosis, leading to expansions, but sometimes contractions, in repeat length, successively inherited by future generations (76). The age of onset is influenced by the length of CAG repetition; in particular a longer length correlates with earlier age of onset, leading to symptoms development at progressively younger ages down the family tree. Moreover, since spermatogenesis and oogenesis are different processes, it is now clear that the anticipation of onset occurs more likely when transmission derives from the paternal bloodline (77). For example, rare cases with CAG repeat length is above 55, HD appears as leading to Juvenile HD (JHD), since the age of onset is less than 20 years old (78).

The correct diagnosis of the disease is helped when the family history is detailed and clear. However, about 8% of patients have no family history. In fact, de novo may derive from intermediate length alleles, leading to the so-called sporadic cases. Obviously, some sporadic cases may be due to non-paternity, misdiagnosis in prior generations, or when family

members died for other causes before the development of characteristic neurological symptoms of HD, hiding the presence of the mutation (79).

The gene *HTT* codes for Huntingtin, which is a large 350 kDa protein comprised of multiple repeated units of 50 amino acids, termed HEAT repeats, which assemble into a superhelical structure with a hydrophobic core. The mutant protein contains an expanded polyQ stretch from residue 18, triggering a pathogenic cascade, with both cell autonomous and non-cell autonomous mechanisms involved (Fig. 4) (80).

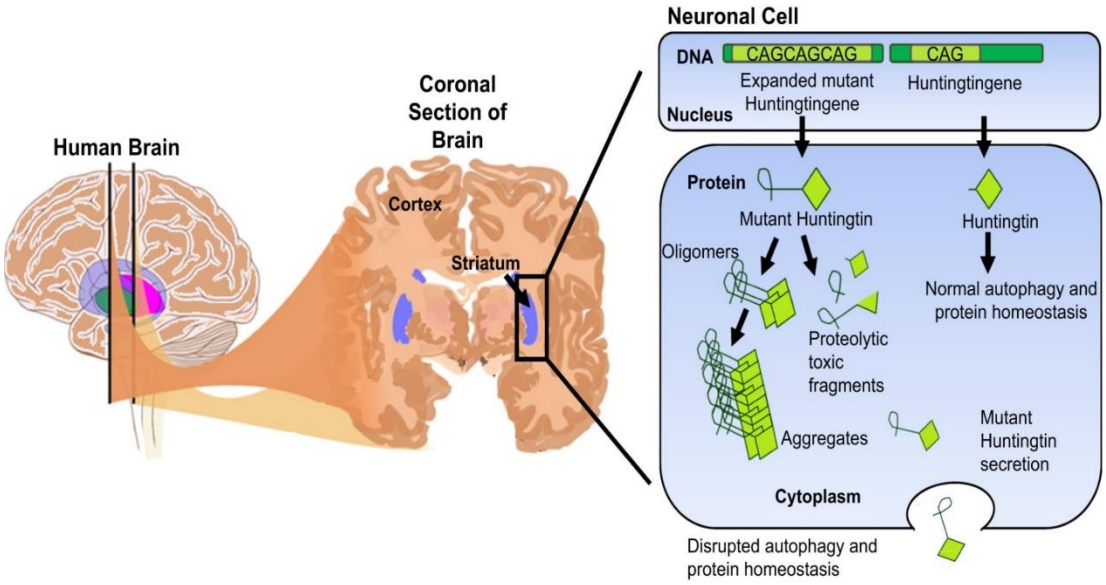

FIGURE 4. PATHOLOGICAL MECHANISMS INVOLVED IN HD (81)

The "toxic fragment hypothesis" suggests that mutant HTT is cleaved into toxic N-terminal fragments containing the expanded polyQ, contributing to cell death because of accumulation (82). The proteolytic toxic fragments can generate intranuclear inclusions of mutant HTT (mHTT), an important feature of HD. In neurons, inclusions can accumulate also in the cytoplasm, dendrites and axon terminals. These inclusions are not homogeneous but are composed of different forms of mHTT (83). Moreover, their role in HD has not yet been established (84). HTT can have several post-translational modifications at diferent sites by phosphorylation, SUMOylation, acetylation, ubiquitination and palmitoylation, and obviously

all these modifications can have an effect on mHTT pathogenicity (85). Microarray studies showed that transcriptional pathways are dysregulated before symptom onset, and usually affects a large number of several transcription factors and regulatory DNA target sequences (Hodges et al., 2006). Another evidence that support a dysregulation in epigenetics of HD patients, is the inhibition of the histone acetyltransferase activity by mHTT, leading to the condensation of chromatin and, thus, a downregulation of gene transcription (86). Interestingly, microglial activation, leading to inflammatory response, has been demonstrated in HD patients, in manifest but also in premanifest disease (87, 88). In particular, seems that microglia expriming mHTT have an increased expression of pro-inflammatory factors (89). Moreover, pro-inflammatory cytokines were found in blood samples of manifest and premanifest HD patients, suggesting an inflammatory response also in a peripheral tissue (90). As seen in other ND, also mHTT was shown to spread from HD mouse model neurons to wild-type human neurons and this was blocked by botulinum neurotoxins, suggesting a possible role of synaptic machinery for the spreading (91). Furthermore, HD patients who have received neural stem cell transplantation as experimental treatment have revealed during the autopsy the presence of HTT inclusions in the grafted donor cells (92). Since HTT regulates vesicular transport and recycling thanks to the interactions with other proteins, it was seen that the expression of mHTT deregulate this transport (93). Since mitochondria are transported on axons to reach the synapses, mHTT affects also this translocation, affecting the normal mitochondrial function. Moreover, it was seen that calcium homeostasis is impaired in HD mitochondria, and transcription of genes needed for the correct functioning of this organelle is largely affected, leading to dysregulation of mitochondrial respiration chain (94). Moreover, mitochondrial DNA mutations have also been found increased in neural tissue of HD patients (95). It was found that excitoxicity can play a pivotal role in HD. For example, the injection of an NMDA receptor agonist into the brain of mouse was found to be a good model to recapitulate several aspects of the disease (96). Moreover, it is now clear that

impairment of the signalling of glutamate occurs through changes in glutamate release, increase in activity of glutamate receptors, decreased levels of transporters, and reduced glutamate uptake (73). Finally, a decrease expression of potassium channels in mHTT astrocytes seems to increase excitability of striatum neurons (97). Another pathway that results altered in HD is the one for degradation of misfolded proteins. Impairment of both the ubiqutine-proteasome system and autophagy occurs in HD (73). Finally, it is now clear that when the pathways necessary for the DNA repair is impaired, CAG repeat can expand in germline cells (as already described) but also in somatic cells, as in striatum neurons, leading to the development of the disease (98). In conclusion, all the pathways described above lead to the degeneration of striatum neurons, causing HD.

1.1.5. Neurodegenerative diseases' modelling

In recent years the knowledge about these diseases has greatly improved, such as early diagnostic with advances in medical imaging (99) and the discovery of specific biomarkers (100). Moreover, many molecular pathways involved in the pathogenesis of neurodegeneration have been discovered. In contrast, the possibility to prevent, treat or simply slowdown the degeneration is a hard goal. Since many investigations on NDDs cannot be performed on human being because of the inaccessibility of brain biopsy, it is necessary to use model that can recapitulate at least some features of the diseases. Thanks to the advances in molecular genetics over the last three decades allowed the modelling neurodegeneration in animals in order to carry out experiments. The most used animal model is represented by transgenic mice (101), but many other species are used, e.g., *Brachydanio rero*, *Caenorhaditis elegans*, and *Drosophila melanogaster* (102).

As yet sentenced, the great development of molecular biology and the improvement of molecular techniques deeply transformed the way researchers normally approach all fields of

biological research. Thus, the major technological breakthroughs permitted the diversification of experimental model organisms.

The first technology that has been widely used is the recombinant DNA cloning which allows the splicing DNA fragments of any origin together with plasmids and vectors, in order to introduce and amplify it in a recipient bacterial host. The technique permitted for the first time to isolate, manipulate, modify genes, and eventually determine their complete nucleotide sequence using the DNA sequencing methods, which became soon available (102). The main consequence has been the rapid increase in the knowledge about genes and the investigation of regulatory mechanisms of their expression, identifying promoters and tissue-specific enhancer elements and opening the possibility to control the expression of cloned genes (102).

The second important discovery in molecular techniques was the development of the permanent integration of exogenous genetic material into the genome of a recipient host and the transmission to its offspring (103). Since the efficiency is weak in many organisms, this approach remained limited until recently and was applied to the mouse in the early 1980s and shortly after to *Drosophila* (104).

In recent years, the development of a site-directed gene editing in mouse embryonic stem cells allowed the generation of a new transgenesis approach, opening the possibility to inactivate or "knock out" a target gene which can be interesting for modelling ND; moreover, the technology allows to replace its coding sequence by "knocking in" the mutated form of the gene or a different gene (Fig. 5) (105). Thus, has been possible to generate numerous animal models of AD, PD, ALS and HD, providing major insights into the cellular and molecular basis of the degeneration processes (101).

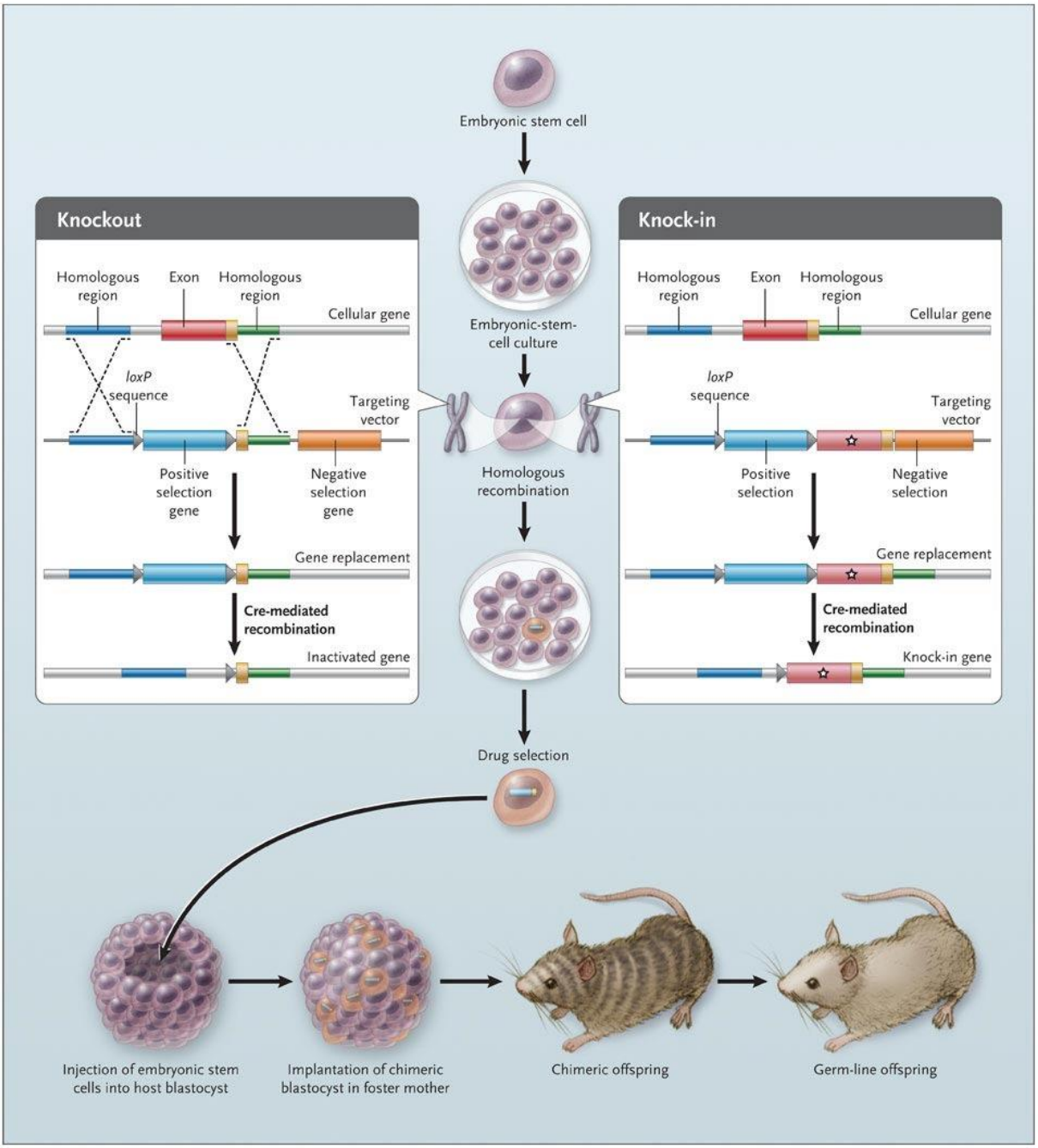

FIGURE 5. GENERATION OF KNOCKOUT AND KNOCK-IN MOUSE GERM-LINE (106)

Finally, the third major advance was the great advance in DNA sequencing and bioinformatics technologies, leading to the development of genomics, giving access without any limitation to whole genome sequences of all living organisms (102). This technology made possible GWAS in order to uncover in human populations some genetic variations

associated with NDDs, leading to the identification of new candidate genes to be investigated for their role in the onset and progression of the disease (107).

More recently, advances in stem cell technology allowed researchers to establish human induced pluripotent stem cell (hiPSC) lines from patients (108), and directly differentiate these cells into neuronal and glial cells. The hope is that iPSCs lines will permit to model more efficiently and in a more realistic way the main features of NDDs at a cellular level, providing an opportunity not only to study disease mechanisms, but also to test therapeutic strategies in patient-specific cell type most affected in these diseases. Since these cells can be maintained and expanded in culture, iPSCs provide for experimentation an unlimited source of disease-relevant human cells. Actually, researchers have established dozens of lines from patients with NDDs, and have modified and expanded differentiation protocols in order to study the cell type usually affected by the disease (109).

1.2. Induced Pluripotent Stem Cells in NDDs' study

One of the most interesting areas of cell biology is considered stem cell research, probably because they have represented in the last years a promising tool for both disease mechanisms studies and regenerative biology. In particular, stem cells are considered an essential tool in order to study NDDs, because of the lack of a realistic cellular model of these disorders.

Embryonic stem cells (ESCs) are the first type of stem cells that were used. ESCs derive from the inner cell mass of blastocysts, and they are considered pluripotent cells because they have the ability to proliferate indefinitely and the capability to differentiate into cells of all three germ layers: ectoderm, mesoderm and endoderm (110, 111). Human ESCs were isolated for the first time in 1998 and since their first appearance they gained a high

importance as a potential treatment of a variety of NDDs (112). However, the main issue in the use of ESCs is the fact that their extraction arises sharp ethical controversies, since they are derived from human embryos, killing it. Moreover, it was seen that their transplantation in patients could present serious risks, such as the possibility of rejection or the generation of tumours (113).

In order to avoid and overcome the ethical issues involved in the establishment of ESCs, some alternative approaches have been developed and are now available. These methodologies allow to generate pluripotent stem cell lines starting from differentiated adult somatic tissue. In particular in 2006, a landmark discovery was published by the Yamanaka group, inducing the expression of only four pluripotency-associated transcription factors, Oct3/4, Sox2, c-Myc, and Klf4 in mouse fibroblast cells (114). The technology resulted in the generation of mouse ESC-like cells line, called induced pluripotent stem cells (iPSCs), and after just one year, two research groups independently reported the generation of iPSCs from human fibroblasts (108, 115).

1.2.1. iPSCs

Human iPSC technology allowed the development of an exciting new era not only for stem cell biology and regenerative medicine, but also for disease modelling and drug discovery. Soon after the establishment of human iPSCs lines, they were rapidly applied to develop human 'disease in a dish' models and used for drug testing to investigate efficacy and toxicity.

Starting from their discovery, iPSCs technology has evolved rapidly. One of the first issues was represented by the introduction of reprogramming factors using integrating viral vectors, rising concerns about the potential clinical application of iPSCs, because of the

possible insertional mutagenesis caused by the integration of transgenes into the genome of host cells (116).

In order to establish iPSCs lines with a clinical application, several non-integrating methods have been developed, avoiding the risk of genetic alterations associated with retroviral and lentiviral transduction (117). These non-integrating methods include reprogramming using microRNAs (118), adenovirus (119), Sendai virus (120), PiggyBac transposons (121), episomal DNAs (122), recombinant proteins (123), minicircles (124), and synthetically modified mRNAs (125).

Some of the previously reported methods are relatively simply and have high efficiency, providing integration-free technologies, such as episomal DNAs, synthetic mRNAs, and Sendai virus. Thus, the use of non-integrating viruses could avoid genomic insertions, reducing associated risks when human iPSCs are used for clinical applications (126).

As expected, a patient-specific approach is now becoming increasingly popular, because drugs can be potentially tested on the desired cell type derived from the patient (127). The advantages of such cells are human derivation, easy accessibility, expandability, ability to differentiate into almost any cell types, lack of ethical issues, and more importantly the potential to develop personalized medicine using patient-specific iPSCs. Moreover, the CRISPR–Cas9 system, one of the most advanced gene editing technologies, enabled the rapid generation of genetically defined human iPSC-based disease models (127).

Thus, it is now clear that human iPSC technology represents a great promise for disease modelling, drug discovery and stem cell-based therapy, and the revolution that they carried it is only beginning in the few last years (127).

1.2.2. iPSCs in Disease Modelling

The discovery of new therapeutic strategies highly depends on the identification of the pathological mechanisms that underlie NDDs. Valuable tools for modelling such disorders are represented by animal models, providing a way to identify many pathological in specific cell types using an *in vivo* setting. Furthermore, with animal models it is possible to compare *in vitro* iPSC-based models with *in vivo* models, providing a better understanding of the advantages and the limitations of iPSCs (127).

The main problem in the use of animal models is the lack of the complete recapitulation of all features of NDDs, mainly due to the substantial differences between diverse species. For example, many transgenic mouse models have been developed for AD, but none has recapitulated all the features of the human disorders, including considerable neurons loss (128). Thus, it is now clear that there is an urgent need to develop a realistic human disease modelling platform, in order to help studies that use animal models for biomedical research.

The most useful method in order to model human NDDs is the use of primary patient-derived cells, but in neural tissues they have critical limitations, such as the lack of expandable source, the hard accessibility. Moreover, NDDs are characterized by the loss of neural cells, and often patients lose the majority of neurons before the diagnosis of a NDD. Therefore, human iPSCs derived from patients are an attractive alternative, because they derive from easily accessible cell types, such as skin fibroblasts and blood cells. Furthermore, because of their intrinsic properties of self-renewal, iPSCs could provide large quantities of disease-relevant cells type. Moreover, iPSCs can potentially be differentiated into any variety of different cell types that were previously inaccessible, such as neurons, allowing to study such cells more easily than before. Finally, they could allow personalized disease modelling approach, because they derive from the relevant patients themselves.

As ESCs, also iPSCs express human pluripotent factors and specific surface markers, exhibiting the developmental potential to differentiate into three germ layers (115). A minor problem is represented by the possible presence of a residual epigenetic memory of somatic cells (129), which may affect the differentiation (130). Although this epigenetic memory issue can affect the effectiveness, similar phenotypes between ESCs and iPSCs have been reported during disease modelling, supporting the advantages of using patient-derived iPSCs (130).

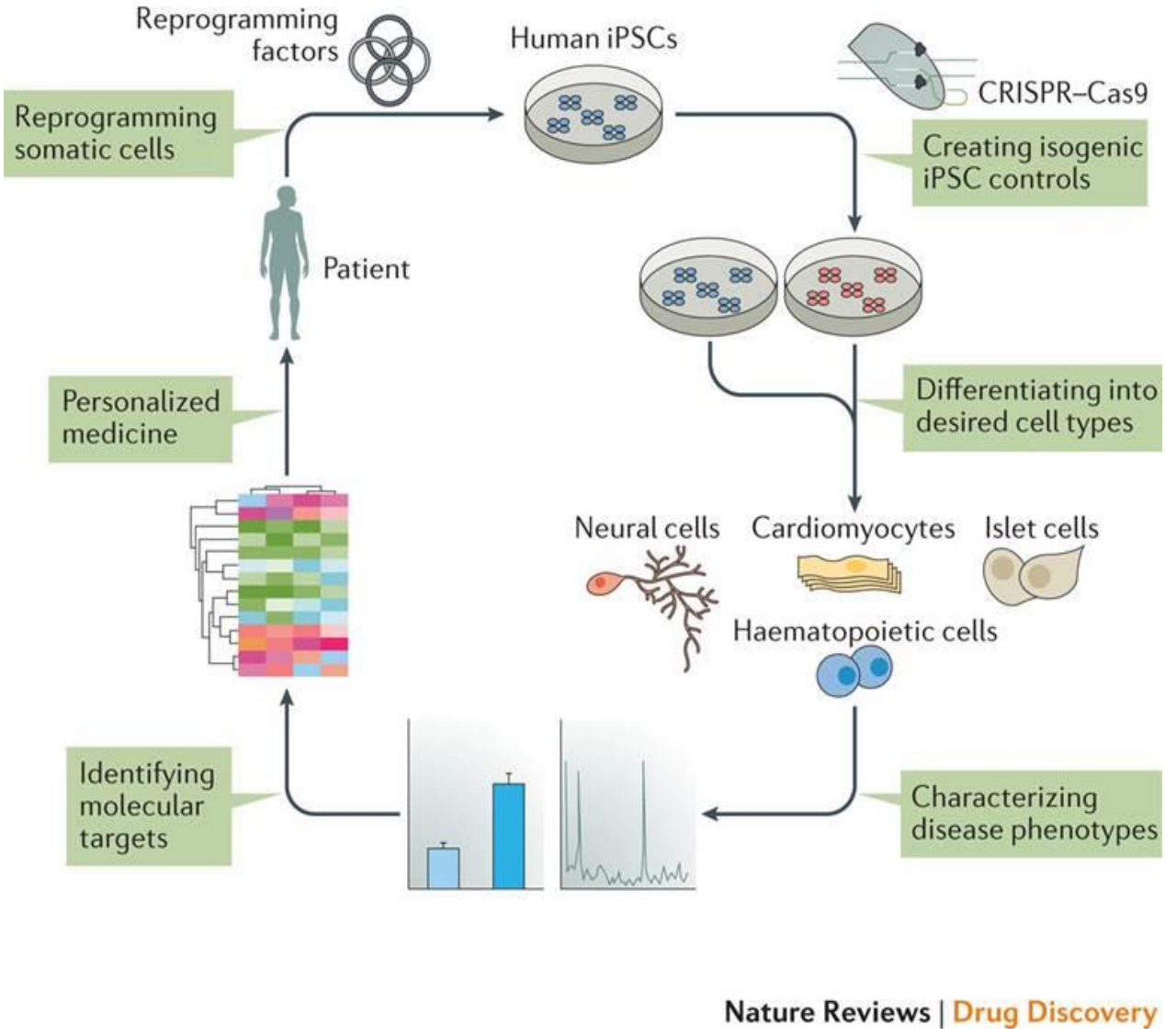

FIGURE 6. POTENTIALITY OF IPSCS IN MODELLING NDDS WITH A PERSONALIZED MEDICINE APPROACH (127)

Disease modelling using human iPSCs begins with the extraction of patient's somatic cells and the following reprogramming using Yamanaka factors in order to obtain iPSCs cell lines (Fig. 6). In the first studies of iPSC-based disease modelling, iPSCs derived from healthy individuals were used as controls for patient-derived iPSCs. The main problem is that iPSCs exhibit line-to-line variations, complicating data interpretation in order to distinguish the true disease-relevant phenotypes. Thanks to the development of genome editing technologies the introduction of genetic changes into iPSCs (e.g., correction of disease-causing gene mutations) is now possible. Obviously, this approach allows the generation of an isogenic iPSCS line, with the disease-causing mutation as sole variable. Genome editing ensures a reliable identification of the pathogenesis of NDDs, avoiding the mistakes that can be made with disparities in genetic background (131). Many site-specific nucleases, including zinc-finger nucleases (132), transcription activator-like effector nucleases (133) and the CRISPR–Cas9 system (134), has been used for iPSCs-based disease modelling. Notably, the CRISPR–Cas9 technology has gained much attention thanks to its simplicity in design and ease of use.

Another challenging issue in modelling NDDs is represented by the fetal-like properties of iPSCs, suggesting that they couldn't be used for late-onset disease (135). However, induced cellular ageing has been used in order to successfully model such diseases (136, 137). For example, cells stressors like MG-132 can be used to induce ageing in iPSCs-derived differentiated neurons (138). The induction of cellular ageing can be achieved also by ectopically express gene products, such as progerin, inducing premature ageing (137). Moreover, recent studies have suggested that cellular maturation and ageing are distinct events ((135, 139). Finally, a direct reprogramming approach, thus converting human fibroblasts into other lineage-specific cells, such as neurons, seems to not erase cellular ageing, offering a realistic cellular model to study late-onset disorders (140).

Sporadic forms of NDDs can be also studied using iPSCs and it is very important because the majority of patients with many have sporadic forms of the disease. Modelling sporadic NDDs is usually more difficult because in such disorder the phenotypic changes are often thought to be caused by multiple genetic risk variants and by environmental factors (127). The main issue is represented by the by line-to-line variations in genetic background that cannot be corrected by gene editing technologies. Thus, the key question for iPSC-based modelling of sporadic NDDs is whether is possible to generate isogenic cell lines, which are different only at relevant risk variants. Obviously, the generation of isogenic cell lines is easier when risk variants are well known. For example, isogenic iPSC lines that differ at a Parkinson disease-associated risk variant were generated, developing a robust strategy that can be used also with other diseases (141).

1.2.3. iPSC-based drug discovery

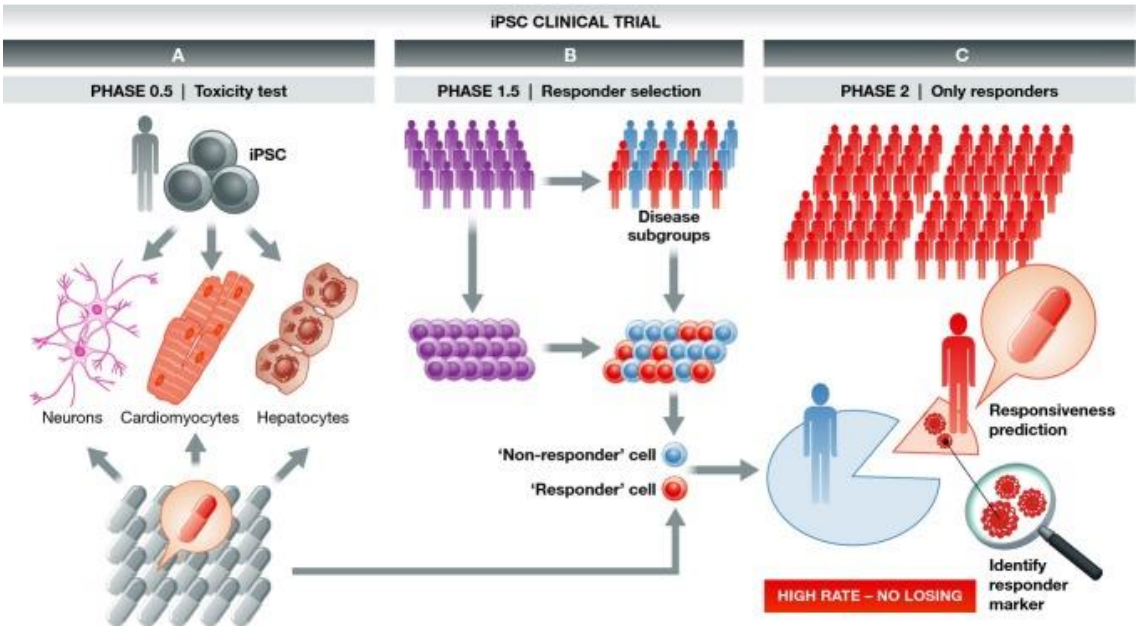

FIGURE 7. DRUG SCREENING APPROACH USING IPSCS AS DISEASE MODEL (142)

Usually, drug screening is based on disease relevant targets, but the low success rates of such approach have led to a phenotypic screening, especially in NDDs field (143). The scalability of iPSC production, which facilitates drug testing, is one of the advantages in using such cells in drug screening. As for disease modeling, the pluripotency of iPSCs allows the possibility to have disease-relevant cell types, which is one of the main issues in neural tissue drug screening (Fig. 7) (142). Patient-derived iPSC models made possible to recapitulate disease phenotypes, which can be confirmed to be used as a good readout by a gene editing approach and by validating it in patient samples or animal models (Fig. 7) (144). The presence of the specific cell type is fundamental in order to have the most reliable result, so it is necessary a high purity on a large scale, using for example purification with specific cell-surface markers (145), cell-specific promoters (146) and microRNAs (147).

In the field of neurodegeneration, Bright and colleagues worked on a patient-derived iPSC model of AD. In this work, the authors found extracellular Tau in the conditioned medium of cortical neurons derived from an iPSCs line of a patient with AD and consequently they developed an antibody-based therapeutic strategy to remove Tau (148). The same group performed disease modeling and drug screening using iPSCs derived from patients with sALS. In this case, they found de novo aggregation of TDP43 in iPSCs-derived motor neurons of patients; they then used as readout for a high-content drug screen such aggregation to investigate compounds that could reduce TDP43 aggregation (149).

A big problem in the use of iPSCs is the time-consuming protocols of reprogramming and differentiation. Therefore, other methods were investigated in order to develop a faster and more stable technology, resulting in higher maturity and purity. For example, the drug screening was performed using cells derived from direct conversion (150, 151). This approach forces somatic cells to express cell-specific transcription factors, in order to directly convert it to another somatic cell state, avoiding the reprogramming through the iPSC state (140). As previously suggested, another advantage of the direct conversion is that, in NDDs field,

neurons reflect important aspects of cellular ageing (140). On the contrary, the lack of a renewable source of cells may not be useful for large-scale drug screening.

As disease modeling, an important point in such research studies using iPSCs is the presence of a reliable control group. For monogenetic disorders, the gene correction approach can be used to validate results of drug screening (142). In case of sporadic form of the disease, it is difficult to establish the nature of the control group.

Obviously, drug screening approach with iPSCs can be used also in drug repositioning, in which drugs already approved for specific diseases are tested to find new applications in other diseases (127). An interesting example is represented by the anti-epileptic drug called ezogabine, which has been demonstrated efficacy also in motor neurons derived from an iPSC line of ALS patients, undergoing now into a clinical trial (152). In this study, authors tested the efficacy of ezogabine on iPSCs-derived motor neurons derived from patients with ALS harboring mutations SOD1, C9ORF72 and FUS genes (152). Moreover, they demonstrated that such motor neurons initially exhibit a hyper-excitable state followed by a decrease in excitability, suggesting that early treatment with ezogabine may be useful for ALS patients (153). Previously described works, it was observed a similar drug response in patients with different phenotypes, enabling the generalization across ALS types. In fact, the use of iPSCs derived from multiple genetic forms of a NDD allows testing drug responsiveness in a broad patient population.

One of the problems in the development of new drugs is the fact that it is enormously costly. In particular, the high costs are mostly due of failures during the late-stage clinical trials, because of toxic side effects (154, 155). Thus, it is obvious that many new candidate drugs can present unpredicted adverse effects, notably concerning with cardiac and liver toxicity. Thus, the development of new approaches in order to test not only the therapeutic effect on diseases, but also the toxicity on particular cell types, enabling a more effective selection of candidates that are less likely to fail in late-stage trials.

Regarding the neural tissue, Schwartz and colleagues have proposed a cellular platform that can test side effects of several drugs using pluripotent stem cells. Notably, they analyzed gene expression alterations of cells in various cell types, such as neural cells, mesenchymal stem cells and vascular endothelial cells (156).

1.2.4. IPSCs in Alzheimer's disease

Many groups used and performed several studies on in vitro models with neural and non-neural cells iPSCs-derived. For examples, Armijo and colleagues hypothesized that iPSC-derived neurons of AD patients might be more susceptible to the treatment of Aβ oligomers compared with cells derived from healthy individuals. In order to test this hypothesis, they analyzed the toxic effects of Aβ42 oligomers using neuronal cultures derived from iPSCs sAD, fAD (with PSEN A246E mutation) and healthy individual as control. The groups found that only neurons derived from fAD iPSCs present a higher susceptibility to the toxic effect of Aβ42 oligomers, while neurons originated from healthy and sAD iPSCs were comparable (157). The authors suggested that fAD neurons might have some intrinsic features that make them more sensitive to the toxic effect of Aβ42, which usually can be in an AD brain. This study highlighted the importance of using an in vitro model using patients' cells in to find new pathological pathways (157).

Another group induced typical fAD mutations, i.e., APP and PSEN1 mutations, by genome editing mutagenesis, in order to generate isogenic iPSC-derived human neurons. This work suggested that amyloid-independent cellular trafficking and transport phenotypes could participate to the development of fAD, in particular leading to increased levels of APP in the soma and decreased levels in the axons (158). Such trans-localization of APP is followed by the concurrent accumulation in the neuronal soma of another protein involved in endosomal trafficking, Rab 11, and its reduction in axons, suggesting the interplay between Rab 11 and

APP. Moreover, the knockdown of Rab11 leads to decrease level of APP axonal density. The study suggests that a common early defect among the two different mutations in APP and PSEN1 is an impairment of a key neuron-specific traffic pathway, the soma-to-axon transcytosis, maybe caused by defects in the recycling endosome (158).

In the previous case, it is very interesting to notice how genome editing tools can be useful in order to induce disease-specific mutations, leading to a realistic and reliable cellular model of the disease. On the contrary, genome editing technology could be used also for mutation's correction, generating the so-called isogenic control. For example, Pires and colleagues reported an A79V-iPSC line in combination with its isogenic control, named A79V-GC-iPSCs, generated using CRISPR/cas9 system. One of the main issues in gene correction is to investigate some side effects caused by such tool, thus firstly the authors validate the nucleotide correction by sequencing. Moreover, they checked also gene-integrity confirming that there was no alteration in the DNA sequence surrounding the mutation (159). Furthermore, the pluripotency of the corrected line was tested by immunocytochemical analysis of the staminality markers, i.e.: OCT4, NANOG, SSEA3, SSEA4, TRA-1-60 and TRA-1-81. Finally, no chromosomal aberrations due to gene correction were found in the isogenic line, performing karyotyping (159).

Finally, also glial cells derived from iPSCs could be very helpful in disease modeling and drug screening. For example, it was found that the generation of mature astroglia cells line from human iPSCs derived from patients with confirmed both familial and sporadic form of AD as well as from a healthy individual. They found that astrocytes derived from AD patients appear with a distorted morphology and cellular phenotype, such cells express the same markers of mature healthy astrocytes (160).

These works suggest that iPSCs-derived neurons from AD patients can be used not only to discover new disease mechanisms, but also to screen new therapeutic drugs and also to find new possible drug targets. Moreover, the authors suggest that, as previously reported,

gene correction is a helpful technology for both generating isogenic controls and inducing AD mutations in healthy controls cell lines. Finally, iPSCs can be also differentiated into non-neural cells, e.g. astrocytes, oligodendrocytes, microglial cells, which in recent years have gained an important role in the study that try to unravel the pathogenesis of several NDDs (161).

1.2.5. IPSCs in Parkinson's disease

Usually iPSCs are differentiated into dopaminergic (DA) neurons to model PD because the disease is characterized by the loss of DA neurons of the *susbtantia nigra* in the midbrain (mDA). For example, mDA neurons derived from patients with either PINK1 or Parkin showed higher levels of α-synuclein expression at both gene and protein levels. Moreover, the PD iPSC-derived mDA neurons seem to have an increased susceptibility to mitochondrial damaged mediated by toxic compounds (162). Furthermore, the authors of this work found mitochondrial abnormalities and a higher level of intracellular DA levels in PD iPSC mDA neurons. These findings highlighted the importance to use the disease-specific neuron for *in vitro* disease modeling (162).

Several evidences suggest that PD is not only a brain disease but could involve other tissues, notably the gastrointestinal one. Thus, Son and colleagues generated iPSC lines carrying a mutation in *LRRK2*, which is involved also in gastrointestinal diseases such as Chron's disease. The group differentiated iPSCs in both neural and intestinal phenotypes, providing the first evidence that mutations in *LRRK2* gene cause changes in gene expression mostly in the intestinal cells (163). This data implies that *LRRK2* mutation might be more involved in the gastrointestinal tissue than in neural tissue (163).

In PD, iPSCs helped also for drug testing. For example, several genetic modifiers were found from screening in a yeast model of α-synuclein toxicity, leading to identification of

early pathogenic phenotypes in patient neurons, e.g., nitrosative stress, accumulation of ER-associated degradation substrates and ER stress (164). Moreover, a small molecule identified with such screen was found to activate the ubiquitin ligase Nedd4, interestingly reversing pathologic phenotypes in cortical neurons differentiated from iPSCs of patients with *SNCA* mutations (164).

Another group wanted to recapitulate the *in vivo* developmental pathway of microglia *in vitro*, exploiting iPSCs technology. In particular, microglia derive from the yolk sac as MYB-independent macrophages, which migrate into the developing brain to differentiate into microglial cells. In their work, Haenseler and colleagues recapitulated the ontogeny of microglia by differentiation of embryonic MYB-independent macrophages derived from PD-iPSC, successively co-cultured with iPSC-derived cortical neurons. They found that co-culture between such cells allows retaining neuronal maturity and functionality for many weeks. As expected, iPSCs-differentiated microglia expressed microglia-specific, developed highly dynamic ramifications, and was phagocytic (165). Moreover, during activation they released several microglia-relevant cytokines. Importantly, co-culture microglia downregulated pathogen-response pathways, upregulated homeostasis, and promoted the expression of pro-inflammatory cytokines. This work, demonstrated the effectiveness of co-cultures between microglia and neurons, suggesting that they are preferable for modeling authentic microglial physiology, which could have an important role in NDDs pathogenesis (165).

Thus, the works previously reported suggest that iPSCs-derived neurons from PD patients can be play a key role in the research of PD pathophysiology and to find new therapeutics' targets. Moreover, iPSCs allow the possibility to have and study non-neuronal cells, such as microglial cells and intestinal cells, helping to unravel the role of immunity response and the gastrointestinal diseases that affect PD patients (161).

1.2.6. IPSCs in amyotrophic lateral sclerosis

Motor neurons derived from iPSCs are the most common neuron type used in ALS modeling. For example, an interesting study shows that oxidative stress and DNA damage are increased in motor neurons derived from iPSCs harboring C9ORF72 expansion. In particular, it was found that poly(GR) binds to mitochondrial ribosomal proteins, impairing mitochondria and leading to increased oxidative stress in human neurons (166). More importantly, the reduction of oxidative stress due to pharmacological treatments partially suppressed these pathogenic effects in human motor neurons, suggesting an interesting new pathogenic mechanism in *C9ORF72*-related ALS (166).

Moreover, the induction of mutation in FUS (P525L) was used to analyze the transcriptome and microRNA. As expected, significant enrichment of pathways previously associated to sporadic ALS was found with the analysis of differentially expressed genes (167). Several microRNAs were found to be deregulated in *FUS* mutant motor neurons. Among these, miR-375 target the neural RNA-binding protein ELAVL4 and other apoptotic factors, which were found unregulated. Thus, the authors suggest that the characterization of transcriptome in motor neurons can contribute to the identification of new pathogenic mechanisms of *FUS*-linked ALS (167).

An interesting approach of iPSCs studies was applied by Qian and colleagues. They transplanted spinal neural progenitors derived from sALS and healthy iPSCs, into the spinal cord of adult mice. After 9 months, they found that such cells differentiated into human astrocytes in large areas of the spinal cord, replacing endogenous astrocytes, and contacting neurons (168). Moreover, mice with sALS cells showed reduced motor neurons number in the host spinal cord, while mice with cells from healthy control did not. The surviving motor neurons in mice with sALS cells showed reduced inputs from inhibitory neurons and disorganized neurofilaments, with aggregation of ubiquitin. Moreover, mice with sALS but

not non-ALS cells showed movement disorder. These data suggested that sALS iPSC-derived astrocytes can cause ALS-like degeneration, providing the evidence that astrocytes can participate to the pathogenesis of ALS (168).

Another study suggesting the role of astrocytes in sALS pathogenesis is represented by the work of Hall and colleagues. They differentiated iPSCs derived from VCP-mutated patients into functional populations of both spinal cord motor neurons and astrocytes, and subsequently they identify ER stress and accumulation of cytoplasmic TDP-43, with secondary oxidative stress, mitochondrial impairment, and synaptic degeneration. Interestingly, thanks to co-culture experiments, the authors found non-cell-autonomous effects of VCP-mutant astrocytes on both control and mutant motor neurons (169).

Genome correction of disease mutations could help to identify new pathological pathways. For example, an upregulation of disease-related pathways was found in patient-derived iPSCs differentiated into motor neurons using deep RNA-sequencing technology. Moreover, the pharmacological inhibition of such upregulated pathways, allowed to find that activation of the AP1 pathway, via MAPK signaling, results in neurodegeneration of motor neurons (170).

As for the other NDDs, for ALS new compounds were also screened on motor neurons derived from patients iPSCs. Osborn and colleagues screened a library of several molecules and identified new IGF-II inducers, that it is known to protect motor neurons from degeneration (171). Interestingly, one of the compounds allowed a complete protection of motor neurons, an effect that was reversed by blocking receptors of IGF-II. Moreover, this compound when was administered to SOD1 transgenic mice, led to a significant delay in motor symptom onset and allowed to prolong survival of the animals (172).

These works suggest that a helpful tool to study the pathological mechanisms that lead to the degeneration of motor neurons in the disease is represented by the use of iSPCs derived from both of mutated and sporadic ALS patients. With such model will be possible several

investigations, e.g. oxidative stress, DNA damage, and transcriptome. Moreover, the co-culture between glial cells, such as astrocytes, and motor neurons can give new information about the interactions between each other and if such interaction could have a pathophysiologic role in ALS.

1.2.7. IPSCs in Huntington's disease

For HD, pathogenesis studies are a bit different respect the other NDDs because in this case the genetic cause is clear. Although this fact, the exact mechanism through which mutant HTT leads to the degeneration of neurons is still unclear. Thus, studies on iPSCs HD models are needed to find new treatments.

Therefore, lines of mouse iPSCs with HD phenotype and iPSCs of HD patients were generated. Both cell types presented several dysregulated cellular pathways, such as ERK-signaling, β-catenin phosphorylation, SOD1 accumulation and the expression of p53, indicating that such events could be considered the earliest markers of HD (173). In summary, this demonstrate that important HD pathological processes are active during an embryonic like cellular conditions, indicating that the alteration in signal transduction of HD patients begins in the early stages of life (173).

Consistent deficits related to neurodevelopment and adult neurogenesis were found also using neural cells differentiated from HD patient-derived iPSC lines with both adult and juvenile-onset CAG repeat expansions, suggesting that specific gene networks could represent potential therapeutic interventions (174). The group tested isoxazole-9, a compound that targets many of such dysregulated gene network, normalizing the phenotype of iPSCs-derived neurons in both juvenile-repeat and adult-onset HD (174).

The possibility to differentiate iPSCs into neurons opened the possibility to discover new therapeutic targets, e.g. pre-mRNA trans-splicing modules. In this work, Rindt and colleagues

expressed pre-mRNA trans-splicing modules in a neural culture derived from HD patient iPSCs, reversing two previously established polyQ-length dependent phenotypes. These data suggest that pre-mRNA repair of mHTT could have a therapeutic effect, generating a new approach in the correction of mRNA product produced by mHTT (175).

Finally, the role of glial cells was investigated in several studies, such as Hsiao and colleagues, that reported that HD astrocytes provide less pericyte coverage by promoting angiogenesis and reducing the number of pericytes (176).

The studies previously described highlight the importance to have a realistic model of the disease to investigate mechanisms that could lead to the neurodegeneration; iPSCs-derived neurons seem to represent a useful tool for such studies. They can be used not just for disease modeling, but also to perform study of drug discovery and drug screening, to better understand the effect of several compounds in patient's neurons. Moreover, the possibility to differentiate iPSCs into non-neuronal cells, such as astrocytes, will help to discover the role of glial cells in HD pathogenesis.

1.3. 3D Bioprinting

The word "bioprinting" was used for the first time in 2009 by Mironov but was firstly defined by Guillemot in 2010 (177, 178):

> *The use of computer-aided transfer processes for patterning and assembling living and non-living materials with a prescribed 2D or 3D organization in order to produce bio-engineered structures serving in regenerative medicine, pharmacokinetic and basic cell biology studies.*
>
> **Guillemot et al., 2010**

Such emerging technology have been used for the generation and fabrication of artificial tissues and organs (179), adding a new interesting approach in the field of tissue engineering (TE) and regenerative medicine (RM). With such technology is now possible both the generation of a scaffold on which seeding cells and the controlled *in situ* deposition of cell suspensions (177).

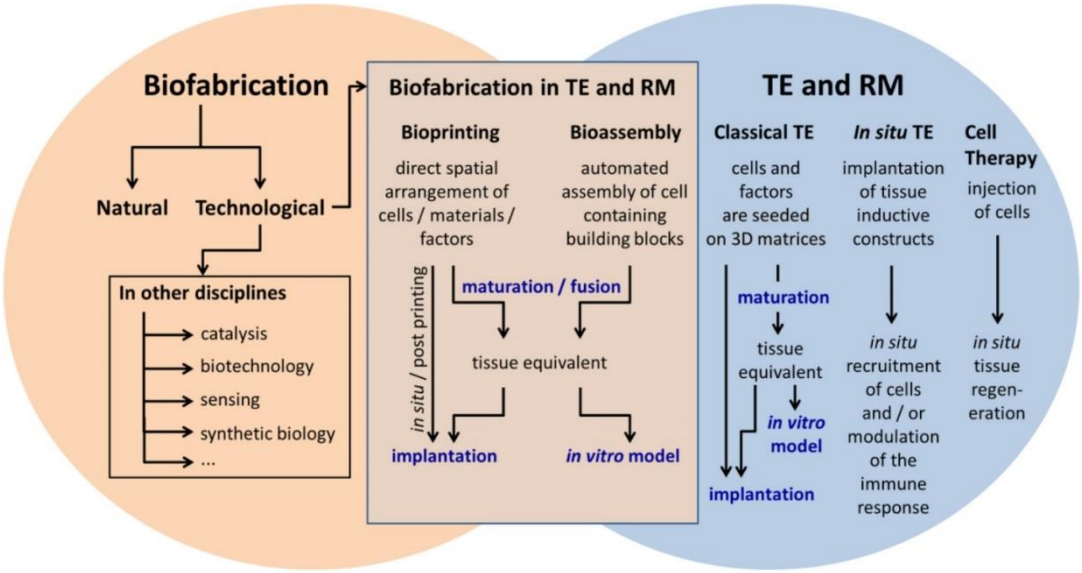

FIGURE 8. DIFFERENCES BETWEEN BIOFABRICATION AND TE/RM. BIOPRINTING IS AN EMERGING APPROACH THAT EXPLOIT ADVANTAGES OF BOTH TECHNOLOGIES (178)

Bioprinting technology allowed to overcome several limits, such as the control of a defined 3D structure and the precise cellular deposition (180). Notably, bioprinting, using specific hardware and software, has been used for the development of organ/tissue-like 3D structures, allowing the generation of cellular models that can be potentially used for mechanism and pharmacological studies, and directly to human patients, using those artificial organs in the field of RM.

Bioprinting requires to fundamental components:

- bioplotter, the machine that allows the software-controlled deposition of the bioink;

- bioink: the compound with a defined composition on which cells can be seeded or added to directly print them.

Thanks to the extreme versatility of such technology, it is possible to vary several parameters, such as the printing technology, the cell type to ecnapsulate into the bioink, the chemical and physical composition of the bioink (181).

1.3.1. Bioprinting techniques

Bioprinting technology can be divided into different bioprinting techniques, which can be specific for some particular bioinks or cell types. Moreover, different technologies have different precision in the deposition of the material. The correct bioprinting technique has to be determined by the composition of the compounds and cell types to be used (179).

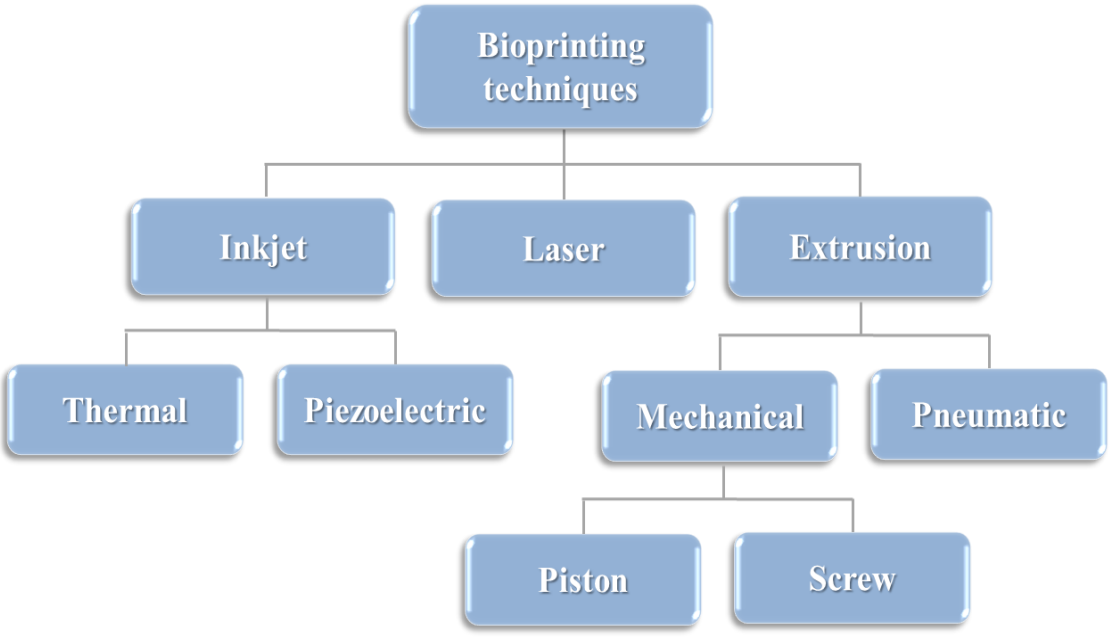

FIGURE 9. CLASSIFICATION OF THE DIFFERENT AVAILABLE BIOPRINTING TECHNIQUES (179)

Inkjet-based

Bioprinting has its origin from the classical office inkjet printers in use since the 1980s. The technology consists of ink droplets deposited on paper using narrow orifices, enabling precise control and giving great flexibility to users. More recently, inks were replaced by cells in cartridges, generating the first bioinks to print living cells in the form of droplets by using a nozzle (182). Only thermal and piezoelectric methods have been adapted for bioprinting technology. The first one consists of increasing the temperature a heating element, allowing the generation of a bubble that forces the ink out of the nozzle. On the other hand, the piezoelectric technology exploits the inward vibration of a piezoelectric element, forcing a small amount of the ink out of the nozzle (Fig. 10). Although this technology is cheap and can use mild conditions, it seems to affect cell viability. Moreover, one of the main restrictions is the low upper limit for viscosity of bioink (183), making the deposition of hydrogels with high viscosity more complicated (184). Many parameters, such as material throughput, reproducibility of droplets, the range of shear forces, cell aggregation and the consequent sedimentation, clogging of the nozzle, and the number of fluids that may be printed during a single experiment are other limitations and challenges associated with this technique (179). Although the presence of these limitations, inkjet technology has a great potential to solve some of the intrinsic problems of TE, thanks to its capacity to print very small droplets of several materials.

Laser-based

A laser-based system was firstly introduced in 2000 in order to generate a 2D cell patterning. In this technique, laser energy excites cells, giving precise patterns to control the cellular environment spatially (Fig. 10) (185). In the case of bioprinting, usually laser-based direct writing (LDW) is considered one of the best methods. In this technology, a laser pulse allows the translocation of an individual cell from a donor source to an acceptor substrate

(186). Notably, the laser pulse generates a bubble, and consequently shock waves created by the bubble formation can force cells to transfer toward the acceptor substrate. Microscale cell patterning is possible thanks to the optimization of several parameters (e.g., bioink viscosity, laser printing speed, laser energy, and pulse frequency) (187). Moreover, multiple cell types are possible by ejecting different cells to the collector substrate. One of the main advantages of this technique is the lack of nozzle, enabling the use of bioink with very high viscosity. Furthermore, laser-based bioprinting has high precision characteristic, offering many benefits for printing the smallest features of an organ (179). On the contrary, this technique, such as the other techniques, has several limitations. For example, the laser energy or the heat produced by the laser can affect cell viability and impair the ability to communicate. One of the most important issues is the limitations in printing in the third dimension and the bioink need to be photocrosslinkable (188).

Extrusion-based

Extrusion-based bioprinting is the most common method and has been used for quite a long time, representing a promising tool for generating living tissue constructs. This technique is composed of a fluid-dispensing system (a pneumatic or mechanical) and an automated robotic system for extrusion (Fig 10) (189). While piston-driven printing allows more direct control over the flow, the screw-driven systems may help to have a more spatial control of bioinks with higher viscosities. The main disadvantage of such system is the generation of larger pressure, which can potentially damage cells.

The main advantage of extrusion-based technique is the controlled deposition by computer software. The bioink can then be crosslink by light, chemical or thermal transitions, allowing a more precise generation of the desired 3D structure and a better structural integrity (188). Although extrusion is considered the best technique for the generation of tissues and organs, it has several limitations, e.g. the shear stress due to the pressure, which can damage

cells, and limited material selection that can be used. Such limits can be overcome optimizing some parameters, such as bioink concentration and viscosity, nozzle diameter, printing pressure and speed.

Each bioprinting technique has its advantages and disadvantages, including printing capabilities, resolution, deposition speed, scalability, bioink, and material compatibility, ease of use, printing speed, and biocompatibility (179).

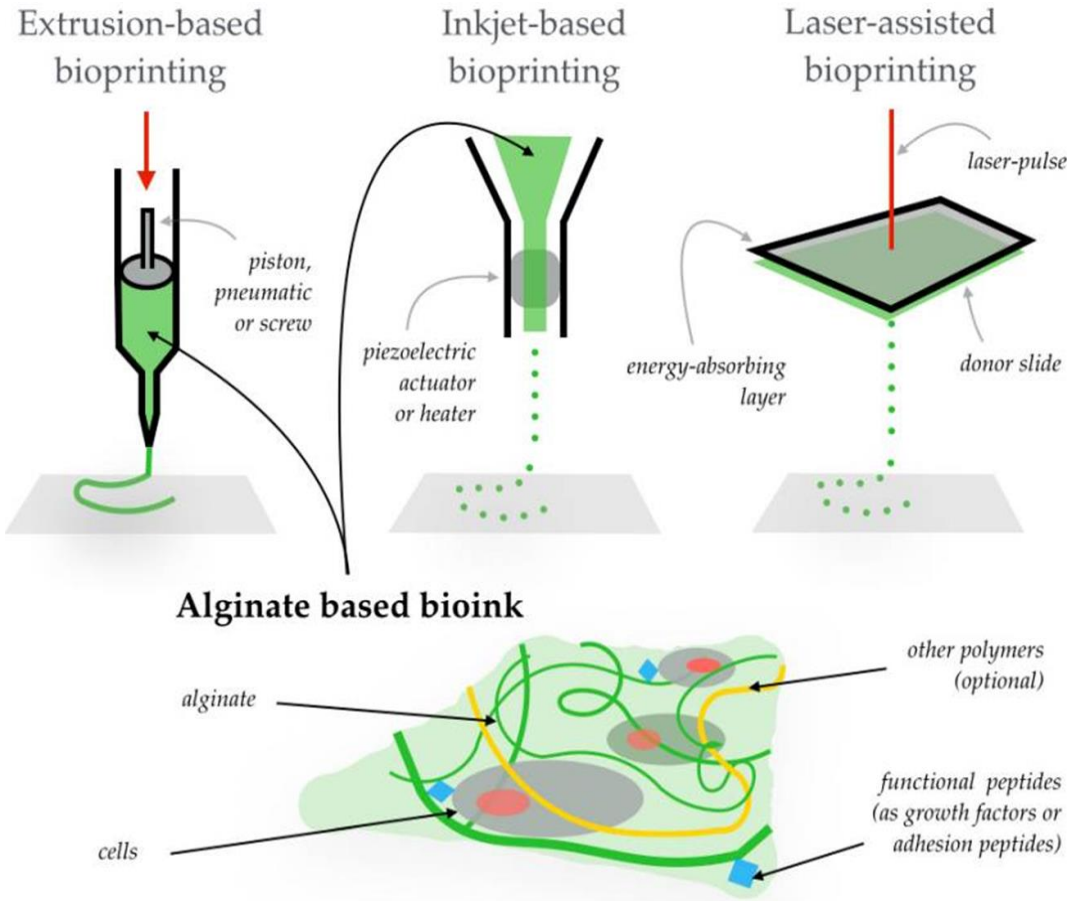

FIGURE 10. DIFFERENT BIOPRINTING TECHNIQUE AND EXAMPLE OF AN ALGINATE BASED BIOINK (190)

1.3.2. Bioplotters

Each bioplotter has common features, which are needed in order to print living cells in a 3D structure:

- robotic system that allows the movement of the nozzles in the tree axis (x, y, and z);
- one or more nozzles;
- sterile chamber with laminar flow in order to guarantee sterility of the construct, otherwise the bioplotter has to have small dimensions in order to place it into the laminar flow hood;
- software that allows the deposition of the bioink with a specific pressure and speed.

The first sold bioplotters had a high cost and they were produced for an industrial aim, features that delay the development of such machines. Only in 2006 were developed new technologies that allow to produce the first versatile and cheap bioplotter, called Fab@Home.

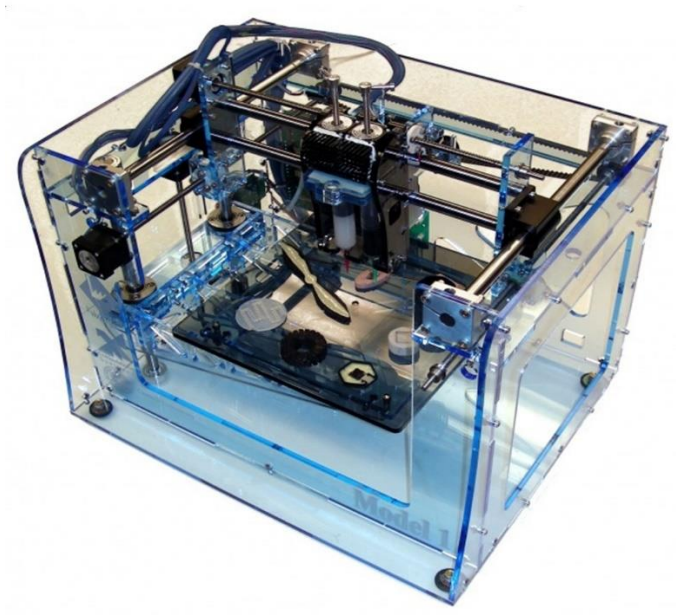

FIGURE 11. BIOPLOTTER FAB@HOME, MODEL 1
HTTP://WWW.CREATIVEMACHINESLAB.COM/FABHOME.HTML

In recent years, many bioplotters were developed by different industries but also some hand-made machines, each one with a specific feature needed by the developer. For example, more nozzles were added to the bioplotter in order to extrude contemporary more materials. Some bioplotters avaiable are listed below:

- **3D Bioplotter®**, developed by EnvisionTEC, is the most costly but also the most complete and versatile bioplotter available. It allows to extrude up to 5 contemporary biomaterials, which can have different chemical features, and can reach a temperature of 150 °C. Because of its very high cost, actually is available in few research laboratories;

- **NovoGen MMX ™**, developed by Organovo, allows the depositions of many *strati* of biocompatible materials such as hydrogel and bioink, in order to generate the desired shape. Such bioplotter is available at the moment just for big pharmaceuticals industries for the creation of bioartificial tissues;

- **Biobot 2**, developed by BioBots, has a heated 6-head extruder, with UV and visible light curing for photo-crosslinking. The extruder is based on compressed air pneumatic system. The print bed can heat up to 120°C and can maintain 37°C cells in the plate. The system allows printing directly onto petri dishes, well-plates and slides.

- **Bio X**, developed by Cellink, offers the most complete stand-alone system, with high flexibility, presenting many features, such as exchangeable print heads, heated and cooled print heads, heated and cooled print bed, a sterile chamber, both piston and pneumatic print heads, multi well plate, and touch screen.

1.3.3. Bioinks

One of the most critical point of the bioprinting process is the development and the characterization of the optimal bioink, which has to have some specific features, such as

biocompatibility, good printability, and the right physical and chemical properties in order to maintain the 3D shape (179). One of the most used bioink in bioprinting and TE fields are the so-called hydrogels, because they are very similar to natural ECM, allowing cell encapsulation in a highly hydrated, hydrophilic and supportive 3D environment (191). Hydrogels can be generally divided into naturally (e.g., alginate, cellulose, collagen, chitosan and fibrin) and synthetic derived polymers (e.g., pluronics and polyethylene glycol) (188). Usually naturally derived polymers are more biocompatible respect than synthetic ones, thus, they have been used more frequently in TE technologies.

Hydrogels were used to encapsulate several types of cells, such as fibroblasts, chondrocytes, hepatocytes, smooth muscle cells, adipocytes, and stem cells (192). A hydrogel with encapsulated cells is usually bioprinted into a well-defined shape, fixed successively by a process called "gelation", which is a crosslinking reaction that can be initiated by physical or chemical processes (193). The first one, physical crosslinking, is defined as a reversible interaction between molecular polymer chains, ionic interaction and hydrogen bridges. Because of its poor mechanical properties, such crosslinking method is not used in many application of 3D bioprinting, otherwise it requires post-processing crosslinking and/or an additional crosslinking agent. On the other hand, chemical crosslinking allows to form new covalent bonds, giving relatively high mechanically stable bioprinted constructs respect than physical crosslinking (193). One of the main issues in the chemical crosslinking is the exposure to chemicals that can be harmful for embedded cells. Furthermore, it reticulates the structures, generating a 3D mesh networks that are smaller than cells, leading to the limitation of the mobility of encapsulated cells (194).

Among hydrogels previously described, in my work I used two types of hydrogels:

- a gelatin- and alginate-based hydrogel;
- a cellulose-based hydrogel mixed with carbon nanotubes (CNTs).

Gelatin. Gelatin is a protein from the hydrolysis of collagen obtained from the connective tissue, present in various animal body parts. Hydrogels composed of gelatin, such as gelatin/alginate, gelatin/chitosan, gelatin/fibrinogen, have many interesting properties, i.e., high biocompatibility, optimal biodegradability, lack of immunogenicity for clinical applications (195, 196).

Gelatin used in TE is usually derived from mammals' skin such as pig's or bovine's skin. Its molecular weight and the length of polypeptide chain depend on its derivation, the degradation with which the collagen was converted into gelatin, pH, and temperature(197).

One important features of gelatin, is the capacity to solidify under the temperature of about 30 °C, forming a hydrogel. Moreover, the jellification is reversible, allowing to liquefy it over 30°C, thanks to the generation of new non-specific bonds, such as, hydrogen bonds, hydrophobic bonds, and electrostatic bonds (195, 196).

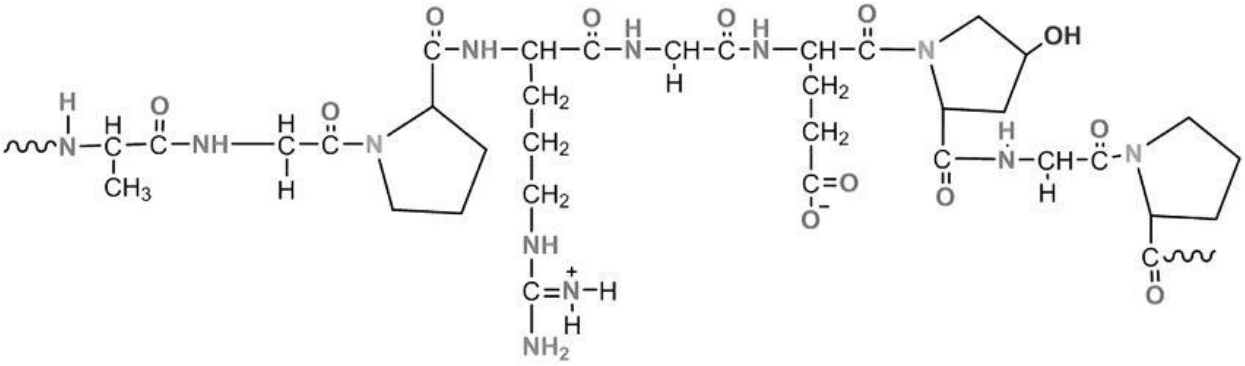

FIGURE 12. CHEMICAL STRUCTURE OF GELATIN

Alginate. Alginate is a polysaccharide distributed widely in the cell walls of brown algae. The empirical formula of sodium salt of alginate is NaC6H7O6 and is a linear copolymer composed of β-D-mannuronate (M) e di α-L-guluronate (G). The polymeric form can be generated by only G residues, only M residues, or the alternation between G and M

residues, depending on the derivation. Molecular weight of sodium alginate is usually between 32000 and 40000, depending on the extraction process (198).

Sodium alginate is one of the most used compounds in hydrogels development in both TE and drug delivery fields, because of its high biocompatibility and its low interaction with other molecules. Sodium alginate dissolved into aqueous solution can be crosslinked and thus solidify using ionic crosslinking, with divalent cations such as Ca^{2+}. Notably, Ca^{2+} allows the bonds between G residues, generating a solid structure .

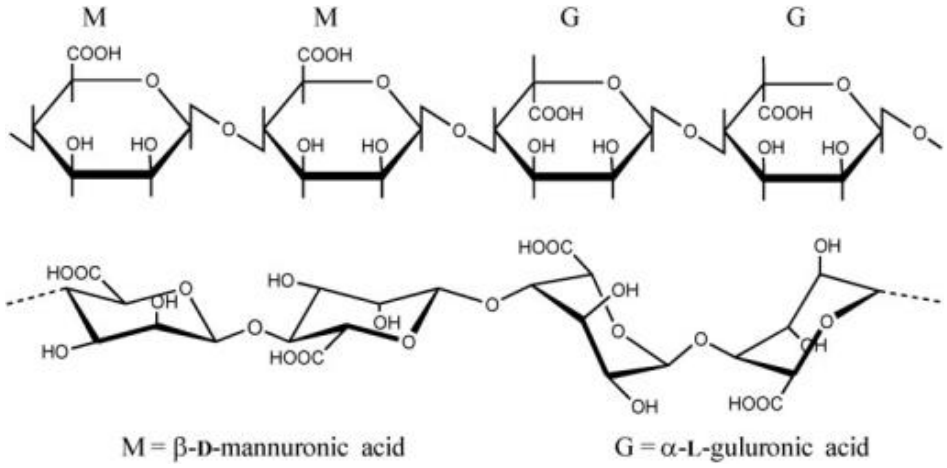

FIGURE 13. CHEMICAL STRUCTURE OF ALGINATE

Cellulose. Cellulose is an organic polysaccharide with the empirical formula (C6H10O5)n, in which "n" represents a number between several hundred to many thousands of β(1→4) linked D-glucose units (199). The main source of cellulose is the primary cell wall of plants, some type of algae, the oomycetes and some species of bacteria.

Most cellulose-based materials are usually chemically treated, to alter their properties. For example, acetylation of cellulose leads to the loss of the native structure and strength (200). In bioengineering field, cellulose nanofibrils, that are fibrils with one dimension in the nanometer range, have gained increased interest during the past decade. Cellulose nanofibrils can be divided into three main categories, depending on the source and its processing

conditions: microfibrillated cellulose, nanocrystalline cellulose, and bacterial nanocellulose (201). Like the previously reported materials, cellulose provides many advantages, such as the biocompatibility, the hydrophilicity, broad range of chemical modification capacity, and good mechanical properties (202).

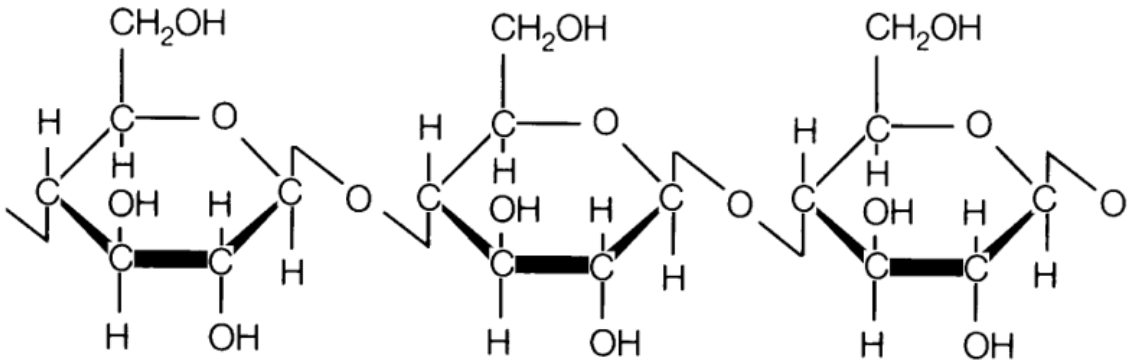

FIGURE 14. CHEMICAL STRUCTURE OF CELLULOSE

1.3.4. Bioprinting and neurodegeneration

In the last decade, the possibility to replace degenerated cells in many degenerative processes, such as NDDs, affecting the central nervous system opened the way for a more accurate and intense study of stem cells research, notably in the TE and RM fields (203). Moreover, the ability of stem cells to secrete cytokines and other growth factors allowed the development of stem cells-based treatments, offering several benefits such as anti-inflammatory effects, protection of neural cells, and endogenous recovery systems. Such therapies have some limits, like low cell survival and limited engraftment (204). To minimize these problems, the development and the use of three-dimensional scaffold, allowed to mimic the complexity both from the biological and functional points of view of the tissue to be replaced (205). The generation of three-dimensional scaffolds suggested promising results for the treatment and the repair of nerve damage, although such method has a great limitation

notably in terms of control of the external and internal structure of the scaffold (206, 207). 3D bioprinting allowed to overcome these problems, leaving to the operator complete freedom regarding the shape, the material and its internal architecture (161). The first 3D bioprinting technologies were developed fort the RM field in order to respond to the growing demand for tissues and organs for transplants, but in the last years, such technology was applied also to basic scientific research, in order to use it in disease modeling. While several studies have been focused on widely studied tissues such as skin, bones, heart tissue, and cartilage, just few studies applied 3D bioprinting for the neural tissue (208). Moreover, the few studies published so fundamental because of the delicacy of the tissue (205, 209). Like the other tissue, also 3D in vitro neural tissue has been proposed in the field of RM, notably for neural regeneration in patients with NDDs (210, 211). The generation of the neural tissue using bioprinting can be exploited also in pharmacological studies, for both drug screening and drug testing. However, for such studies it is important to underline how recent is the 3D bioprinting field, thus will be necessary to validate such models for the applications described up to now, in order to prove that the model completely recapitulates the pathophysiology of NDDs (205).

2. AIM

NDDs affect more than 50 million people in the world, and this number is destined to grow because of the longer duration of the average life. Despite such high number, to date there are only a few treatments for the treatment of such diseases, and often concern only the treatment of a single symptom of the disease. To date only some cellular and animal models allow us to give answers to the many questions that characterize neurodegenerative diseases.

Given the latest developments in the field of biological 3D printers and the evidence that a 3D environment improves the proliferation and the spatial organization of cells, the first part of the thesis is focused on the creation of a bioink based on sodium alginate and gelatin. Such materials must be able to maintain good cellular viability and proliferation and have to allow cells to migrate across the environment, to create cell-cell interconnections in the most natural way. Moreover, we developed a printing protocol for such bioink for an extrusion bioplotter, with which repeatability tests of the bioink without cells have been carried out, in order to be able to do the subsequent experiments in a reproducible way.

The second part of this work consisted in the generation of a conductive hydrogel cellulose-based, because conductivity can help the cultivation, maturation and differentiation of neural cells. Thus, we firstly develop such bioink, characterized it and finally evaluated the effect of such bioink to SH-SY5Y maturation and differentiation, in order to understand if conductivity is suitable to generate a realistic 3D neural tissue model.

Lastly, we developed a protocol for reprogramming of somatic cells deriving from peripheral blood and from skin of patients suffering from neurodegenerative diseases and from healthy control subjects, to obtain induced pluripotent stem cells (iPSCs) , which can be subsequently differentiated into the various neuronal phenotypes, and thus obtain a cellular model that possesses the genetic patrimony of the subject of origin. Such cells were included into the gelatin-based bioink, in order to to print "simple" constructs containing aiPSCs, and to to assess whether the printing process affect cellular viability and proliferation, and how

such environment allows cells to grow in a 3D spatial organization, not possible with the traditional in vitro models in two dimensions.

3. MATERIALS AND METHODS

3.1. Gelatin-based hydrogel

Hydrogel preparation. Hydrogel was composed of sodium alginate (SA) and gelatine (GEL), both used individually and in combination with each other at different concentrations for a more accurate analysis. SA (Sigma Aldrich, Italy) and GEL (Sigma Aldrich, Italy) were dissolved separately into sterile phosphate buffer saline (PBS) and subsequently they were mixed at different concentrations (Table IV).

Sample	Alginate (SA)	Gelatin (GEL)
1	0%	0%
2	0%	1%
3	0%	2%
4	1%	0%
5	1%	1%
6	1%	2%
7	2%	0%
8	2%	1%
9	2%	2%
10	4%	4%
11	6%	4%

TABLE IV. DIFFERENT CONCENTRATIONS OF ALGINATE AND GELATINE USED IN THE WORK

Briefly, GEL was stirred into hot PBS (72° C) to improve its solubility using a magnetic plate and SA solution was added to GEL solution. All these steps were performed in sterile conditions. Hydrogel were centrifuged ad 500 g x 3 min before their utilization to eliminate air bubbles.

Sterilization process. One of the first issues we encountered was the choosing of the best sterilization process. We tried four sterilization methods to obtain a sterile hydrogel: filtration, autoclaving, UV exposure and pasteurization. The first method we tried was filtration, based on the insertion of the two components dissolved in PBS in 20 mL syringes and then passed into a 0.20 μm filter (Corning, USA). The second method was UV exposure, where the two powders, dissolved in PBS, were placed under UV rays for 1 hour. The third method tested was pasteurization where the SA and GEL solutions, placed in 50 mL centrifuge tubes, were placed in a 72° C bath for 1 hour. Finally, the last method tested was autoclaving: dissolved SA and GEL were collected in 50 mL centrifuge tubes, autoclaved at the temperature of 121° C for 20 minutes.

Cell cultures. Hydrogels were tested on two different cell lines, the human neuroblastoma cell line SH-SY5Y and the cervical cancer cell line HeLa. Both cell lines were cultivated in DMEM (Carlo Erba, Italy) supplemented with 15% fetal bovine serum (FBS) (Carlo Erba, Italy), penicillin/streptomycin (100 U/mL; 100 mg/mL) (Carlo Erba, Italy), and 2 mM L-glutamine (Carlo Erba Italy). Cells were cultivated at 37°C in a humidified atmosphere containing 5% CO_2.

Encapsulation of HeLa and SH-SY5Y cell lines. After sterilization and mixing, hydrogels were transferred in a 5 mL syringe. We used the luer connector to improve cell mixing and to encapsulate them in the hydrogel. For proliferation and viability assays, we suspended cells at a concentration of $1x10^6$ cells/mL for HeLa cell lines and $5x10^4$ cells/ mL for SH-SY5Y cell line. Since HeLa and SH-SY5Y have a different phenotype, we used the ideal concentration for each cell line.

Proliferation-viability assay. Both cell lines were cultivated as previously described for 5 days in 12-well plate encapsulated in the hydrogel and the medium surrounding the hydrogel was changed daily. The proliferation and viability tests were carried out using an automatic cell counter (TC20-Automated Cell Counter, Biorad, Italy) using Trypan blue exclusion method. Briefly, it is based on the principle that intact cell membranes of live cells exclude the dye, while dead cells do not (212). Thus, we mixed 10 µl of cell suspension and 10 µl of Trypan blue dye. The suspension was then loaded into a counter slide (Biorad, Italy) and read with the cell counter. Proliferation was evaluated considering total cells number, while viability considering only live cells number.

Bioprinting. For the first project the bioplotter Cellink INKREDIBLE+ (Cellink AB, Sweden) was used to print SA/GEL-based hydrogels. The bioplotter was equipped with a chamber ventilated through HEPA filters, to guarantee a sterile environment during the printing process. Encapsulated cells were printed using a 0.41 mm nozzle in order to avoid cell death. We set two temperatures, 25° and 37° C, and pressure was manually controlled, and it changed according to the temperature and the composition of the bioink. An open source CAD software was used to design STL grid model (FreeCAD©, ver. 0.16). Slicing process was assessed using Slic3r (version 1.2.9), print-head speed was set at 600 mm/min and layer height at 0.4 mm.

Crosslinking process. Alginate can be crosslinking in presence of bivalent ions and the most used compound is 2% calcium chloride ($CaCl_2$) that reticulate SA residue very rapidly. Thus, crosslinking was performed with 2% $CaCl_2$ powder (Sigma Aldrich, Italy) diluted in sterile distilled water and was maintained for 5 minutes on the printed structure. After this time, $CaCl_2$ was removed and the structures were washed three times with PBS.

Viability assay on crosslinked structures. Since crosslinking harden the structure, the Trypan blue exclusion test is not executable. Thus, viability test was performed using LIVE/DEAD Cell Viability Assays following manufacture instructions (ThermoFisher, USA).

It is based on two fluorescent dyes, calcein AM (green) for living cells, and ethidium homodimer-1 (red) for dead cells.

Immunofluorescence analysis. 3D printed constructs were washed and fixed with 4% paraformaldehyde for 25 minutes and subsequently rinsed with ice cold PBS. The structures were incubated for 2 hours at RT with blocking solution (10% Normal Goat Serum and 0.3% Triton X100 in PBS). Subsequently, the structures were incubated with primary antibody overnight at 4° C. After two washes in ice cold PBS, they were incubated for 3 hours at 4° C with the secondary antibody and rinsed with ice cold PBS. Each construct was placed on a microscope slide, mounted with Prolong® Gold anti fade reagent DAPI (Invitrogen) and finally the sample was dried and nail-polished. Cells were stained with GAPDH (GeneTex, USA) at a concentration of 1:200 (2nd Rabbit 1:700, Sigma Aldrich, Italy) and α-tubulin (Cell Signaling, USA) at a concentration of 1:100 (2nd Mouse 1:700, Sigma Aldrich, Italy). The images were obtained using an Axio Imager 2 fluorescence microscope (Zeiss, USA), with an Axiocam Mrm camera.

Statistical analysis. All the tests were performed three times or more. Each parameter and result is shown as means ± SD. We performed statistical analysis using GraphPad Prism (ver. 7, GraphPad Software), adopting the one-way analysis of variance test (ANOVA). Values were considered statistically significant when p-values were <0.05.

3.2. Conductive hydrogel

This part of my work and the following experiments were carried out in the 3D Bioprinting Center, Chalmers University (Göteborg, Sweden) leaded by Prof. Paul Gatenholm, which welcomed me in his laboratory.

Bioinks preparation. Firstly, we prepared CNTs dispersion, mixing 1% SWCNTs (P3-SWNT, Carbon Solution, USA) and 0.25% of Pluronic F-127 (Sigma Aldrich, Sweden) in water. In order to improve the dispersion of CNTs, the solution was sonicated at 70° C for 8 h followed by sonication at room temperature overnight. The dispersion was successively mixed with 2% NFC dispersion in water (StoraEnso, Sweden) and with 2% alginate solution to obtain conductive bioinks with two different CNTs content: NFC/CNTs/Alginate dry weight ratio of 60/20/20 and 70/10/20. The final mixtures were finally homogenized using SpeedMixer (DAC 150.1 FV-K, FlackTek).

SH-SY5Y cells cultivation. Human neuroblastoma cell line SH-SY5Y was cultured as previously reported. For this project involving differentiation, cells were derived from the same batch at passage 19 and were never cultivated beyond passage 25.

SH-SY5Y cells differentiation. Differentiation was performed following the protocol proposed by Forster and colleagues (213). Briefly, the first day of differentiation cells were cultivated in DMEM (Invitrogen, Sweden) with 1% P/S further supplemented with 10 µM all-trans retinoic acid (Sigma Aldrich, Sweden). After three days, the medium was changed with Neurobasal-A medium minus phenol red (Invitrogen, Sweden) with 1% l-glutamine, 1% P/S, 1% N-2 supplement 100× (Invitrogen, Sweden) and Human BDNF (Invitrogen, Sweden) at a concentration of 50 ng/mL. Cells to be differentiated were cultivated on pure NFC as negative control, and on bioinks with 10% and 20% of CNTs.

Confocal microscopy. Following producer instructions, few drops of NucBlue (Invitrogen, Sweden) were added to the medium of the culture and incubated for 30 min. Successively, cells were rinsed three times with PBS 1X and fixed with 4% PFA in PBS 1X for 15 min. After that, cells were rinsed again and permeabilized with Triton X-100 0.2 % in PBS 1X for 15 min. ActinGreen 488 (Invitrogen, Sweden) was added directly in the permeabilization solution (2 drops for mL) and samples were incubated for 30 min. Finally, samples were rinsed three times with PBS 1X and placed in a microscope slide, covered with

a coverslip and nail-polished. Samples were imaged by confocal microscope (LSM 710 NLO, Zeiss).

Scanning Electron Microscopy (SEM). Samples were washed three times in PBS 1X and the fixed in 2% glutaraldehyde dissolved in PBS 1X for 1 h at room temperature. Cells were rinsed three times in PBS 1X and dehydrate using a series of increasing ethanol concentration (60%, 70%, 80%, 90%, and 100%), each step 30 min. After samples were completely dried, they were sputter-coated (Fine Coat Ion Sputter JFC-1100, JEOL Ltd., Tokyo, Japan) with 10 nm thick gold layer in a vacuum for 80 s at 10 mA. A LEO Ultra 55 FEG SEM Zeiss scanning electron microscope was operated in secondary electron mode at an acceleration voltage of 3 kV.

Electrical conductivity measurements. The electrical conductivity was measured on crosslinked and not-crosslinked bioinks at dry state before cells seeding. The conductivity measurements were performed using a two-point probe system (Parameter Analyzer-Keithley 4200-SCS). The working distance between the probes was kept at 3 mm during the measurements.

RT-qPCR. Total RNA from SH-SY5Y cells was extracted with TRIzol® (Invitrogen, Italy) following the manufacturer's instructions. RNA quality and quantity were determined using NanoDrop spectrophotometer (Invitrogen, Italy) and 1 μg was reverse-transcribed using the iScriptcDNA Synthesis Kit (BioRad, Italy) following the manufacturer's protocol. PCR amplifications were carried out with the CFX Connect™ Real-Time PCR Detection System (BioRad) using SYBR Green Master Mix (BioRad). GAPDH gene was used as housekeeping gene to normalize values. Primer sequences: NESTIN Fw: 5'- GGA AGA GAA CCT GGG AAA GG-3', Rv: 5'- GAT TCA GCT CTG CCT CAT CC-3'; TUBB3 Fw: 5'- CAG ATG TTC GAT GCC AAG AA-3', Rv: 5'- GGG ATC CAC TCC ACG AAG TA-3'; GAPDH Fw: 5′-CAG CAA GAG CAC AAG AGG AAG-3′, Rv: 5′-CAA CTG TGA GGA GGG GAG ATT-3′.

3.3. Induced Pluripotent Stem Cells

Patients' enrolment. Fibroblasts and PBMCs were isolated from NDDS patients. NDD diagnosis was made at the IRCCS Mondino Foundation. Patients were tested for genetic mutations with next generation sequencing and only patients without mutations were used for this work. Healthy volunteers were recruited at the IRCCS Policlinico S. Matteo Foundation in Pavia. Healthy volunteers were all unrelated and the normal phenotype was confirmed by interviews based on personal health histories. The study design was examined by the IRBs of the enrolling Institutions.

Isolation of PBMCs. PBMCs were immediately isolated from blood using Histopaque®-1077 (Sigma-Aldrich, Italy) following manufacturer's instructions. The same volume of Histopaque and blood were put in a centrifuge tube. Blood was added slowly with a plastic Pasteur pipette to avoid the mixture with Histopaque. It was centrifuged at 1800 rpm for 30 min with low deceleration. The layer of PBMCs was collected with a glass pipette, transferred into another centrifuge tube, the volume was adjusted to 14 mL with PBS 1X and centrifuged at 1600 rpm for 10 min to separate PBMCs from plasma. Cells viability was assessed by trypan blue exclusion test with an automatic cells counter. Supernatant is discarded, and the pellet was re-suspended in 1 mL of mixture composed of 900 µL of FBS and 100 µL of dimethyl sulfoxide (DMSO) in order to prevent cells death. PBMCs were placed at -80° C into a container which provides a rate of cooling very close to -1° C/min. Finally, cells were stored into cryogenic storage tank with liquid nitrogen.

Isolation of fibroblasts. Fibroblasts were obtained from skin biopsy taken with a 4 mm punch. Using sterile forceps, the biopsy was placed in a dish and dissected into 15 small pieces with sterile scissors. The small pieces were then placed into T25 flasks in RPMI (Carlo Erba, Italy) supplemented with 20% fetal bovine serum (FBS) (Carlo Erba, Italy), penicillin/streptomycin (100 U/mL; 100 mg/mL) (Carlo Erba, Italy), and 2 mM L-glutamine (Carlo Erba Italy). After one week of cultivation at 37°C in a humidified atmosphere

containing 5% CO2, cells were monitored daily and media changed every 2-3 days. Once fibroblasts are confluent in each flask, fibroblasts were trypsininzed and placed into T75 flasks. At passage 2, cells were cryopreserved as previously described.

Fibroblasts reprogramming. About $1x10^5$ fibroblasts were plated in 6 well-plates. They were allowed to grow in RPMI until 70% confluence. The correct amount of viruses was evaluated counting cells in a well. Viruses provided by CytoTune®-iPS 2.0 Sendai Reprogramming Kit (Invitrogen) were incubated for 24h. Spent RPMI was replaced every day. After 7 days from transduction cells were trypsinized and about $8x10^4$ cells were plated on vitronectin-coated wells and were grown in Essential 8 Medium. Spent medium were replaced every day for 3 weeks. Undifferentiated colonies were manually picked and plated on vitronectin-coated well. Colonies were splitted using 0.5 mM EDTA for 3 passages. Finally cells were collected using 0.5 mM EDTA and cryopreserved in liquid nitrogen in Essential 8 Medium + 10% DMSO.

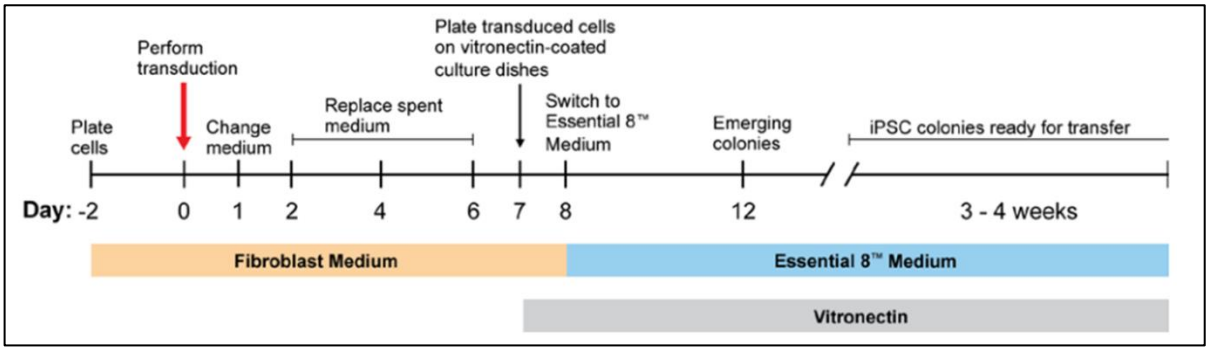

FIGURE 15. FIBROBLASTS DIFFERENTIATION PROTOCOL (THERMOFISHER)

PBMCs reprogramming. About $5x10^5$ PBMCs were resuspended in 24 well-plates with PBMC medium (StemPro™-34 + SCF 100 ng/mL, FLT-3 100 ng/mL, IL-3 20 ng/mL, IL-6 20 ng/mL). After 4 days, the correct amount of viruses was evaluated counting cells in a well. Viruses provided by CytoTune®-iPS 2.0 Sendai Reprogramming Kit (Invitrogen) were incubated for 24h. The medium was replaced with fresh complete PBMC medium to remove the CytoTune™ 2.0 Sendai reprogramming vectors. After 2 days, transduced cells were plated

on vitronectin-coated culture dishes in complete StemPro™-34 medium (Invitrogen, Italy) and the spent medium was replaced every week for 4 days. After 7 days from transduction cells were grown in Essential 8 Medium. Spent medium were replaced every day for 3 weeks. Undifferentiated colonies were manually picked and plated on vitronectin-coated well. Colonies were splitted using 0.5 mM EDTA for 3 passages. Finally, cells were collected using 0.5 mM EDTA and cryopreserved in liquid nitrogen in Essential 8 Medium + 10% DMSO.

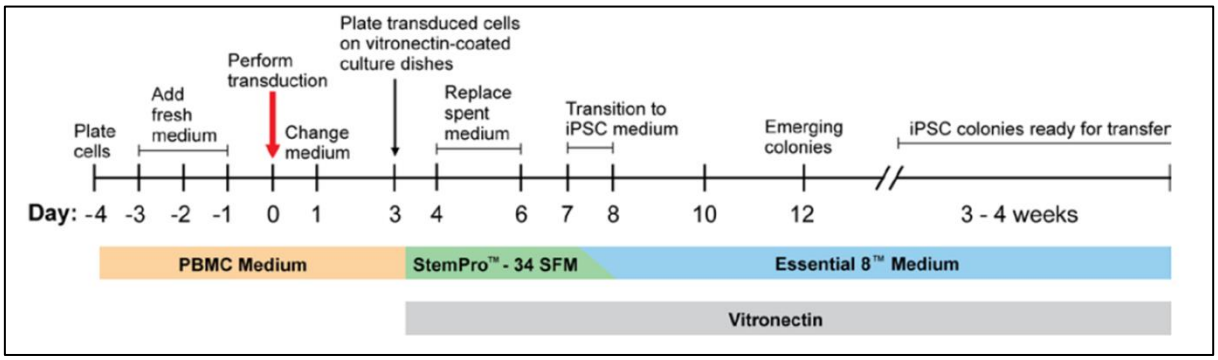

FIGURE 16. PBMCS DIFFERENTIATION PROTOCOL (THERMOFISHER)

Immunofluorescence. Efficient reprogramming was assessed with immunofluorescence analysis of stemness markers. Colonies of iPSCs were picked manually and plated in vitronectin-coated microscope plates. They were cultured 7 days, replacing spent medium daily. After removing medium, cells were incubated with 4% PFA for 15 min at RT and successively permeabilized with saponin 1% for 15 min. After incubation with blocking solution for 30 min, primary antibodies were added, and cells were incubated overnight at 4° C. The next day cells were rinsed with wash buffer 3 times and secondary antibodies were added for 1 h. Finally, samples were washed, mounted with Prolong® Gold anti fade reagent with DAPI (Invitrogen), dried, nail-polished and analyzed by immunofluorescence microscopy

Antibody	Host Species	Dilution
anti-OCT4	rabbit	1:100
anti-SSEA4	mouse IgG3	1:200
anti-SOX2	rat	1:200
anti-TRA-1-60	mouse IgM	1:200
Alexa Fluor™ 594 anti-rabbit	donkey	1:250
Alexa Fluor™ 488 anti-mouse IgG3	goat	1:250
Alexa Fluor™ 488 anti-rat	donkey	1:250
Alexa Fluor™ 594 anti-mouse IgM	goat	1:250

TABLE V. LIST OF ANTIBODIES USED TO CONFIRM CELLS REPROGRAMMING

4. RESULTS

4.1. Gelatin-Based Hydrogel

The first hydrogel tested on this work was composed of two biocompatible materials, sodium alginate (SA), which confers rigidity and support to the 3D structure, and gelatin (GEL), which mimics the extracellular matrix thank to its derivation from collagen. Thus, several mixtures with different concentration were tested, to better understand the best mixture that combines biocompatibility and stiffness. In a second time, a robust repeatable printing protocol was established, to allow a precise cell deposition and to generate a well-defined structure.

4.1.1. Pasteurization is the best sterilization method available

Sterilization of hydrogel is one of the critical issues in 3D bioprinting, because it is essential for cultivating cells, but it could alter the chemical and physical properties of the materials. Thus, we observed that pasteurization is actually the best method to guarantee the sterility of the hydrogel, thus suitable for cell cultures, without affecting their features. The other tested methods presented defects, i.e., loss of viscosity properties during autoclaving, sensitivity of the material when exposed to UV rays and impossibility to filter due to the polymeric nature of the materials (Table VI).

	SA	GEL
Pasteurization	✓	✓
UV	X	✓
Autoclaving	X	X
Filtration	X	X

TABLE VI. STERILIZATION METHODS TESTED. PASTEURIZATION IS THE ONLY METHOD COMPATIBLE WITH BOTH SA AND GEL SOLUTIONS.

4.1.2. Gelatin seems to improve cells viability

Sterile hydrogel was mixed with HeLa cell suspension to obtain about $1x10^6$ cells/mL and cells were grown in a 12 multiwell plate in a final volume of 500 µL (about $5x10^5$ cells) for 5 days. Viability and proliferation tests were obtained using trypan blue exclusion method. Proliferation results showed the same data compared to 2D control model, in all samples the number of cells is tripled compared to the starting cells number (Fig. 17A). This result demonstrates that the gelatin-based hydrogel does not affect cell proliferation. Moreover, viability results showed that GEL at concentration of 2% and 1% (sample 1, 2 and 4 in Fig. 17B) increased cell viability compared with control sample without it (sample 3 and 6, Fig. 17B), proving that GEL played an important role for cellular growth (statistically significant difference between sample 1 vs 3, 2 vs 3 *$p<0.05$, Figure 17B, 4 vs 6 **$p<0.01$, Figure 17B). Moreover, the presence of SA, at the concentration of 2% and 1% (sample 1-6, Fig. 17B) did not lead to any decrease in cell viability, suggesting that SA does not interfere with the positive effect of GEL on cells viability. This result confirmed the biocompatibility of SA with this kind of cells, with good results combined with GEL. We noticed a high mortality in sample 9 (Fig. 17B), probably due to an elevated seeded number of cells.

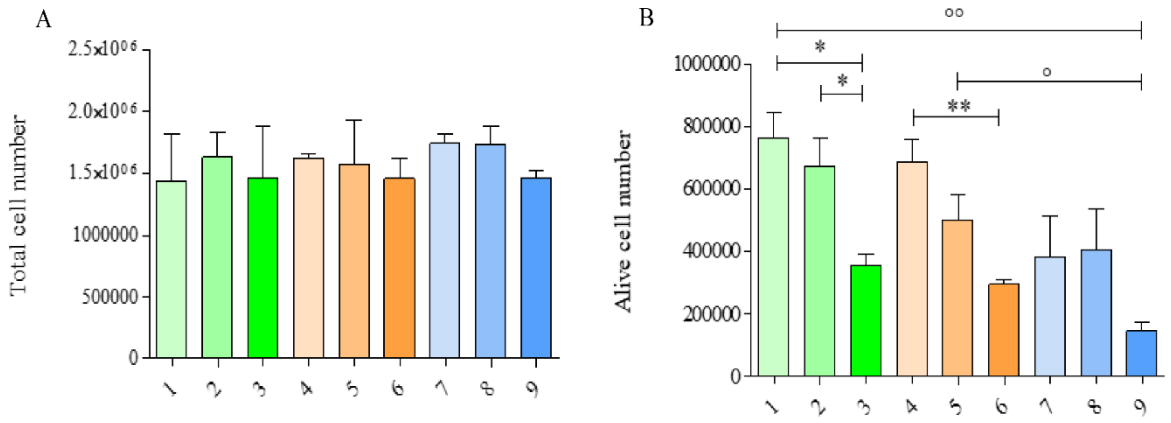

FIGURE 17. A) PROLIFERATION TEST OF CULTURE OF HELA CELL LINE AFTER 5 DAYS OF CULTURE IN THE DIFFERENT BIOINKS. SAMPLES ON THE X-AXIS ARE THE SAME REPORTED IN TABLE 1. ON THE Y-AXIS THE TOTAL NUMBER OF CELLS IS INDICATED. ALL THE SAMPLES SHOW AN EQUAL PROLIFERATION, ABOUT THREE TIMES MORE THAN THE INITIAL CELL NUMBER (500.000 PER SAMPLE). B) VIABILITY TEST OF HELA CELL LINE AFTER 5 DAYS OF CULTURE IN THE DIFFERENT BIOINKS. SAMPLES ON THE X-AXIS ARE THE SAME REPORTED IN TABLE 1. ON THE Y-AXIS THE NUMBER OF ALIVE CELLS IS INDICATED. OUR RESULTS SHOW A SIGNIFICANT INCREASE IN CELL VIABILITY IN ALL SAMPLES CONTAINING GELATIN (1, 2, 4, 5) COMPARED WITH THEIR NEGATIVE CONTROL (3 AND 6) (* P<0.05, ** P<0.001). THE SAMPLES CONTAINING ALGINATE (1-6) SHOW AN INCREASED VIABILITY COMPARED WITH THE NO-ALGINATE SAMPLES (7-9), IN PARTICULAR WITH THE NEGATIVE CONTROL (9) (° P<0.05, °° P<0.001).

4.1.3. Viability tests in SH-SY5Y cell line

Previously reported data showed a high viability and proliferation, but structure of the hydrogel was not maintained in the incubator for 5 days. Thus, we decided to increase both SA and GEL concentration in order to improve mainly the printability, and to verify if good viability is maintained. We tested the samples that showed the best results during the first test (Fig. 18), adding a new sample, 4% SA and 4% GEL, as suggested by the literature.

Moreover, we decided to use a significantly lower concentration of cells due to the different characteristics between HeLa and SH-SY5Y cell lines, and to avoid a drastic cell death in the control sample without SA and GEL. We mixed the sterile hydrogel with SH-SY5Y cell suspension, in order to have $5x10^4$ cells/mL, and cells were grown in a 12 multiwell plate in a final volume of 500 µL. Viability results were obtained with trypan blue

exclusion method, and they confirmed the good cellular viability also with a neural cell line in all tested samples, even with higher concentration of SA and GEL. Checked the good viability of the sample 4 (Fig. 18), we obtained a statistically significant difference between sample 1 and sample 4 (*p<0.05, Fig. 18). These data reflected results obtained in HeLa cell line and demonstrated that GEL improved the viability and SA allowed to keep cells in a well-defined 3D space, in which they could grow more and faster, maintaining a good viability.

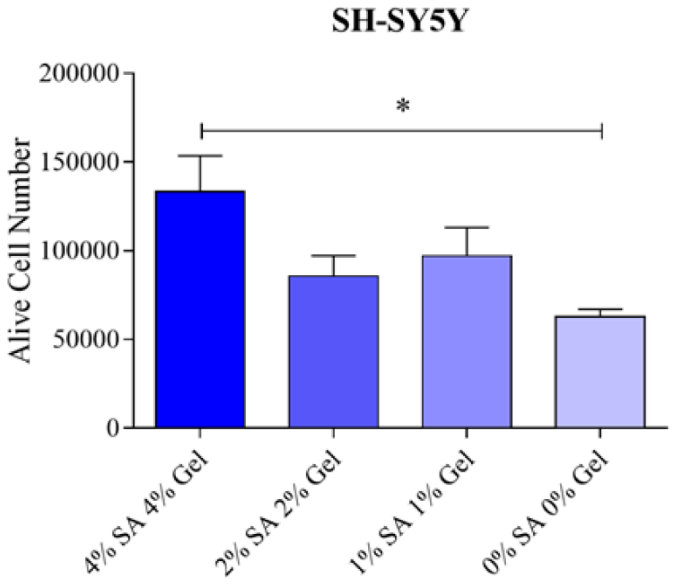

FIGURE 18. VIABILITY RESULTS OF SH-SY5Y CELL LINE AFTER 5 DAYS OF CULTURE IN THE BIOINK. ON THE Y-AXIS THE NUMBER OF ALIVE CELLS IS INDICATED. SAMPLE WITH THE HIGHEST CONCENTRATION OF BOTH ALGINATE AND GELATIN (4% SA 4% GEL) SHOWS THE HIGHEST VIABILITY COMPARED WITH NEGATIVE CONTROL (0% SA 0% GEL) (* P<0.05).

4.1.4. The 4% SA / 4% GEL hydrogel maintains the 3D structure

The hydrogel we developed was thought for 3D bioprinting, thus it is necessary that maintains the structure, in order to potentially allow a 3D localization of cells included in it. We confirmed this feature hardening the 3D bioprinted structure using a crosslinker, thus after printing process, structures were crosslinked with incubation for 5 min with 2% $CaCl_2$

dissolved in water, obtaining a hard structure as illustrated in Fig. 19A. Fig. 19B-C and shows a phase-contrast microscope image (EVOS XL Core Cell Imaging System, ThermoFisher, Italy) of a printed grid with Cellink INKREDIBLE+ bioplotter.

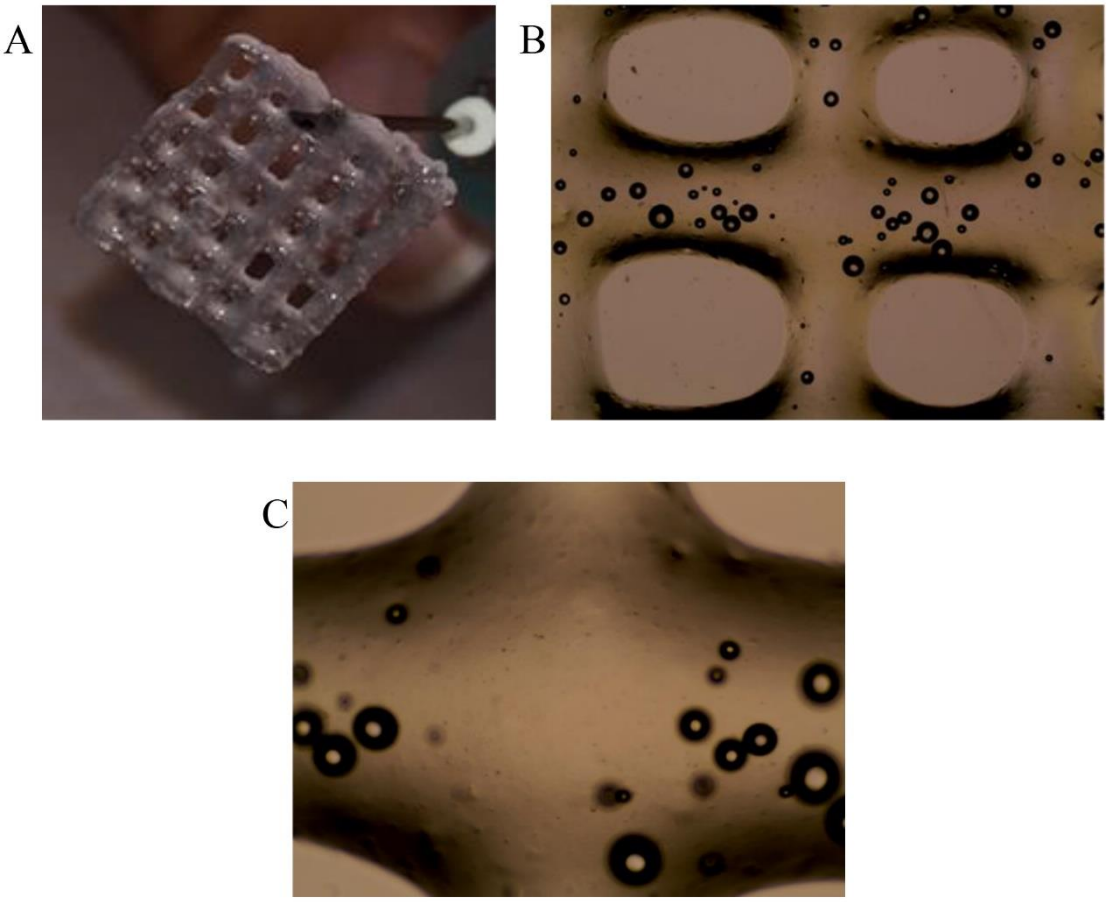

FIGURE 19. A) STRUCTURE PRINTED WITH CELLINK INKREDIBLE + AND CROSSLINKED WITH 2% CACL2 FOR 5 MIN. B) PHASE-CONTRAST MICROSCOPE IMAGE OF A PRINTED GRID. PRESENCE OF BUBBLES IN BIOINK DOES NOT INTERFERE WITH THE STABILITY OF STRUCTURE AND WITH CELL VIABILITY. C) MAGNIFICATION OF PHASE-CONTRAST IMAGE WHERE THEY CAN SEE CELLS DISPERSED IN A HYDROGEL

4.1.5. Cells organize themselves into 3D clumps

Moreover, it essential that cells maintain a 3D organization in order to improve the beneficial effects of 3D cell cultures. To confirm that, we included cells in the 4% SA / 4% GEL hydrogel, cultivated them for 5 days and finally we marked cells with GAPDH to detect

cells dispersed in 3D space and DAPI for the detection of nuclei. We noticed that cells grew in some clumps, to indicate that cells proliferate without migrating in the hydrogel. Fig. 20A shows a clump with a large number of cells, to indicate a good proliferation during 5 days of culture and the immobility of cells. With this kind of spatial organization, we can further investigate a single cell clone. Fig. 20B shows a 3D confocal reconstruction of a group of cells taken from the same immunofluorescence staining, where it is appreciable the three-dimensional proliferation of the cells within the hydrogel. Fig. 20C shows a reconstruction of z-stack in which two colonies can be seen, marked with DAPI. These two colonies were organized spatially in a 3D environment; they maintained their position during 5 days of proliferation, confirming the 3D structure of our hydrogel.

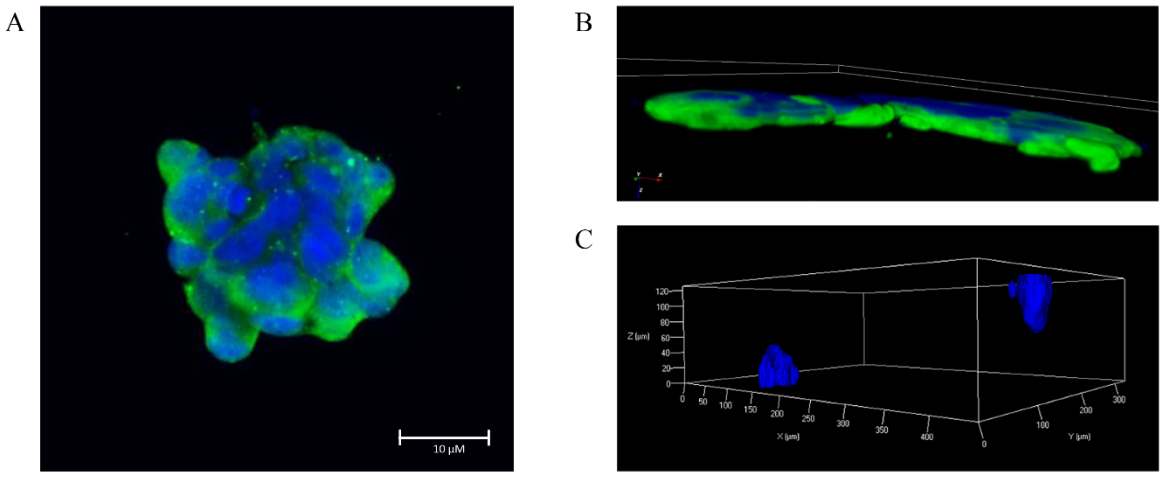

FIGURE 20. A) IMMUNOFLUORESCENCE IMAGE OF CELL COLONY 5 DAYS AFTER CULTURING. B) 3D RECONSTRUCTION OF CONFOCAL IMAGES. C) RENDERING IN 3 DIMENSIONS OF Z-STACK OBTAINED FROM AXIO IMAGER 2 IN WHICH CELLS WERE LABELED. THE IMAGE SHOWS THE FORMATION OF TWO AGGREGATION CLUSTERS TO INDICATE CELL PROLIFERATION WITHIN 5 DAYS OF CULTURING WITHIN BIOINK. IN GREEN: GAPDH, IN BLUE: DAPI

4.1.6. Analysis of repeatability

Based on preliminary results we decided to perform printing and repeatability tests using 4% SA / 4% GEL hydrogel without cells, to assess precision and printing quality

performed with Cellink INKREDIBLE+ bioplotter (Cellink AB, Sweden). We added a sample with 6% of SA and 4% GEL to verify if a highest concentration improves further the printability. In Table VII, all samples with temperatures and printing pressure are reported. We noticed that sample 2 and sample 4 required a lower print pressure than sample 1 and 3. Such difference is due to the presence of GEL, a dependent temperature biomaterial, which liquefies with increasing temperature. We could also appreciate the difference in printing pressure between sample 1, which is characterized by a higher concentration of SA, and sample 3, to indicate a major viscosity due to the high concentration of SA.

Sample	Alginate (SA)	Gelatin (GEL)	Printing Temperature	Printing Pressure (kPa)
1	6%	4%	25 °C	45-70
2	6%	4%	37 °C	30-50
3	4%	4%	25 °C	35-60
4	4%	4%	37 °C	30-40

TABLE VII. TWO COMPOSITIONS OF HYDROGEL, 6% SA AND 4% GEL, 4% SA AND 4% GEL, PRINTED EACH AT TWO DIFFERENT TEMPERATURES, 25°C AND 37°C. IN THE LAST COLUMN ARE REPORTED THE PRINTING PRESSURE (KPA) UTILIZED TO EXTRUDE HYDROGEL FOR PRINTING REPEATABILITY TESTS.

Moreover, we assessed printing repeatability to define which is the best concentration. This test consists of three printed grids with 10x10x1.2 mm dimensions testing daily fresh hydrogel, and tests were repeated 3 days consecutively. Each sample was imaged by a camera at distance of 12 cm, obtaining a planar picture. The images were acquired and analyzed by ImageJ software (ver. 1.50i, NIH) and grid gap and grid side (Fig. 21A) were measured. Fig. 21B and C indicate side and gap measures respectively, 9 tests for each sample. Dotted line indicates pre-established dimension set during printing set-up. This parameter was used to evaluate the printing accuracy. Both side and gap showed a statistically significant difference between sample 1 and sample 4 due to both printing temperature and SA concentration

(*p<0.05, Fig. 21B and C), while sides showed a statistically significant difference between sample 3 and sample 4, due to a different printing temperature (*p<0.05, Fig. 21B). Sample 2 and sample 4 showed a high standard deviation, due to a high variability during printing protocol, probably due to a major viscosity of hydrogel printed at 37°C. This data was also evaluated varying in the pre-established dimension of the printed grid. These results showed a major printing accuracy of sample 1, and for these reasons sample 1, composed of 6% SA and 4% GEL, printed at 25°C, and it was used for the next experiment.

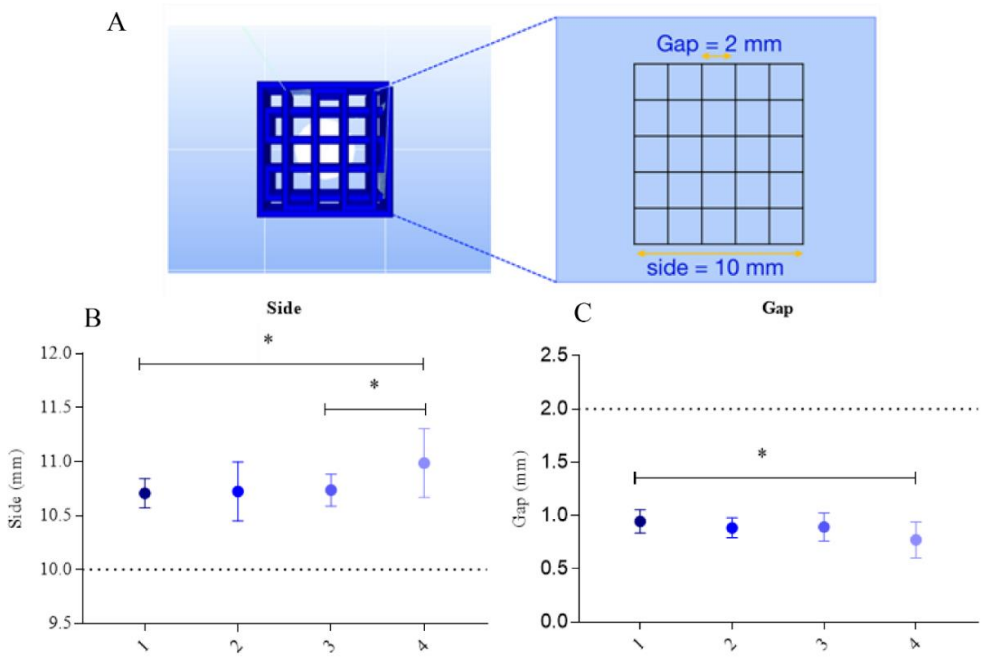

FIGURE 21. A) FREE-CAD IMAGE OF A GRID WITH GAP DIMENSION AND SIDE DIMENSION. B) DIMENSION RESULTS OF SIDE OF SAMPLE SHOWN IN TABLE 2. BOTH SAMPLE 1 AND SAMPLE 3 SHOW A STATISTICALLY SIGNIFICANT DIFFERENCE WITH SAMPLE 4 (* P<0.05). C) DIMENSION RESULTS OF GAP OF SAMPLE SHOWN IN TABLE 2. SAMPLE 1 SHOW A STATISTICALLY SIGNIFICANT DIFFERENCE WITH SAMPLE 4 (* P<0.05). DOTTED LINE INDICATES THE REFERENCE VALUE.

4.1.7. 3D bioprinting of SH-SY5Y cell line

Using repeatability results, we decided to encapsulate SH-SY5Y in hydrogel composed of 6% SA and 4% GEL, in order to obtain the best stiffness for the 3D structure. To

perform this experiment, we decided to use two types of geometry, 10x10x1.2 mm grid previously used, and a more complex structure, composed of two layers of 0.4 mm: the first layer is composed of only hydrogel, 10x10 mm, used to support second layer, composed of ten 1 mm strips with and without cells alternatively (Fig. 22A). This last geometry can be used for future biological study in co-culture with different cell phenotypes. We measured cell viability using LIVE/DEAD Cell Viability Assays immediately after printing process. Three measures were taken from the same staining and results was plotted as mean percentage of viability ± SD. Results in Fig. 22B shows a viability of 74% of each printed structure, grid and double extrusion. Printing process did not affect cell viability and maintained printed geometry. In addition, the geometry printed did not affect cell viability, opening the possibility to print many types of structures for different cell types. Fig. 22C shows the cell distribution, marked with α-tubulin.

We could see the exact distribution of cells in strip with cells and other strips without cells, to assess printing precision and the good viscosity of hydrogel that could lead cells to maintain their position after printing process.

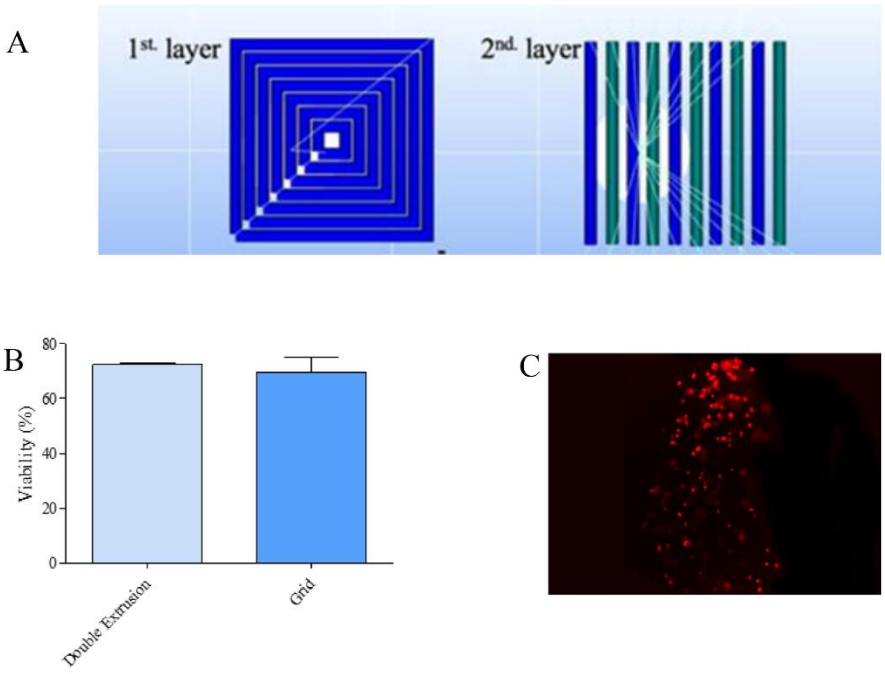

FIGURE 22. A) DOUBLE EXTRUSION SAMPLE. FIRST LAYER, CELL-FREE, AS SUPPORT, AND SECOND LAYER FORMED BY TEN ALTERNATED 1 MM STRIPES, ONE CELL-FREE AND ONE CELL-LADEN WITH SH-SY5Y. B) VIABILITY RESULTS OF SH-SY5Y CELL LINE ENCAPSULATED IN A 6% ALGINATE AND 4% GELATINE WITH TWO DIFFERENT GEOMETRIES. THE PRINTING PROCESS AND THE DIFFERENT GEOMETRY DID NOT AFFECT CELLULAR VIABILITY. C) IMMUNOFLUORESCENCE IMAGE OF DOUBLE EXTRUSION PRINTED CONSTRUCT, IMMEDIATELY AFTER PRINTING PROCESS. IN RED THE LABELLING WITH ALFA-TUBULIN, TO DETECT CELLS DISPERSE IN A HYDROGEL. PRECISION DEPOSITION OF MATERIAL WAS MAINTAINED.

4.2. Conductive hydrogel

The hydrogel we developed showed many advantages respect to classical 2D models, but obviously we decided to improve our 3D bioprinting technique, thus I visited for several months, the laboratory of 3D Bioprinting Center leaded by Prof. Paul Gatenholm, who kindly thought me many aspects of 3D cell cultures. We decided to develop a conductive hydrogel specific for neural cells, using cellulose, because of its high abundancy in Sweden, and CNTs, which provide conductivity.

4.2.1. Finding the best drying method for scaffolds

One of the main issues with NFC-based bioinks is their structural instability when used during classical biological experiments (214). Thus, it is important to harden the bioprinted scaffold by drying it. Moreover, drying is essential to allow the percolation of CNTs. We decided to try freeze-drying and air-drying techniques. Fig. 23A shows the differences between freeze-dried, air-dried and pristine (not dried) samples. The shape is maintained for both drying methods, but the dimensions of the air-dried samples are significantly reduced. Using the ImageJ software, we found that X and Y dimensions of air-dried samples are reduced by more than half compared to not dried samples, while the freeze-dried samples are reduced by about only 20 % (Fig. 23B). Moreover, the air-dried samples maintain an area of only 20 % of the not dried samples, while the area of freeze-dried samples is about 60 % of the not dried sample.

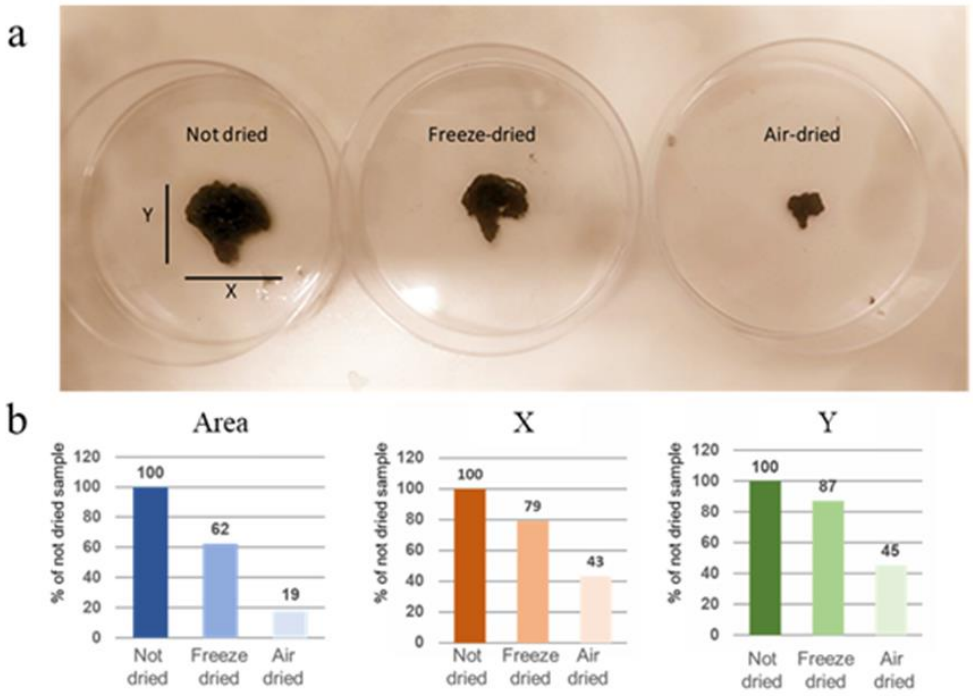

FIGURE 23. A) PHOTO OF NOT DRIED SCAFFOLD COMPARED TO FREEZE-DRIED AND AIR-DRIED SAMPLE. B) ANALYSIS OF X, Y AND AREA MEASURES USING IMAGEJ SOFTWARE. VALUES ARE % OF NOT DRIED SAMPLE.

4.2.2. The attachment of SH-SY5Y cells is charge-dependent

It is critical to fabricate ECM that can satisfy specific cell types, because cell adhesion usually occurs due to cell membrane proteins. As suggested by other works, NFC provides properties that mimic the neural extracellular matrix (ECM): cell-material interfacial interaction, optimal stiffness, high surface to volume ratios and high porosity (215-217).

We seeded cells on scaffolds printed using bioinks that have different level of oxidation and t different number of charged functional groups. In order to evaluate the effect of charges on cell attachment, one ink was composed of a non-charged NFC (NFC1, StoraEnso, Sweden), while the other was based on negatively charged NFC (NFC8, StoraEnso, Sweden). As shown in Fig. 24, cells have attached only to the non-charged NFC1, suggesting that the abundant negative charges of NFC8 repulse cells that have a negatively charged membrane (218).

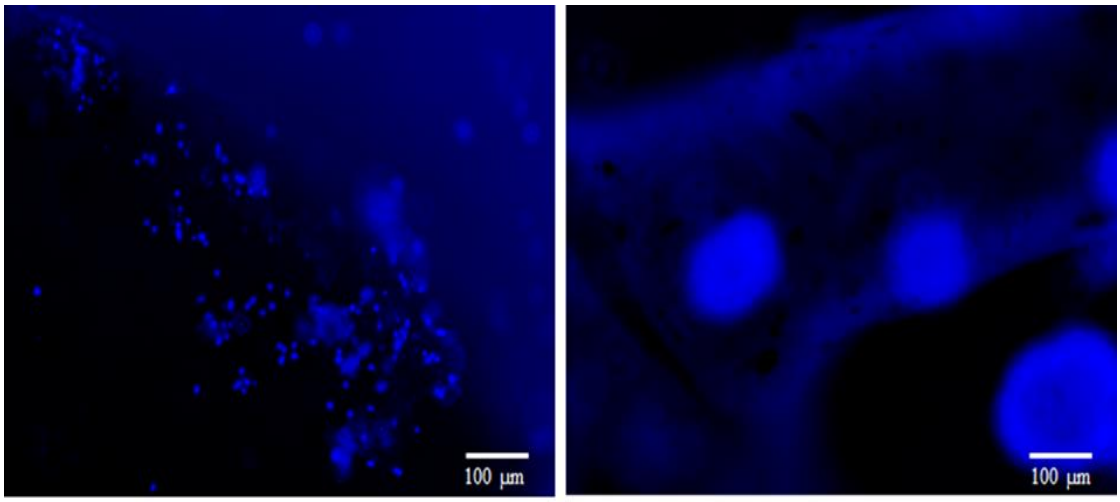

FIGURE 24. CELLS ATTACHED TO NFC1 SCAFFOLD (LEFT) WHILE THEY SEEM TO NOT ATTACH TO THE NEGATIVELY CHARGED NFC8 SCAFFOLD (RIGHT). CELLS NUCLEI WERE STAINED IN BLUE USING NUCBLUE. SCALE BAR: 100 µM.

4.2.3. Functionalization with CNTs allows conductivity improvement of NFC

NFC is an electrically inert material; thus, it is necessary to functionalize it with conductive additives. We mixed NFC with SWCNTs that previously have been characterized as a biocompatible material (219).

The conductivity of NFC/SWCNT mixtures with various CNT content was measured at both crosslinked and non-crosslinked states. As shown in Fig. 25, non-crosslinked samples have rather high electrical conductivity with a mean of 1.9 S/cm and 0.12 S/cm respectively for the bioink with 20% and 10% of CNTs, which means that the percolation threshold of CNTs is reached (220). According to previous works, this level of conductivity is high enough to promote neural cell development (221, 222). On the contrary, the crosslinked bioink with 10 % of CNTs entirely loses ability to conduct electrons, while the one with 20% of CNTs has very low conductivity. We can assume that crosslinked alginate network penetrates through SWCNTs, obstructing their interconnectivity and leading to the undesired effect of lost conductivity. Moreover, crosslinking affects the repeatability of measurements, also leading to the high value of standard error, which can be explained by inhomogeneous distribution of alginate clusters during crosslinking.

NAME	CNF	CNTs	Alginate	Cross linking	Cond. (S/cm)
Gel 1	70%	10%	20%	✓	0
Gel 2	60%	20%	20%	✓	$1.8x10^{-4}$
Gel 3	70%	10%	20%	×	0.12
Gel 4	60%	20%	20%	×	1.9

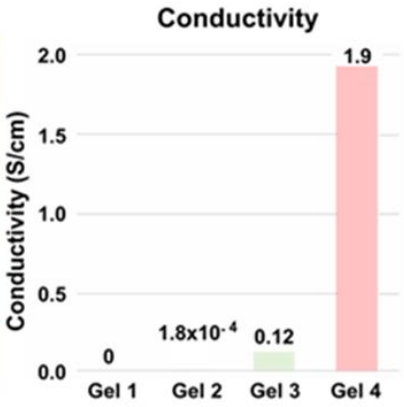

FIGURE 25. ANALYSIS OF THE EFFECT OF CROSSLINKING IN CONDUCTIVITY AND EVALUATION OF CONDUCTIVE PROPERTIES OF SCAFFOLDS COMPOSED OF EITHER 10% OR 20% OF CNTS. CROSSLINKING SEEMS TO PRODUCE LOSS OF CONDUCTIVE EFFECT OF CNTS, WHILE NOT CROSSLINKED SCAFFOLDS HAVE GOOD CONDUCTIVITY (0.12 AND 1.9 S/CM RESPECTIVELY FOR 10% AND 20% OF CNTS).

4.2.4. The conductive ink improves differentiation of SH-SY5Y cells

Moreover, we want to study the effect of the conductive bioinks on the neural cell differentiation. Interestingly, we could not observe any cells on the most conductive 20 % CNTs bioink constructs, while there were many cells on less conductive 10 % CNT constructs. Probable cell death or detachment from the 20% CNT-inks could have happened due to several factors such as increased hydrophobicity and stiffness of scaffolds with the addition of more CNTs impeding strong connection with cell proteins. As expected, cells cultivated with differentiation factors on pure NFC films, matured into neural cells after 10 days of differentiation process, failing to generate a realistic neural network (Fig. 26A). Moreover, when they were not exposed to differentiation medium, they did not differentiate and maintain an undifferentiated shape (Fig. 26B). On the contrary, when cells were cultivated for 10 days in presence of differentiation factors on the 10 % CNTs bioink constructs, they highly differentiated, organizing into an extended neural network with many connections between cells (Fig. 26C). Surprisingly, when cells were cultivated on 10 % CNTs bioink constructs without differentiation factors, they managed to show great progress in differentiation after 10 days (Fig. 26D), starting to generate a neural network presenting synapses (Fig. 26E).

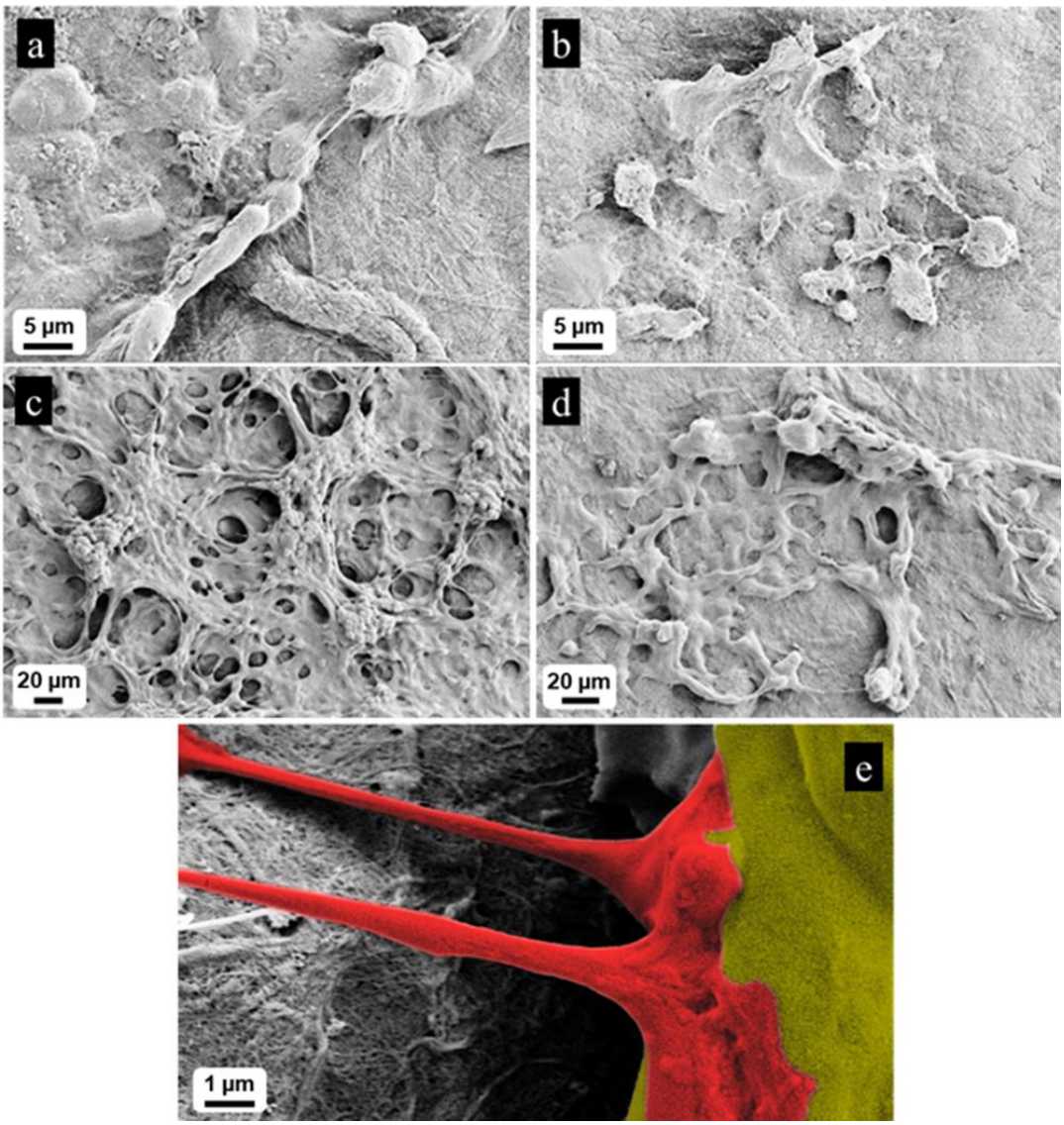

FIGURE 26. A) CELLS CULTIVATED ON PURE NFC SCAFFOLD IN PRESENCE OF DIFFERENTIATION FACTORS. SCALE BAR: 5 µM. B) CELLS CULTIVATED ON PURE NFC SCAFFOLD WITHOUT DIFFERENTIATION FACTORS. SCALE BAR: 5 µM. C) CELLS CULTIVATED ON NFC/10% CNTS WITH DIFFERENTIATION FACTORS. SCALE BAR: 20 µM. D) CELLS CULTIVATED ON NFC/10% CNTS WITHOUT DIFFERENTIATION FACTORS. SCALE BAR: 20 µM. E) EXAMPLE OF A SYNAPSE FOUND IN THE SAMPLE OF CELLS CULTIVATED IN CONDUCTIVE SCAFFOLD WITHOUT DIFFERENTIATION FACTORS. SCALE BAR: 1 µM.

We decided to analyze cells additionally with confocal microscopy. Thus, we seeded cells on pure NFC and on 10 % CNTs cellulose films. After 10 days, we fixed and stained cells using Actingreen in order to image cells morphology. We can see in Fig. 27A that cells cultivated on pure NFC films present a typical undifferentiated cancer cell shape with immature phenotype; they have sharp edges and tend to generate colonies. Moreover, they do

not have neurites. On the contrary, cells on 10 % CNTs films appear differentiated, with many and long neurites (white arrows, Fig. 27B). We can see a magnification of 10 % CNTs samples, showing a neural network between 3 cells (Fig. 27C) and a neural cell with a very long neurite (about 150 µm) that seems to contact another cell (Fig. 27D).

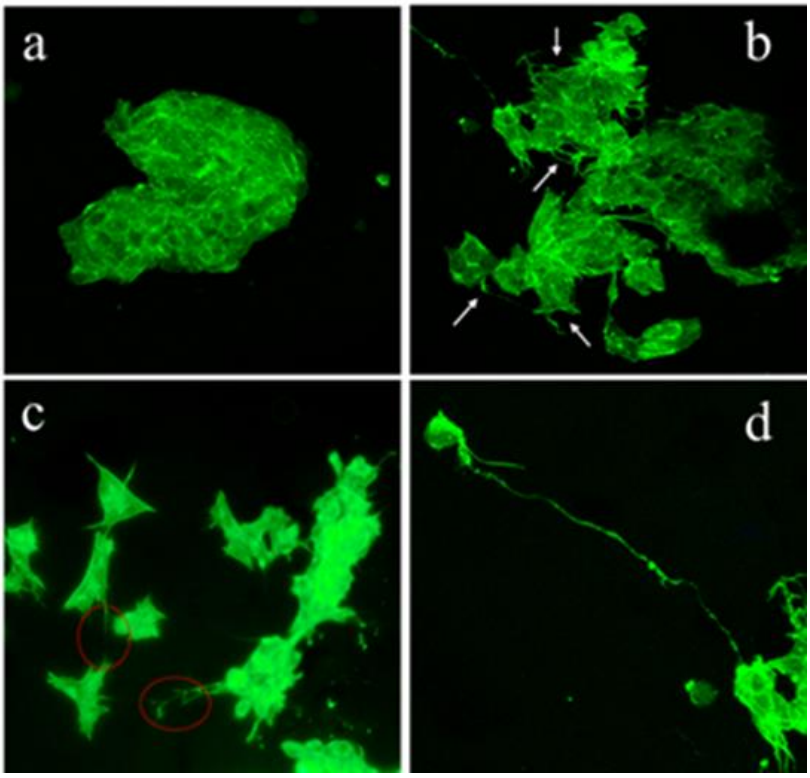

FIGURE 27. A) CELLS CULTIVATED ON PURE NFC WITHOUT DIFFERENTIATION FACTORS. B) CELLS CULTIVATED ON CONDUCTIVE SCAFFOLD WITHOUT DIFFERENTIATION. C) INTERACTION BETWEEN NEURAL CELLS CULTIVATED ON CONDUCTIVE INK. D) VERY LONG NEURITE OF A NEURAL CELL CULTIVATED ON C.

Finally, in order to confirm the morphologic data, we analyzed the expression of differentiation markers by RT-qPCR. We investigated TUBB3, a marker that increases in differentiated cells, and Nestin, a marker that decreases during differentiation. In line with previous results, we found (Fig. 28A) an increase in TUBB3 gene expression in the cells cultivated on 10 % CNTs bioink construct compared to the cells cultivated on pure NFC and to the negative control (cells not cultivated). Moreover, Nestin gene expression decreased in cells cultivated on both bioink constructs, compared to the negative control, especially on the

samples cultivated on the 10 % CNTs bioink (Fig. 28B). The small decrease on cells cultivated on pure NFC is probably due to the time of cultivation.

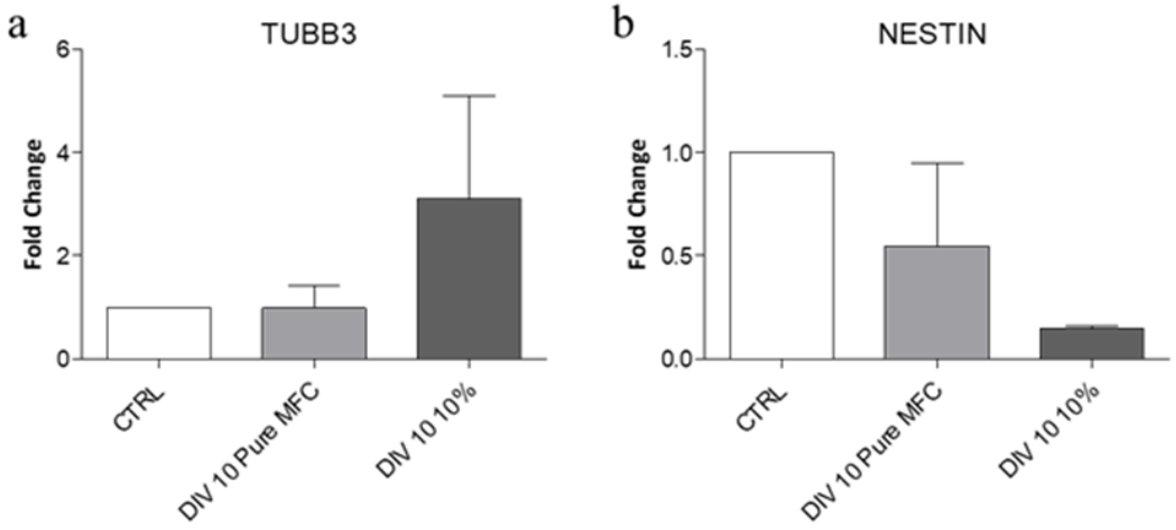

FIGURE 28. A) TUBB3 EXPRESSION, A MATURE NEURON MARKER, INCREASED WHEN CELLS WERE CULTIVATED ON CONDUCTIVE INK. B) NESTIN EXPRESSION, AN IMMATURE NEURON MARKER, DECREASED IN CELLS CULTIVATED ON CONDUCTIVE INK.

4.3. iPSCs

4.3.1. Fibroblasts and PBMCs reprogramming

During the first step of hydrogels development, we started to reprogram fibroblasts and PBMCs of both neurodegenerative patients and healthy controls, using CytoTune™-iPS 2.0 Sendai Reprogramming Kit (ThermoFisher, Italy). Firstly, we confirmed the efficiency of reprogramming by morphological analysis. As we can see in Fig. 29, over time cells changed their shape and their spatial organization, forming colonies of round-shaped cells.

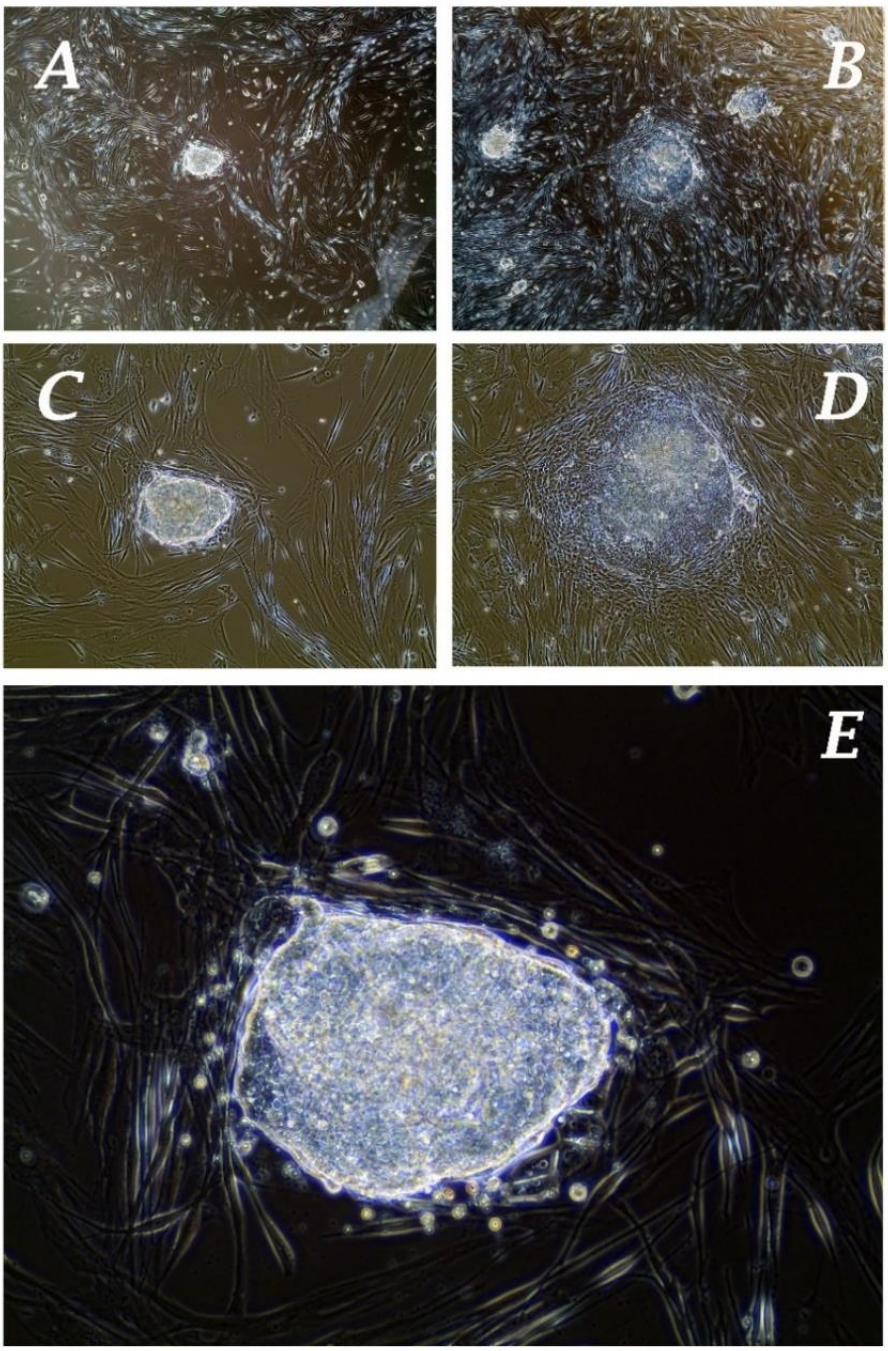

FIGURE 29. CELLS REPROGRAMMING STEP. A) CELLS AFTER 7 DAYS FROM TRANSDUCTION. B) CELLS AFTER 14 DAYS FROM TRANSDUCTION. C) IPSCS AFTER 21 DAYS FROM REPROGRAMMING. D) BIG IPSCS COLONY AFTER 28 DAYS. E) MAGNIFICATION OF D.

We confirmed the efficient cells reprogramming by analysing the products of transgene by RT-PCR. In particular, we found (Fig. 30) the expression of virus genome (SeV) the 3 transgenes (Klf4, c-Myc, KOS).

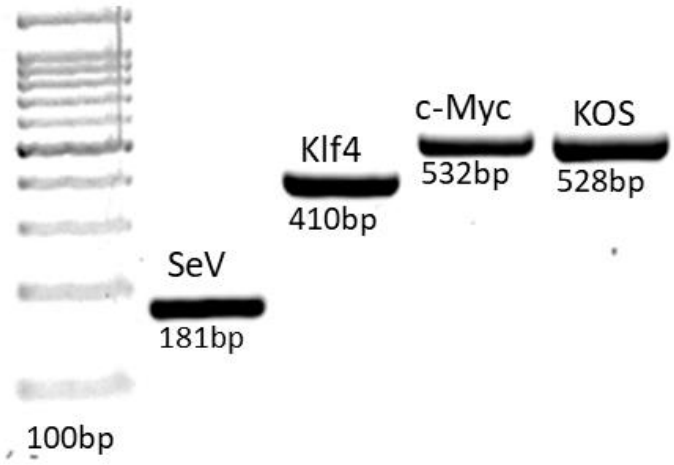

FIGURE 30. EXPRESSION OF GENES TRANSFECTED WITH SENDAI VIRUS: SEV, KLF4, C-MYC, KOS.

Finally, we confirmed the stemness of reprogrammed iPSCs, utinsg PSC 4-Marker Immunocytochemistry Kit (ThermoFisher, Italy), which marks SSEA4 (Stage-specific embryonic antigen-4), OCT4 (octamer-binding transcription factor 4), SOX2 (SRY-Box2) and TRA-1-60 (Tumor Rejection Antigen 1-60). All the cells of the colonies, presented the expression of such markers, indicating an optimal efficiency of transfection and reprogramming processes (Fig. 31).

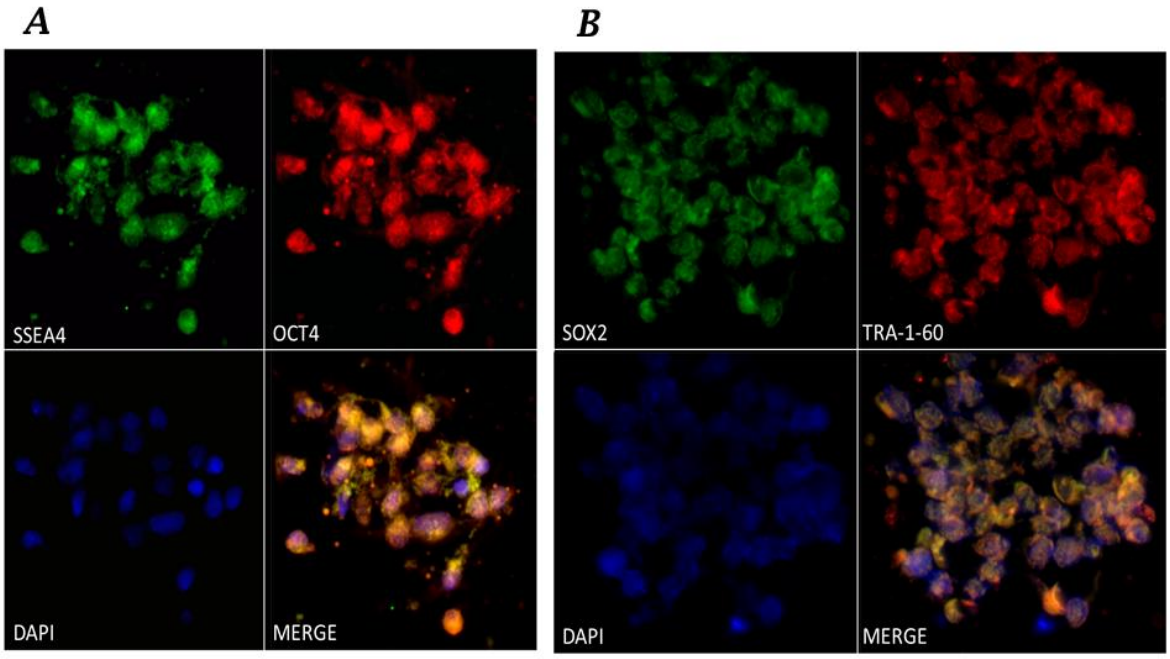

FIGURE 31. PROTEIN EXPRESSION OF STEMNESS MARKER.

4.3.2. iPSCs bioprinting

Finally, we wanted to include iPSCs into the gelatin-based alginate, in order to verify cell viability after bioprinting process. Thus, we measured cell viability on 6% SA/ 4% GEL after 0 (T0), 3 (T3) and 7 (T7) days. As showed in Fig. 32, bioprinting did not affected cell viability and also cultivation into the hydrogel structure did not interfere with viability and proliferation, indicating a good biocompatibility of the hydrogel also using iPSCs.

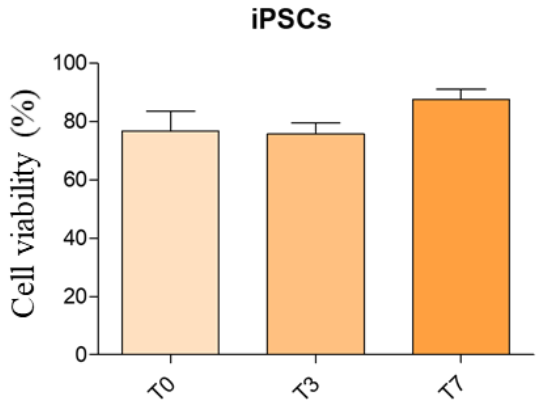

FIGURE 32. CELL VIABILITY AFTER 0, 3 AND 7 DAYS FROM BIOPRINTING PROCESS.

5. DISCUSSION AND CONCLUSION

3D bioprinting is an emerging technique, which consists in printing the hydrogel with a 3D bioplotter. The materials that compose the hydrogel can be various and they can have many specific features. Several cell types are actually used in 3D cell culture field, to create several tissues, e g. cartilage, bone, and heart. Actually, studies that combine neural cells and 3D bioprinting are poor, badly characterized and do not have a standard hydrogel composition, due to a frailty of the neural cells and a lack of a direct applicability in clinical therapies and in regenerative medicine. We tested many types of gelatine-based and conductive hydrogels concentrations, combining them with many types of cells, including HeLa, SH-SY5Y and iPSCs. We can conclude that the gelatin-based bioink we developed, combined with both HeLa and SH-SY5Y cell lines, improves cellular proliferation and viability, compared with 2D standard cultures, obtaining in less time a large number of cells, with an increased viability. With such bioink, the three-dimensionality, fundamental for cell-to-cell communication, more physiologically relevant for further mechanistic studies, is also maintained. The printing process was standardized in term of print pression, temperature and rapidity, to print hydrogel composed of SA and GEL with Cellink INKREDIBLE+ bioplotter, with a good repeatability and a robust preparation protocol. Viability results of SH-SY5Y encapsulated in hydrogel composed of SA-GEL after printing process also showed good results, demonstrating how 3D bioprinting will be suitable for printing neural cells. It is also necessary to establish a repeatable 3D bioprinting protocol, which leads to control cells and differentiation factors deposition, to facilitate cell organization, because actually matrigel-based cell cultures do not guarantee a defined 3D spatial assembling.

Moreover, we developed a conductive ink cellulose-based, because conductivity seems to help neural cells cultivation, while NFC seems to provide many properties that mimic the ECM found in the neural tissue, because of the stiffness, and the high surface/volume ratio due to its porosity. Moreover, NFC was found to enhance cell-material interfacial interaction, probably because of the presence of integrins in cell membran.

Another problem that we faced was the mechanical instability of printed cellulose, because of the high content of water, thus, the printed scaffold structure was dried in order to stabilize the structure. Notably, we found freeze drying as the best drying technique, which allows maintenance of the structure, while dimensions are reduced by only about 20%. As the result, we obtained a more suitable scaffold on which cells can be easily cultivated for biological experiments. Moreover, our results suggest that the surface properties of the scaffold play key roles in the cell attachment, because of membrane's proteins interactions with the scaffold and the repulsion caused by the negatively charged cell membrane, thus negatively charged scaffold do not allow cell attachment (218).

The peculiar feature of neural cells to conduct electrical stimuli and to transmit it to other cells shall be utilized via making electrically conductive scaffolds. For example, previously studies reported the beneficial effect of cultivating neural cells on conductive material (221, 222). Thus, we firstly investigated the conductive properties of hydrogels composed of NFC/CNTs and the effect of crosslinking, finding that both 10% and 20% concentrations of CNTs provide enough electrical properties for neural cells. Finally, we investigated the effect of such electrical conductivity, finding that CNTs promote neural cells differentiation without providing external electrical stimulation. The maturation of SH-SY5Y cells into a more neural phenotype could be explained with the ability of the scaffold to transfer current between separated neurons. The conductive surfaces can even promote cell differentiation and generation of a neural network without specific differentiation factors. Our data provided evidences that in some cell lines conductive scaffolds could be replaced to neural differentiation factors.

Finally, our first aim is to generate a suitable and reproducible neural 3D tissue in vitro in order to obtain a more realistic model for studying NDDs. Thus, we want to exploit the pluripotency of iPSCs to differentiate into many cell types, including neurons, but also glial cells, like astrocytes, oligodendrocytes and microglia, with which brain tissue is composed of.

Firstly, we reprogrammed several lines of fibroblasts and PBMCs derived from NDDs and healthy controls. Our protocol resulted highly efficient and reproducible. In a second time we included iPSCs onto the gelatin-based hydrogel, but in feature we want to combine conductive scaffold and iPSCs to generate a neural model of NDDs.

In conclusion, 3D bioprinting represents one of the main pivotal techniques in the future, because it allows to cultivate cells in a more realistic way respect to traditional 2D cells. The gelatin-based hydrogel convinced us that 3D cell cultures have a big potentiality because they can improve proliferation without affecting viability. Moreover, the presence of a 3D environment mimics in a better way physiological conditions of human tissues. The conductive hydrogel showed an intriguing characteristic, the capacity to help the maturation and differentiation of neural cells. Such hydrogel, combined with iPSCs technology, opens many new scenarios in the innovative field of 3D bioprinting, allowing for the first time the generation of a realistic neural tissue.

6. REFERENCES

1. Peden AH, Ironside JW. Molecular pathology in neurodegenerative diseases. Curr Drug Targets. 2012;13(12):1548-59.
2. Hagenaars SP, Radaković R, Crockford C, Fawns-Ritchie C, Harris SE, Gale CR, et al. Genetic risk for neurodegenerative disorders, and its overlap with cognitive ability and physical function. PLoS One. 2018;13(6):e0198187.
3. Schlachetzki JC, Saliba SW, Oliveira AC. Studying neurodegenerative diseases in culture models. Rev Bras Psiquiatr. 2013;35 Suppl 2:S92-100.
4. Becker LA, Huang B, Bieri G, Ma R, Knowles DA, Jafar-Nejad P, et al. Therapeutic reduction of ataxin-2 extends lifespan and reduces pathology in TDP-43 mice. Nature. 2017;544(7650):367-71.
5. Elden AC, Kim HJ, Hart MP, Chen-Plotkin AS, Johnson BS, Fang X, et al. Ataxin-2 intermediate-length polyglutamine expansions are associated with increased risk for ALS. Nature. 2010;466(7310):1069-75.
6. Gitler AD, Chesi A, Geddie ML, Strathearn KE, Hamamichi S, Hill KJ, et al. Alpha-synuclein is part of a diverse and highly conserved interaction network that includes PARK9 and manganese toxicity. Nat Genet. 2009;41(3):308-15.
7. Gitler AD, Dhillon P, Shorter J. Neurodegenerative disease: models, mechanisms, and a new hope. Dis Model Mech. 2017;10(5):499-502.
8. McKhann GM, Knopman DS, Chertkow H, Hyman BT, Jack CR, Kawas CH, et al. The diagnosis of dementia due to Alzheimer's disease: recommendations from the National Institute on Aging-Alzheimer's Association workgroups on diagnostic guidelines for Alzheimer's disease. Alzheimers Dement. 2011;7(3):263-9.
9. Shampo MA, Kyle RA, Steensma DP. Alois Alzheimer--Alzheimer disease. Mayo Clin Proc. 2013;88(12):e155.
10. Masters CL, Bateman R, Blennow K, Rowe CC, Sperling RA, Cummings JL. Alzheimer's disease. Nat Rev Dis Primers. 2015;1:15056.
11. Ferri CP, Prince M, Brayne C, Brodaty H, Fratiglioni L, Ganguli M, et al. Global prevalence of dementia: a Delphi consensus study. Lancet. 2005;366(9503):2112-7.
12. Mayeux R, Stern Y. Epidemiology of Alzheimer disease. Cold Spring Harb Perspect Med. 2012;2(8).
13. Evans DA, Funkenstein HH, Albert MS, Scherr PA, Cook NR, Chown MJ, et al. Prevalence of Alzheimer's disease in a community population of older persons. Higher than previously reported. JAMA. 1989;262(18):2551-6.
14. Cacace R, Sleegers K, Van Broeckhoven C. Molecular genetics of early-onset Alzheimer's disease revisited. Alzheimers Dement. 2016;12(6):733-48.
15. Karch CM, Goate AM. Alzheimer's disease risk genes and mechanisms of disease pathogenesis. Biol Psychiatry. 2015;77(1):43-51.
16. Goate A, Chartier-Harlin MC, Mullan M, Brown J, Crawford F, Fidani L, et al. Segregation of a missense mutation in the amyloid precursor protein gene with familial Alzheimer's disease. Nature. 1991;349(6311):704-6.
17. Levy-Lahad E, Wasco W, Poorkaj P, Romano DM, Oshima J, Pettingell WH, et al. Candidate gene for the chromosome 1 familial Alzheimer's disease locus. Science. 1995;269(5226):973-7.
18. Sherrington R, Froelich S, Sorbi S, Campion D, Chi H, Rogaeva EA, et al. Alzheimer's disease associated with mutations in presenilin 2 is rare and variably penetrant. Hum Mol Genet. 1996;5(7):985-8.
19. Athan ES, Williamson J, Ciappa A, Santana V, Romas SN, Lee JH, et al. A founder mutation in presenilin 1 causing early-onset Alzheimer disease in unrelated Caribbean Hispanic families. JAMA. 2001;286(18):2257-63.
20. Tanzi RE. The genetics of Alzheimer disease. Cold Spring Harb Perspect Med. 2012;2(10).

21. Corder EH, Saunders AM, Strittmatter WJ, Schmechel DE, Gaskell PC, Small GW, et al. Gene dose of apolipoprotein E type 4 allele and the risk of Alzheimer's disease in late onset families. Science. 1993;261(5123):921-3.
22. Chartier-Harlin MC, Parfitt M, Legrain S, Pérez-Tur J, Brousseau T, Evans A, et al. Apolipoprotein E, epsilon 4 allele as a major risk factor for sporadic early and late-onset forms of Alzheimer's disease: analysis of the 19q13.2 chromosomal region. Hum Mol Genet. 1994;3(4):569-74.
23. Yu JT, Tan L, Hardy J. Apolipoprotein E in Alzheimer's disease: an update. Annu Rev Neurosci. 2014;37:79-100.
24. Jones L, Holmans PA, Hamshere ML, Harold D, Moskvina V, Ivanov D, et al. Genetic evidence implicates the immune system and cholesterol metabolism in the aetiology of Alzheimer's disease. PLoS One. 2010;5(11):e13950.
25. Lambert JC, Ibrahim-Verbaas CA, Harold D, Naj AC, Sims R, Bellenguez C, et al. Meta-analysis of 74,046 individuals identifies 11 new susceptibility loci for Alzheimer's disease. Nat Genet. 2013;45(12):1452-8.
26. Carmona S, Hardy J, Guerreiro R. The genetic landscape of Alzheimer disease. Handb Clin Neurol. 2018;148:395-408.
27. Dauer W, Przedborski S. Parkinson's disease: mechanisms and models. Neuron. 2003;39(6):889-909.
28. Hirsch EC, Jenner P, Przedborski S. Pathogenesis of Parkinson's disease. Mov Disord. 2013;28(1):24-30.
29. de Lau LM, Breteler MM. Epidemiology of Parkinson's disease. Lancet Neurol. 2006;5(6):525-35.
30. Lee A, Gilbert RM. Epidemiology of Parkinson Disease. Neurol Clin. 2016;34(4):955-65.
31. Katzenschlager R, Head J, Schrag A, Ben-Shlomo Y, Evans A, Lees AJ, et al. Fourteen-year final report of the randomized PDRG-UK trial comparing three initial treatments in PD. Neurology. 2008;71(7):474-80.
32. Lees AJ, Hardy J, Revesz T. Parkinson's disease. Lancet. 2009;373(9680):2055-66.
33. Gillies GE, Pienaar IS, Vohra S, Qamhawi Z. Sex differences in Parkinson's disease. Front Neuroendocrinol. 2014;35(3):370-84.
34. Georgiev D, Hamberg K, Hariz M, Forsgren L, Hariz GM. Gender differences in Parkinson's disease: A clinical perspective. Acta Neurol Scand. 2017;136(6):570-84.
35. Martinez-Martin P, Falup Pecurariu C, Odin P, van Hilten JJ, Antonini A, Rojo-Abuin JM, et al. Gender-related differences in the burden of non-motor symptoms in Parkinson's disease. J Neurol. 2012;259(8):1639-47.
36. Noyce AJ, Bestwick JP, Silveira-Moriyama L, Hawkes CH, Giovannoni G, Lees AJ, et al. Meta-analysis of early nonmotor features and risk factors for Parkinson disease. Ann Neurol. 2012;72(6):893-901.
37. Polymeropoulos MH, Lavedan C, Leroy E, Ide SE, Dehejia A, Dutra A, et al. Mutation in the alpha-synuclein gene identified in families with Parkinson's disease. Science. 1997;276(5321):2045-7.
38. Corti O, Lesage S, Brice A. What genetics tells us about the causes and mechanisms of Parkinson's disease. Physiol Rev. 2011;91(4):1161-218.
39. Sidransky E, Lopez G. The link between the GBA gene and parkinsonism. Lancet Neurol. 2012;11(11):986-98.
40. Sidransky E, Nalls MA, Aasly JO, Aharon-Peretz J, Annesi G, Barbosa ER, et al. Multicenter analysis of glucocerebrosidase mutations in Parkinson's disease. N Engl J Med. 2009;361(17):1651-61.
41. Kalia LV, Lang AE. Parkinson's disease. Lancet. 2015;386(9996):896-912.

42. Bezard E, Przedborski S. A tale on animal models of Parkinson's disease. Mov Disord. 2011;26(6):993-1002.
43. Braak H, Del Tredici K, Rüb U, de Vos RA, Jansen Steur EN, Braak E. Staging of brain pathology related to sporadic Parkinson's disease. Neurobiol Aging. 2003;24(2):197-211.
44. Hawkes CH, Del Tredici K, Braak H. Parkinson's disease: a dual-hit hypothesis. Neuropathol Appl Neurobiol. 2007;33(6):599-614.
45. Visanji NP, Brooks PL, Hazrati LN, Lang AE. The prion hypothesis in Parkinson's disease: Braak to the future. Acta Neuropathol Commun. 2013;1:2.
46. Nalls MA, Pankratz N, Lill CM, Do CB, Hernandez DG, Saad M, et al. Large-scale meta-analysis of genome-wide association data identifies six new risk loci for Parkinson's disease. Nat Genet. 2014;46(9):989-93.
47. Körner S, Kollewe K, Fahlbusch M, Zapf A, Dengler R, Krampfl K, et al. Onset and spreading patterns of upper and lower motor neuron symptoms in amyotrophic lateral sclerosis. Muscle Nerve. 2011;43(5):636-42.
48. Charcot J-M, Joffroy A. Deux cas d'atrophie musculaire progressive avec lesions de la substance grise et des faisceaux antero-lateraux de la moelle epiniere. Arch Physiol Neurol Pathol1869. p. 744–54.
49. Rowland LP, Shneider NA. Amyotrophic lateral sclerosis. N Engl J Med. 2001;344(22):1688-700.
50. Logroscino G, Traynor BJ, Hardiman O, Chiò A, Mitchell D, Swingler RJ, et al. Incidence of amyotrophic lateral sclerosis in Europe. J Neurol Neurosurg Psychiatry. 2010;81(4):385-90.
51. Haverkamp LJ, Appel V, Appel SH. Natural history of amyotrophic lateral sclerosis in a database population. Validation of a scoring system and a model for survival prediction. Brain. 1995;118 (Pt 3):707-19.
52. Logroscino G, Traynor BJ, Hardiman O, Chio' A, Couratier P, Mitchell JD, et al. Descriptive epidemiology of amyotrophic lateral sclerosis: new evidence and unsolved issues. J Neurol Neurosurg Psychiatry. 2008;79(1):6-11.
53. Rosen DR, Siddique T, Patterson D, Figlewicz DA, Sapp P, Hentati A, et al. Mutations in Cu/Zn superoxide dismutase gene are associated with familial amyotrophic lateral sclerosis. Nature. 1993;362(6415):59-62.
54. Andersen PM, Al-Chalabi A. Clinical genetics of amyotrophic lateral sclerosis: what do we really know? Nat Rev Neurol. 2011;7(11):603-15.
55. Renton AE, Chiò A, Traynor BJ. State of play in amyotrophic lateral sclerosis genetics. Nat Neurosci. 2014;17(1):17-23.
56. Neumann M, Sampathu DM, Kwong LK, Truax AC, Micsenyi MC, Chou TT, et al. Ubiquitinated TDP-43 in frontotemporal lobar degeneration and amyotrophic lateral sclerosis. Science. 2006;314(5796):130-3.
57. Corcia P, Couratier P, Blasco H, Andres CR, Beltran S, Meininger V, et al. Genetics of amyotrophic lateral sclerosis. Rev Neurol (Paris). 2017;173(5):254-62.
58. Vance C, Rogelj B, Hortobágyi T, De Vos KJ, Nishimura AL, Sreedharan J, et al. Mutations in FUS, an RNA processing protein, cause familial amyotrophic lateral sclerosis type 6. Science. 2009;323(5918):1208-11.
59. Kwiatkowski TJ, Bosco DA, Leclerc AL, Tamrazian E, Vanderburg CR, Russ C, et al. Mutations in the FUS/TLS gene on chromosome 16 cause familial amyotrophic lateral sclerosis. Science. 2009;323(5918):1205-8.
60. Valdmanis PN, Daoud H, Dion PA, Rouleau GA. Recent advances in the genetics of amyotrophic lateral sclerosis. Curr Neurol Neurosci Rep. 2009;9(3):198-205.
61. Lattante S, Rouleau GA, Kabashi E. TARDBP and FUS mutations associated with amyotrophic lateral sclerosis: summary and update. Hum Mutat. 2013;34(6):812-26.

62. Johnson JO, Mandrioli J, Benatar M, Abramzon Y, Van Deerlin VM, Trojanowski JQ, et al. Exome sequencing reveals VCP mutations as a cause of familial ALS. Neuron. 2010;68(5):857-64.
63. DeJesus-Hernandez M, Mackenzie IR, Boeve BF, Boxer AL, Baker M, Rutherford NJ, et al. Expanded GGGGCC hexanucleotide repeat in noncoding region of C9ORF72 causes chromosome 9p-linked FTD and ALS. Neuron. 2011;72(2):245-56.
64. Shaw PJ. Molecular and cellular pathways of neurodegeneration in motor neurone disease. J Neurol Neurosurg Psychiatry. 2005;76(8):1046-57.
65. Gonzalez de Aguilar JL, Echaniz-Laguna A, Fergani A, René F, Meininger V, Loeffler JP, et al. Amyotrophic lateral sclerosis: all roads lead to Rome. J Neurochem. 2007;101(5):1153-60.
66. Wijesekera LC, Leigh PN. Amyotrophic lateral sclerosis. Orphanet J Rare Dis. 2009;4:3.
67. Okamoto K, Mizuno Y, Fujita Y. Bunina bodies in amyotrophic lateral sclerosis. Neuropathology. 2008;28(2):109-15.
68. Pasinelli P, Brown RH. Molecular biology of amyotrophic lateral sclerosis: insights from genetics. Nat Rev Neurosci. 2006;7(9):710-23.
69. Blackstone C. Huntington's disease: from disease mechanisms to therapies. Drug Discov Today. 2014;19(7):949-50.
70. Wexler A. Huntington's Disease - A Brief Historical Perspective. J Huntingtons Dis. 2012;1(1):3-4.
71. Rawlins MD, Wexler NS, Wexler AR, Tabrizi SJ, Douglas I, Evans SJ, et al. The Prevalence of Huntington's Disease. Neuroepidemiology. 2016;46(2):144-53.
72. Warby SC, Visscher H, Collins JA, Doty CN, Carter C, Butland SL, et al. HTT haplotypes contribute to differences in Huntington disease prevalence between Europe and East Asia. Eur J Hum Genet. 2011;19(5):561-6.
73. Ghosh R, Tabrizi SJ. Clinical Features of Huntington's Disease. Adv Exp Med Biol. 2018;1049:1-28.
74. Snell RG, MacMillan JC, Cheadle JP, Fenton I, Lazarou LP, Davies P, et al. Relationship between trinucleotide repeat expansion and phenotypic variation in Huntington's disease. Nat Genet. 1993;4(4):393-7.
75. Rubinsztein DC, Leggo J, Coles R, Almqvist E, Biancalana V, Cassiman JJ, et al. Phenotypic characterization of individuals with 30-40 CAG repeats in the Huntington disease (HD) gene reveals HD cases with 36 repeats and apparently normal elderly individuals with 36-39 repeats. Am J Hum Genet. 1996;59(1):16-22.
76. Zühlke C, Riess O, Bockel B, Lange H, Thies U. Mitotic stability and meiotic variability of the (CAG)n repeat in the Huntington disease gene. Hum Mol Genet. 1993;2(12):2063-7.
77. Kremer B, Almqvist E, Theilmann J, Spence N, Telenius H, Goldberg YP, et al. Sex-dependent mechanisms for expansions and contractions of the CAG repeat on affected Huntington disease chromosomes. Am J Hum Genet. 1995;57(2):343-50.
78. Barbeau A. Parental ascent in the juvenile form of Huntington's chorea. Lancet. 1970;2(7679):937.
79. Siesling S, Vegter-van de Vlis M, Losekoot M, Belfroid RD, Maat-Kievit JA, Kremer HP, et al. Family history and DNA analysis in patients with suspected Huntington's disease. J Neurol Neurosurg Psychiatry. 2000;69(1):54-9.
80. Zuccato C, Valenza M, Cattaneo E. Molecular mechanisms and potential therapeutical targets in Huntington's disease. Physiol Rev. 2010;90(3):905-81.
81. Zhang N, Bailus BJ, Ring KL, Ellerby LM. iPSC-based drug screening for Huntington's disease. Brain Res. 2016;1638(Pt A):42-56.

82. Halliday GM, McRitchie DA, Macdonald V, Double KL, Trent RJ, McCusker E. Regional specificity of brain atrophy in Huntington's disease. Exp Neurol. 1998;154(2):663-72.
83. Sun CS, Lee CC, Li YN, Yao-Chen Yang S, Lin CH, Chang YC, et al. Conformational switch of polyglutamine-expanded huntingtin into benign aggregates leads to neuroprotective effect. Sci Rep. 2015;5:14992.
84. Arrasate M, Finkbeiner S. Protein aggregates in Huntington's disease. Exp Neurol. 2012;238(1):1-11.
85. Hughes A, Jones L. Pathogenic mechanisms in Huntington's disease. 2014.
86. Butler R, Bates GPJNRN. Histone deacetylase inhibitors as therapeutics for polyglutamine disorders. 2006;7(10):784.
87. Pavese N, Gerhard A, Tai Y, Ho A, Turkheimer F, Barker R, et al. Microglial activation correlates with severity in Huntington disease A clinical and PET study. 2006;66(11):1638-43.
88. Tai YF, Pavese N, Gerhard A, Tabrizi SJ, Barker RA, Brooks DJ, et al. Microglial activation in presymptomatic Huntington's disease gene carriers. 2007;130(7):1759-66.
89. Crotti A, Benner C, Kerman BE, Gosselin D, Lagier-Tourenne C, Zuccato C, et al. Mutant Huntingtin promotes autonomous microglia activation via myeloid lineage-determining factors. 2014;17(4):513.
90. Björkqvist M, Wild EJ, Thiele J, Silvestroni A, Andre R, Lahiri N, et al. A novel pathogenic pathway of immune activation detectable before clinical onset in Huntington's disease. 2008;205(8):1869-77.
91. Pecho-Vrieseling E, Rieker C, Fuchs S, Bleckmann D, Esposito MS, Botta P, et al. Transneuronal propagation of mutant huntingtin contributes to non–cell autonomous pathology in neurons. 2014;17(8):1064.
92. Cicchetti F, Lacroix S, Cisbani G, Vallières N, Saint- Pierre M, St- Amour I, et al. Mutant huntingtin is present in neuronal grafts in Huntington disease patients. 2014;76(1):31-42.
93. Roux J-C, Zala D, Panayotis N, Borges-Correia A, Saudou F, Villard LJNod. Modification of Mecp2 dosage alters axonal transport through the Huntingtin/Hap1 pathway. 2012;45(2):786-95.
94. Jin YN, Johnson GVJJobab. The interrelationship between mitochondrial dysfunction and transcriptional dysregulation in Huntington disease. 2010;42(3):199-205.
95. Siddiqui A, Rivera-Sánchez S, Castro MdR, Acevedo-Torres K, Rane A, Torres-Ramos CA, et al. Mitochondrial DNA damage is associated with reduced mitochondrial bioenergetics in Huntington's disease. 2012;53(7):1478-88.
96. Beal MF, Kowall NW, Ellison DW, Mazurek MF, Swartz KJ, Martin JBJN. Replication of the neurochemical characteristics of Huntington's disease by quinolinic acid. 1986;321(6066):168.
97. Tong X, Ao Y, Faas GC, Nwaobi SE, Xu J, Haustein MD, et al. Astrocyte Kir4. 1 ion channel deficits contribute to neuronal dysfunction in Huntington's disease model mice. 2014;17(5):694.
98. Dragileva E, Hendricks A, Teed A, Gillis T, Lopez ET, Friedberg EC, et al. Intergenerational and striatal CAG repeat instability in Huntington's disease knock-in mice involve different DNA repair genes. 2009;33(1):37-47.
99. Schuster C, Elamin M, Hardiman O, Bede P. Presymptomatic and longitudinal neuroimaging in neurodegeneration--from snapshots to motion picture: a systematic review. J Neurol Neurosurg Psychiatry. 2015;86(10):1089-96.
100. Fiandaca MS, Kapogiannis D, Mapstone M, Boxer A, Eitan E, Schwartz JB, et al. Identification of preclinical Alzheimer's disease by a profile of pathogenic proteins in neurally derived blood exosomes: A case-control study. Alzheimers Dement. 2015;11(6):600-7.e1.

101. JPNDGroup. Experimental models for neurodegenerative diseases. 2014.
102. Lepesant JA. The promises of neurodegenerative disease modeling. C R Biol. 2015;338(8-9):584-92.
103. Lu B, Vogel H. Drosophila models of neurodegenerative diseases. Annual Review of Pathological Mechanical Disease. 2009;4:315-42.
104. Gama Sosa MA, De Gasperi R, Elder GA. Animal transgenesis: an overview. Brain Struct Funct. 2010;214(2-3):91-109.
105. Thomas KR, Capecchi MR. Site-directed mutagenesis by gene targeting in mouse embryo-derived stem cells. Cell. 1987;51(3):503-12.
106. Manis JP. Knock Out, Knock In, Knock Down — Genetically Manipulated Mice and the Nobel Prize. New England Journal of Medicine. 2007;357(24):2426-9.
107. Stranger BE, Stahl EA, Raj T. Progress and promise of genome-wide association studies for human complex trait genetics. Genetics. 2010.
108. Takahashi K, Tanabe K, Ohnuki M, Narita M, Ichisaka T, Tomoda K, et al. Induction of pluripotent stem cells from adult human fibroblasts by defined factors. Cell. 2007;131(5):861-72.
109. Srikanth P, Young-Pearse TL. Stem cells on the brain: modeling neurodevelopmental and neurodegenerative diseases using human induced pluripotent stem cells. Journal of neurogenetics. 2014;28(1-2):5-29.
110. Evans MJ, Kaufman MH. Establishment in culture of pluripotential cells from mouse embryos. Nature. 1981;292(5819):154-6.
111. Martin GR. Isolation of a pluripotent cell line from early mouse embryos cultured in medium conditioned by teratocarcinoma stem cells. Proc Natl Acad Sci U S A. 1981;78(12):7634-8.
112. Thomson JA, Itskovitz-Eldor J, Shapiro SS, Waknitz MA, Swiergiel JJ, Marshall VS, et al. Embryonic stem cell lines derived from human blastocysts. Science. 1998;282(5391):1145-7.
113. Lo B, Parham L. Ethical issues in stem cell research. Endocr Rev. 2009;30(3):204-13.
114. Takahashi K, Yamanaka S. Induction of pluripotent stem cells from mouse embryonic and adult fibroblast cultures by defined factors. Cell. 2006;126(4):663-76.
115. Yu J, Vodyanik MA, Smuga-Otto K, Antosiewicz-Bourget J, Frane JL, Tian S, et al. Induced pluripotent stem cell lines derived from human somatic cells. Science. 2007;318(5858):1917-20.
116. Yamanaka S. Induced pluripotent stem cells: past, present, and future. Cell Stem Cell. 2012;10(6):678-84.
117. Hawley RG. Does retroviral insertional mutagenesis play a role in the generation of induced pluripotent stem cells? Mol Ther. 16. United States2008. p. 1354-5.
118. Lin SL, Chang DC, Chang-Lin S, Lin CH, Wu DT, Chen DT, et al. Mir-302 reprograms human skin cancer cells into a pluripotent ES-cell-like state. Rna. 2008;14(10):2115-24.
119. Stadtfeld M, Nagaya M, Utikal J, Weir G, Hochedlinger K. Induced pluripotent stem cells generated without viral integration. Science. 2008;322(5903):945-9.
120. Fusaki N, Ban H, Nishiyama A, Saeki K, Hasegawa M. Efficient induction of transgene-free human pluripotent stem cells using a vector based on Sendai virus, an RNA virus that does not integrate into the host genome. Proc Jpn Acad Ser B Phys Biol Sci. 2009;85(8):348-62.
121. Woltjen K, Michael IP, Mohseni P, Desai R, Mileikovsky M, Hamalainen R, et al. piggyBac transposition reprograms fibroblasts to induced pluripotent stem cells. Nature. 2009;458(7239):766-70.

122. Yu J, Hu K, Smuga-Otto K, Tian S, Stewart R, Slukvin, II, et al. Human induced pluripotent stem cells free of vector and transgene sequences. Science. 2009;324(5928):797-801.
123. Kim D, Kim CH, Moon JI, Chung YG, Chang MY, Han BS, et al. Generation of human induced pluripotent stem cells by direct delivery of reprogramming proteins. Cell Stem Cell. 2009;4(6):472-6.
124. Jia F, Wilson KD, Sun N, Gupta DM, Huang M, Li Z, et al. A nonviral minicircle vector for deriving human iPS cells. Nat Methods. 2010;7(3):197-9.
125. Warren L, Manos PD, Ahfeldt T, Loh YH, Li H, Lau F, et al. Highly efficient reprogramming to pluripotency and directed differentiation of human cells with synthetic modified mRNA. Cell Stem Cell. 2010;7(5):618-30.
126. Takahashi K, Yamanaka S. A decade of transcription factor-mediated reprogramming to pluripotency. Nat Rev Mol Cell Biol. 2016;17(3):183-93.
127. Shi Y, Inoue H, Wu JC, Yamanaka S. Induced pluripotent stem cell technology: a decade of progress. Nat Rev Drug Discov. 2017;16(2):115-30.
128. Onos KD, Sukoff Rizzo SJ, Howell GR, Sasner M. Toward more predictive genetic mouse models of Alzheimer's disease. Brain Res Bull. 2016;122:1-11.
129. Kim K, Zhao R, Doi A, Ng K, Unternaehrer J, Cahan P, et al. Donor cell type can influence the epigenome and differentiation potential of human induced pluripotent stem cells. Nat Biotechnol. 2011;29(12):1117-9.
130. Avior Y, Sagi I, Benvenisty N. Pluripotent stem cells in disease modelling and drug discovery. Nat Rev Mol Cell Biol. 2016;17(3):170-82.
131. Hockemeyer D, Jaenisch R. Induced Pluripotent Stem Cells Meet Genome Editing. Cell Stem Cell. 2016;18(5):573-86.
132. Hockemeyer D, Soldner F, Beard C, Gao Q, Mitalipova M, DeKelver RC, et al. Efficient targeting of expressed and silent genes in human ESCs and iPSCs using zinc-finger nucleases. Nat Biotechnol. 2009;27(9):851-7.
133. Hockemeyer D, Wang H, Kiani S, Lai CS, Gao Q, Cassady JP, et al. Genetic engineering of human pluripotent cells using TALE nucleases. Nat Biotechnol. 2011;29(8):731-4.
134. Shalem O, Sanjana NE, Hartenian E, Shi X, Scott DA, Mikkelson T, et al. Genome-scale CRISPR-Cas9 knockout screening in human cells. Science. 2014;343(6166):84-7.
135. Studer L, Vera E, Cornacchia D. Programming and Reprogramming Cellular Age in the Era of Induced Pluripotency. Cell Stem Cell. 2015;16(6):591-600.
136. Cooper O, Seo H, Andrabi S, Guardia-Laguarta C, Graziotto J, Sundberg M, et al. Pharmacological rescue of mitochondrial deficits in iPSC-derived neural cells from patients with familial Parkinson's disease. Sci Transl Med. 2012;4(141):141ra90.
137. Miller JD, Ganat YM, Kishinevsky S, Bowman RL, Liu B, Tu EY, et al. Human iPSC-based modeling of late-onset disease via progerin-induced aging. Cell Stem Cell. 2013;13(6):691-705.
138. Nguyen HN, Byers B, Cord B, Shcheglovitov A, Byrne J, Gujar P, et al. LRRK2 mutant iPSC-derived DA neurons demonstrate increased susceptibility to oxidative stress. Cell Stem Cell. 2011;8(3):267-80.
139. Ho R, Sances S, Gowing G, Amoroso MW, O'Rourke JG, Sahabian A, et al. ALS disrupts spinal motor neuron maturation and aging pathways within gene co-expression networks. Nat Neurosci. 2016;19(9):1256-67.
140. Mertens J, Marchetto MC, Bardy C, Gage FH. Evaluating cell reprogramming, differentiation and conversion technologies in neuroscience. Nat Rev Neurosci. 2016;17(7):424-37.

141. Soldner F, Stelzer Y, Shivalila CS, Abraham BJ, Latourelle JC, Barrasa MI, et al. Parkinson-associated risk variant in distal enhancer of alpha-synuclein modulates target gene expression. Nature. 2016;533(7601):95-9.
142. Inoue H, Nagata N, Kurokawa H, Yamanaka S. iPS cells: a game changer for future medicine. Embo j. 2014;33(5):409-17.
143. Vincent F, Loria P, Pregel M, Stanton R, Kitching L, Nocka K, et al. Developing predictive assays: the phenotypic screening "rule of 3". Sci Transl Med. 2015;7(293):293ps15.
144. Matsa E, Burridge PW, Yu KH, Ahrens JH, Termglinchan V, Wu H, et al. Transcriptome Profiling of Patient-Specific Human iPSC-Cardiomyocytes Predicts Individual Drug Safety and Efficacy Responses In Vitro. Cell Stem Cell. 2016;19(3):311-25.
145. Doi D, Samata B, Katsukawa M, Kikuchi T, Morizane A, Ono Y, et al. Isolation of human induced pluripotent stem cell-derived dopaminergic progenitors by cell sorting for successful transplantation. Stem Cell Reports. 2014;2(3):337-50.
146. Egawa N, Kitaoka S, Tsukita K, Naitoh M, Takahashi K, Yamamoto T, et al. Drug screening for ALS using patient-specific induced pluripotent stem cells. Sci Transl Med. 2012;4(145):145ra04.
147. Miki K, Endo K, Takahashi S, Funakoshi S, Takei I, Katayama S, et al. Efficient Detection and Purification of Cell Populations Using Synthetic MicroRNA Switches. Cell Stem Cell. 2015;16(6):699-711.
148. Bright J, Hussain S, Dang V, Wright S, Cooper B, Byun T, et al. Human secreted tau increases amyloid-beta production. Neurobiol Aging. 2015;36(2):693-709.
149. Burkhardt MF, Martinez FJ, Wright S, Ramos C, Volfson D, Mason M, et al. A cellular model for sporadic ALS using patient-derived induced pluripotent stem cells. Mol Cell Neurosci. 2013;56:355-64.
150. Pereira CF, Lemischka IR, Moore K. Reprogramming cell fates: insights from combinatorial approaches. Ann N Y Acad Sci. 2012;1266:7-17.
151. Wang H, Li X, Gao S, Sun X, Fang H. Transdifferentiation via transcription factors or microRNAs: Current status and perspective. Differentiation. 2015;90(4-5):69-76.
152. McNeish J, Gardner JP, Wainger BJ, Woolf CJ, Eggan K. From Dish to Bedside: Lessons Learned While Translating Findings from a Stem Cell Model of Disease to a Clinical Trial. Cell Stem Cell. 2015;17(1):8-10.
153. Devlin AC, Burr K, Borooah S, Foster JD, Cleary EM, Geti I, et al. Human iPSC-derived motoneurons harbouring TARDBP or C9ORF72 ALS mutations are dysfunctional despite maintaining viability. Nat Commun. 2015;6:5999.
154. Avorn J. The $2.6 billion pill--methodologic and policy considerations. N Engl J Med. 2015;372(20):1877-9.
155. DiMasi JA, Grabowski HG, Hansen RW. Innovation in the pharmaceutical industry: New estimates of R&D costs. J Health Econ. 2016;47:20-33.
156. Schwartz MP, Hou Z, Propson NE, Zhang J, Engstrom CJ, Santos Costa V, et al. Human pluripotent stem cell-derived neural constructs for predicting neural toxicity. Proc Natl Acad Sci U S A. 2015;112(40):12516-21.
157. Armijo E, Gonzalez C, Shahnawaz M, Flores A, Davis B, Soto C. Increased susceptibility to Aβ toxicity in neuronal cultures derived from familial Alzheimer's disease (PSEN1-A246E) induced pluripotent stem cells. Neurosci Lett. 2017;639:74-81.
158. Woodruff G, Reyna SM, Dunlap M, Van Der Kant R, Callender JA, Young JE, et al. Defective Transcytosis of APP and Lipoproteins in Human iPSC-Derived Neurons with Familial Alzheimer's Disease Mutations. Cell Rep. 2016;17(3):759-73.
159. Pires C, Schmid B, Petræus C, Poon A, Nimsanor N, Nielsen TT, et al. Generation of a gene-corrected isogenic control cell line from an Alzheimer's disease patient iPSC line carrying a A79V mutation in PSEN1. Stem Cell Res. 2016;17(2):285-8.

160. Jones VC, Atkinson-Dell R, Verkhratsky A, Mohamet L. Aberrant iPSC-derived human astrocytes in Alzheimer's disease. Cell Death Dis. 2017;8(3):e2696.
161. Bordoni M, Fantini V, Pansarasa O, Cereda C. From neuronal differentiation of iPSCs to 3D neurorganoids: modelling of neurodegenerative diseases. IntechOpen; 2018.
162. Chung SY, Kishinevsky S, Mazzulli JR, Graziotto J, Mrejeru A, Mosharov EV, et al. Parkin and PINK1 Patient iPSC-Derived Midbrain Dopamine Neurons Exhibit Mitochondrial Dysfunction and α-Synuclein Accumulation. Stem Cell Reports. 2016;7(4):664-77.
163. Son MY, Sim H, Son YS, Jung KB, Lee MO, Oh JH, et al. Distinctive genomic signature of neural and intestinal organoids from familial Parkinson's disease patient-derived induced pluripotent stem cells. Neuropathol Appl Neurobiol. 2017;43(7):584-603.
164. Chung CY, Khurana V, Auluck PK, Tardiff DF, Mazzulli JR, Soldner F, et al. Identification and rescue of α-synuclein toxicity in Parkinson patient-derived neurons. Science. 2013;342(6161):983-7.
165. Haenseler W, Sansom SN, Buchrieser J, Newey SE, Moore CS, Nicholls FJ, et al. A Highly Efficient Human Pluripotent Stem Cell Microglia Model Displays a Neuronal-Co-culture-Specific Expression Profile and Inflammatory Response. Stem Cell Reports. 2017;8(6):1727-42.
166. Lopez-Gonzalez R, Lu Y, Gendron TF, Karydas A, Tran H, Yang D, et al. Poly(GR) in C9ORF72-Related ALS/FTD Compromises Mitochondrial Function and Increases Oxidative Stress and DNA Damage in iPSC-Derived Motor Neurons. Neuron. 2016;92(2):383-91.
167. De Santis R, Santini L, Colantoni A, Peruzzi G, de Turris V, Alfano V, et al. FUS Mutant Human Motoneurons Display Altered Transcriptome and microRNA Pathways with Implications for ALS Pathogenesis. Stem Cell Reports. 2017;9(5):1450-62.
168. Qian K, Huang H, Peterson A, Hu B, Maragakis NJ, Ming GL, et al. Sporadic ALS Astrocytes Induce Neuronal Degeneration In Vivo. Stem Cell Reports. 2017;8(4):843-55.
169. Hall CE, Yao Z, Choi M, Tyzack GE, Serio A, Luisier R, et al. Progressive Motor Neuron Pathology and the Role of Astrocytes in a Human Stem Cell Model of VCP-Related ALS. Cell Rep. 2017;19(9):1739-49.
170. Bhinge A, Namboori SC, Zhang X, VanDongen AMJ, Stanton LW. Genetic Correction of SOD1 Mutant iPSCs Reveals ERK and JNK Activated AP1 as a Driver of Neurodegeneration in Amyotrophic Lateral Sclerosis. Stem Cell Reports. 2017;8(4):856-69.
171. Hedlund E, Karlsson M, Osborn T, Ludwig W, Isacson O. Global gene expression profiling of somatic motor neuron populations with different vulnerability identify molecules and pathways of degeneration and protection. Brain. 2010;133(Pt 8):2313-30.
172. Osborn TM, Beagan J, Isacson O. Increased motor neuron resilience by small molecule compounds that regulate IGF-II expression. Neurobiol Dis. 2018;110:218-30.
173. Szlachcic WJ, Switonski PM, Krzyzosiak WJ, Figlerowicz M, Figiel M. Huntington disease iPSCs show early molecular changes in intracellular signaling, the expression of oxidative stress proteins and the p53 pathway. Dis Model Mech. 2015;8(9):1047-57.
174. Consortium Hi. Developmental alterations in Huntington's disease neural cells and pharmacological rescue in cells and mice. Nat Neurosci. 2017;20(5):648-60.
175. Rindt H, Tom CM, Lorson CL, Mattis VB. Optimization of trans-Splicing for Huntington's Disease RNA Therapy. Front Neurosci. 2017;11:544.
176. Hsiao HY, Chen YC, Huang CH, Chen CC, Hsu YH, Chen HM, et al. Aberrant astrocytes impair vascular reactivity in Huntington disease. Ann Neurol. 2015;78(2):178-92.
177. Guillemot F, Mironov V, Nakamura M. Bioprinting is coming of age: Report from the International Conference on Bioprinting and Biofabrication in Bordeaux (3B'09). Biofabrication. 2010;2(1):010201.
178. Groll J, Boland T, Blunk T, Burdick JA, Cho DW, Dalton PD, et al. Biofabrication: reappraising the definition of an evolving field. Biofabrication. 2016;8(1):013001.

179. Dababneh AB, Ozbolat IT, editors. Bioprinting Technology : A Current State-ofthe-Art Review2014.
180. Nakamura M, Iwanaga S, Henmi C, Arai K, Nishiyama Y. Biomatrices and biomaterials for future developments of bioprinting and biofabrication. Biofabrication. 2010;2(1):014110.
181. Giovanelli A. Bioprinting: stato dell'arte ed applicazioni biomediche - Master thesis in Clinical Engineering 2015.
182. Wilson WC, Jr., Boland T. Cell and organ printing 1: protein and cell printers. Anat Rec A Discov Mol Cell Evol Biol. 2003;272(2):491-6.
183. Calvert P. Inkjet Printing for Materials and Devices. Chemistry of Materials. 2001;13(10):3299-305.
184. Moon S, Hasan SK, Song YS, Xu F, Keles HO, Manzur F, et al. Layer by layer three-dimensional tissue epitaxy by cell-laden hydrogel droplets. Tissue Eng Part C Methods. 2010;16(1):157-66.
185. Odde DJ, Renn MJ. Laser-guided direct writing of living cells. Biotechnol Bioeng. 2000;67(3):312-8.
186. Koch L, Kuhn S, Sorg H, Gruene M, Schlie S, Gaebel R, et al. Laser printing of skin cells and human stem cells. Tissue Eng Part C Methods. 2010;16(5):847-54.
187. A O, M G, M P, L K, F M, M W, et al. Laser printing of cells into 3D scaffolds. Biofabrication. 2010;2(1):014104.
188. Ozbolat IT, Yu Y. Bioprinting toward organ fabrication: challenges and future trends. IEEE Trans Biomed Eng. 2013;60(3):691-9.
189. Mironov V. Printing technology to produce living tissue. Taylor & Francis; 2003.
190. Axpe E, Oyen ML. Applications of Alginate-Based Bioinks in 3D Bioprinting. Int J Mol Sci. 2016;17(12).
191. Patterson J, Martino MM, Hubbell JA. Biomimetic materials in tissue engineering. Materials Today. 2010;13(1):14-22.
192. Lutolf MP, Gilbert PM, Blau HM. Designing materials to direct stem-cell fate. Nature. 2009;462(7272):433-41.
193. Malda J, Visser J, Melchels FP, Jüngst T, Hennink WE, Dhert WJA, et al. 25th Anniversary Article: Engineering Hydrogels for Biofabrication. Advanced Materials. 2013;25(36):5011-28.
194. Nuttelman CR, Rice MA, Rydholm AE, Salinas CN, Shah DN, Anseth KS. Macromolecular Monomers for the Synthesis of Hydrogel Niches and Their Application in Cell Encapsulation and Tissue Engineering. Progress in polymer science. 2008;33(2):167-79.
195. Yan Y, Wang X, Xiong Z, Liu H, Liu F, Lin F, et al. Direct Construction of a Three-dimensional Structure with Cells and Hydrogel. Journal of Bioactive and Compatible Polymers. 2005;20(3):259-69.
196. Zhang T, Yan Y, Wang X, Xiong Z, Lin F, Wu R, et al. Three-dimensional Gelatin and Gelatin/Hyaluronan Hydrogel Structures for Traumatic Brain Injury. Journal of Bioactive and Compatible Polymers. 2007;22(1):19-29.
197. Foox M, Zilberman M. Drug delivery from gelatin-based systems. Expert Opin Drug Deliv. 2015;12(9):1547-63.
198. Lee KY, Mooney DJ. Alginate: properties and biomedical applications. Prog Polym Sci. 2012;37(1):106-26.
199. Updegraff DM. Semimicro determination of cellulose in biological materials. Anal Biochem. 1969;32(3):420-4.
200. Klemm D, Heublein B, Fink H-P, Bohn A. Cellulose: Fascinating Biopolymer and Sustainable Raw Material. Angewandte Chemie International Edition. 2005;44(22):3358-93.

201. Klemm D, Kramer F, Moritz S, Lindstrom T, Ankerfors M, Gray D, et al. Nanocelluloses: a new family of nature-based materials. Angew Chem Int Ed Engl. 2011;50(24):5438-66.
202. Backdahl H, Helenius G, Bodin A, Nannmark U, Johansson BR, Risberg B, et al. Mechanical properties of bacterial cellulose and interactions with smooth muscle cells. Biomaterials. 2006;27(9):2141-9.
203. Yoo J, Kim HS, Hwang DY. Stem cells as promising therapeutic options for neurological disorders. J Cell Biochem. 2013;114(4):743-53.
204. Wu KH, Mo XM, Han ZC, Zhou B. Stem Cell Engraftment and Survival in the Ischemic Heart. The Annals of Thoracic Surgery. 2011;92(5):1917-25.
205. Hsieh FY, Hsu SH. 3D bioprinting: A new insight into the therapeutic strategy of neural tissue regeneration. Organogenesis. 2015;11(4):153-8.
206. Panseri S, Cunha C, Lowery J, Del Carro U, Taraballi F, Amadio S, et al. Electrospun micro- and nanofiber tubes for functional nervous regeneration in sciatic nerve transections. BMC Biotechnol. 2008;8:39.
207. Cao H, Liu T, Chew SY. The application of nanofibrous scaffolds in neural tissue engineering. Adv Drug Deliv Rev. 2009;61(12):1055-64.
208. Lee W, Pinckney J, Lee V, Lee JH, Fischer K, Polio S, et al. Three-dimensional bioprinting of rat embryonic neural cells. Neuroreport. 2009;20(8):798-803.
209. Lee YB, Polio S, Lee W, Dai G, Menon L, Carroll RS, et al. Bio-printing of collagen and VEGF-releasing fibrin gel scaffolds for neural stem cell culture. Exp Neurol. 2010;223(2):645-52.
210. Censi R, Vermonden T, van Steenbergen MJ, Deschout H, Braeckmans K, De Smedt SC, et al. Photopolymerized thermosensitive hydrogels for tailorable diffusion-controlled protein delivery. Journal of Controlled Release. 2009;140(3):230-6.
211. Ho L, Hsu SH. Cell reprogramming by 3D bioprinting of human fibroblasts in polyurethane hydrogel for fabrication of neural-like constructs. Acta Biomater. 2018;70:57-70.
212. Strober W. Trypan blue exclusion test of cell viability. Curr Protoc Immunol. 2001;Appendix 3:Appendix 3B.
213. Forster JI, Köglsberger S, Trefois C, Boyd O, Baumuratov AS, Buck L, et al. Characterization of Differentiated SH-SY5Y as Neuronal Screening Model Reveals Increased Oxidative Vulnerability. J Biomol Screen. 2016;21(5):496-509.
214. Isobe N, Komamiya T, Kimura S, Kim UJ, Wada M. Cellulose hydrogel with tunable shape and mechanical properties: From rigid cylinder to soft scaffold. Int J Biol Macromol. 2018;117:625-31.
215. Gnavi S, Fornasari BE, Tonda-Turo C, Ciardelli G, Zanetti M, Geuna S, et al. The influence of electrospun fibre size on Schwann cell behaviour and axonal outgrowth. Mater Sci Eng C Mater Biol Appl. 2015;48:620-31.
216. Seidlits SK, Lee JY, Schmidt CE. Nanostructured scaffolds for neural applications. Nanomedicine (Lond). 2008;3(2):183-99.
217. Tamayol A, Akbari M, Annabi N, Paul A, Khademhosseini A, Juncker D. Fiber-based tissue engineering: Progress, challenges, and opportunities. Biotechnol Adv. 2013;31(5):669-87.
218. Hjortso MA, Roos JW. Cell Adhesion in Bioprocessing and Biotechnology 1995. 288 p.
219. Wang R, Hughes T, Beck S, Vakil S, Li S, Pantano P, et al. Generation of toxic degradation products by sonication of Pluronic(R) dispersants: implications for nanotoxicity testing. Nanotoxicology. 2013;7(7):1272-81.
220. Hwang HC, Woo JS, Park SY. Flexible carbonized cellulose/single-walled carbon nanotube films with high conductivity. Carbohydr Polym. 2018;196:168-75.

221. Kuzmenko V, Karabulut E, Pernevik E, Enoksson P, Gatenholm P. Tailor-made conductive inks from cellulose nanofibrils for 3D printing of neural guidelines. Carbohydr Polym. 2018;189:22-30.
222. Ostrakhovitch EA, Byers JC, O'Neil KD, Semenikhin OA. Directed differentiation of embryonic P19 cells and neural stem cells into neural lineage on conducting PEDOT–PEG and ITO glass substrates. Archives of Biochemistry and Biophysics. 2012;528(1):21-31.